SUPERCRITICAL FLOW EXPERIMENTAL FACILITY

A Thesis
Submitted to Faculty of Graduate Studies
In Partial Fulfillment of the Requirements for the Degree of

Master of Science
In
Mechanical and Manufacturing Engineering

Department of Mechanical and Manufacturing Engineering
University of Manitoba
Winnipeg, Manitoba
Canada

by

S. K. Varaprasad Babu Tummalapalli

THE UNIVERISTY OF MANITOBA

FACULTY OF GRADUATE STUDIES

****

COPYRIGHT PERMISSION

SUPERCRITICAL FLOW EXPERIMENTAL FACILITY

BY

S. K. Varaprasad Babu Tummalapalli

A Thesis/Practicum submitted to the Faculty of Graduate Studies of University of Manitoba in partial fulfillment of the requirements of the degree

OF

MASTER OF SCIENCE

ABSTRACT

In the present work, a supercritical flow experimental facility was designed and constructed to understand the behavior of supercritical fluid flow. The primary objective of the experimental facility is to study the supercritical flow instabilities in fluids, while the experimental facility can be employed to conduct other studies, such as heat transfer and pressure drop characteristics. The experimental facility was designed for supercritical water as the working fluid. Most of the components required for water were procured. However, as the first phase of study will use carbon dioxide at supercritical conditions, some components installed are specific to carbon dioxide and will be replaced for the water experiments. The facility was completely constructed and assembled as per design. Pre-experimental procedures such as chemical cleaning and leak tests were performed. Pressure testing was also conducted to verify the pressure rating (10 MPa) of the facility for carbon dioxide experiments.

Steady-state numerical simulations of the loop with carbon dioxide flowing in a single channel distributed heat system were conducted using modified SPORTS code. About sixty simulations were conducted for varying parameters, such as channel inlet K-factor, channel outlet K-factor, inlet temperature and pressure.

ACKNOWLEDGMENTS

I would like to express my sincere appreciation and gratitude to my advisor, Dr. Vijay Chatoorgoon for giving me the opportunity to work in this challenging field of research. His invaluable help with all aspects of this thesis as well as with my graduate course work is greatly appreciated.

My heartful thanks goes to Paul Krueger, who helped me during the construction of the experimental facility. My appreciation also goes to Dr. Igor Pioro and Yvan Lachance of AECL for their support and timely suggestion in course of this project.

Lastly, but certainly not least, I would like to thank my dearest fiancé, Geetha, my parents, family, and friends for their support and encouragement through out the work.

DEDICATION

I whole heartedly dedicate this thesis to my beloved guru.

TABLE OF CONTENTS

LIST OF TABLES

LIST OF FIGURES

CHAPTER 1

INTRODUCTION

The energy crisis has become an important issue for many nations all over the world. Researchers predict that worldwide demand for energy will increase severalfold during the 21st century. Nuclear power seems to be one of the promising energy sources for the next generation's power needs, and has drawn the attention of many nations around the world. Unlike fossil-fuel power plants, nuclear power plants do not produce greenhouse gas effects.

Supercritical water-cooled reactors (SCWR) are being investigated by several organizations worldwide. Among them, researchers at Atomic Energy of Canada Limited (AECL) are studying an advanced CANada Deuterium Uranium (CANDU) reactor concept with supercritical light water as the coolant (Dimmick et al., 1998). A supercritical water cooled reactor is among one of the six new generation reactor concepts suggested in the generation IV nuclear reactors of the US Department of Energy. The use of a supercritical coolant would allow for higher thermal efficiency and more compact design than the existing light water reactors (LWR) and pressurized water reactors (PWR).

By using supercritical water on the primary side, researchers are aiming to increase the overall plant efficiency. Natural circulation of the coolant is very attractive for removing 100% of core heat. However, it is too early to know if this would be feasible. The use of supercritical water in power reactors has not yet been fully explored and much work is ongoing at the moment. A unique feature of supercritical water is that

the density varies by a factor of eight across the critical point. This could lead to flow instabilities; hence, research must be done to study the dynamic behavior of these supercritical fluids. Keeping in view the advantages of supercritical fluids in nuclear reactors, a thorough study will contribute to a better understanding of the behavior of supercritical fluids (carbon dioxide and water).

1.1 Objectives

The objectives of the present work are motivated by the need to better understand supercritical flow behavior under reactor type conditions. The following were the goals of this endeavor:

1. Finalize and complete the design and construction of the supercritical flow experimental research facility to study supercritical flow phenomena such as flow instability, deteriorated heat transfer, pressure-drop characteristics etc., of carbon dioxide and water.
2. Manage the complete project, oversee the purchases, install and construct all necessary components and co-ordinate with various personnel/departments commissioned to perform specific tasks required to achieve objective 1.
3. Test the experimental facility to determine that all components work at the rated pressure.
4. Conduct steady-state numerical simulations of the supercritical flow experimental facility with carbon dioxide in a single channel heated system using the SPORTS code. Presents steady-state results.

1.2 Background Information

1.2.1 Supercritical Fluids

A supercritical fluid is defined as a fluid at a pressure and temperature above the critical point (Duffey and Pioro, 2005), where the critical point represents the highest temperature and pressure at which the substance can exist as a vapor and liquid in equilibrium. The phenomenon can be easily explained with reference to the phase diagram in Figure 1.1. Supercritical fluids have unique features (Pioro et al., 2004). One of their distinctive features is the large change in thermophysical properties as the fluid temperature crosses the critical point. This pattern of behavior is not restricted to water, but is also followed by many other fluids (carbon dioxide, Freon-114, helium etc.,). The density varies drastically between 280 °C and 500 °C for water, which are approximately the core inlet and outlet temperatures for several supercritical water reactors. The density change that occurs as the fluid (water) is heated through the critical point is capable of generating a substantial driving head for natural circulation. Figure 1.2 shows the variation of density with temperature across the critical point for water and carbon dioxide.

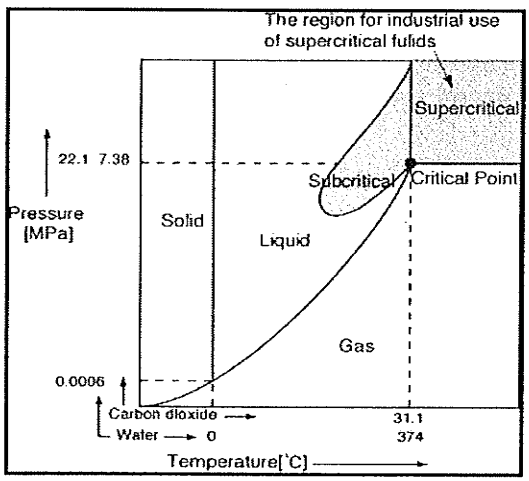

Figure 1.1: Phase diagram showing critical point for H_2O and CO_2 (Kang, 2007).

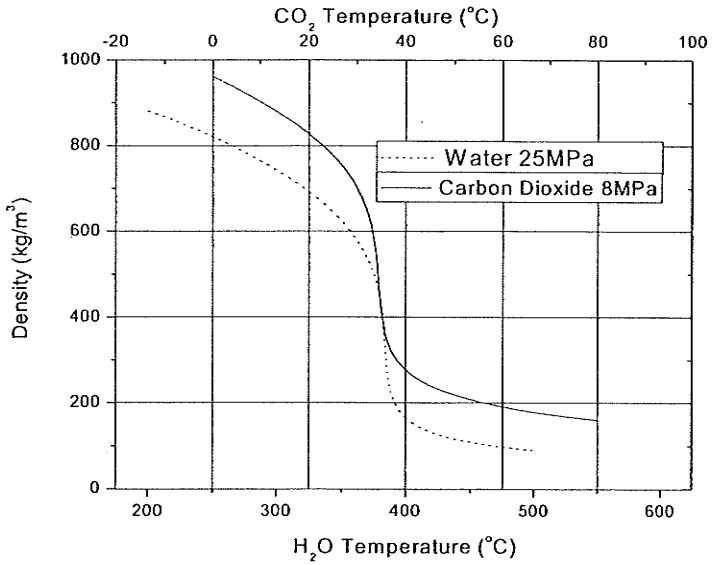

Figure 1.2: Variation of density about the critical point for H_2O and CO_2 (Upadhye, 2007).

1.2.2 Flow Instabilities

In a heat transfer system, such as emergency reactor cooling systems, solar heating and cooling systems, geothermal power systems and many other energy conversion systems, unstable flow can occur in the form of flow oscillations or flow reversals. Flow oscillations may occur in two-phase, or supercritical flows. A flow oscillation in one reactor coolant channel sometimes causes flow oscillations in the surrounding coolant channels due to flow redistribution. Flow oscillations are undesirable for several reasons. Sustained flow oscillations can cause undesirable forced mechanical vibration of components, which could lead to failure of those components due to fatigue. Flow oscillations can also cause system control problems of particular importance in liquid-cooled nuclear reactors because the coolant is also used as the moderator.

Lastly flow oscillations can affect the local heat transfer characteristics and boiling phenomena.

Flow instability studies in boiling water reactors have been investigated extensively; the instabilities studied were in the subcritical region and mostly pertained to two-phase flow. These instability phenomena may cause self-sustained or even divergent flow oscillations in operating power reactors. Such flows could induce a boiling crisis, disturbance in control systems, or may cause mechanical damage due to excitation of flow-induced vibrations. Literature on flow instability at supercritical pressure and temperature is limited and most of the investigators have concentrated on the heat transfer characteristics instead.

1.2.3 Supercritical Water Reactors

Supercritical water reactors are basically light water reactors operating at higher temperature and pressure (Roelofs, 2004). By operating the reactors above the critical point, boiling is absent, thus eliminating the need for jet pumps, pressurizer, steam-generator and dryer. Moreover, because of the high heat capacity of supercritical water, comparatively less coolant would be needed and, thus, the operating costs would be significantly reduced. One more advantage of using supercritical water is a significant reduction in cost through an increase in thermal efficiency and plant simplification. In view of these advantages many nations are investigating the supercritical water reactor concept to assess its technical viability, plant safety, stability characteristics and to identify suitable materials (Buongiorno, 2003). However, flow instabilities may be present in these reactors, as observed in boiling water reactors because of the unique

thermodynamic properties of supercritical water (Figure 1.3). Flow instabilities in the supercritical region have not been investigated to a great extent as most of the present fossil-fuel power plants operate at sub-critical flow conditions.

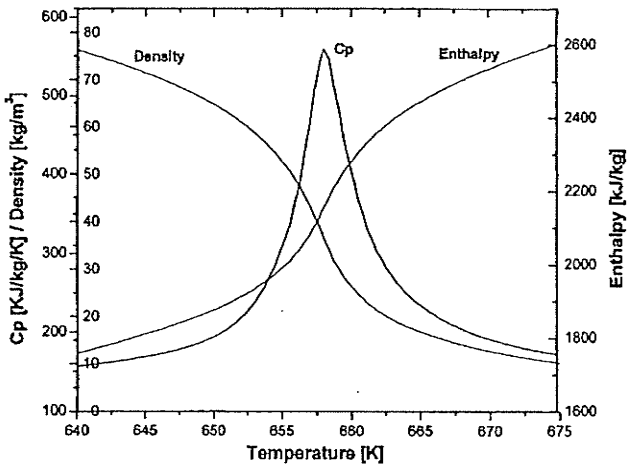

Figure 1.3: Properties of water at supercritical pressure (P = 25MPa) (Jain, 2005).

1.2.4 Supercritical Carbon Dioxide

Carbon dioxide is considered to be a good substitute for water in experimental research due to its analogous change in physical properties across the critical point. Because of its low critical point, carbon dioxide (critical temperature: 31 °C and critical pressure: 7.83 MPa) is an easier fluid to handle in experiments than water (critical temperature: 374.1 °C and critical pressure: 22.1 MPa). Table 1.1 lists nominal operating parameters of the SCW CANDU reactor concept in water and carbon dioxide equivalent values. Furthermore, supercritical carbon dioxide is proposed as a working fluid in the Brayton cycle of the STAR-LM fast reactor concept (Sienicki et al., 2003), where the supercritical carbon dioxide is directly employed to transfer heat to the secondary circuit by natural circulation.

Table 1.1: Critical and nominal operating parameters (Pioro and Khartabil, 2005).

Parameter	Unit	Water	Carbon Dioxide
Critical Parameters			
Critical Pressure	MPa	22.1	7.83
Critical Temperature	°C	374.1	30.98
Critical Density	kg/m^3	315	467.60
SCWR Operating Parameters			
Operating Pressure	MPa	25	8.50
Inlet Temperature	°C	350	25
Outlet Temperature	°C	625	150

Supercritical carbon dioxide has also been extensively used in fluid extraction, semiconductor cleaning, polymer processing, drug delivery and in other applications. These numerous and varied applications of supercritical carbon dioxide has necessitated an in depth study of supercritical fluid behavior.

1.3 Outline

An experimental facility was designed and constructed to study supercritical carbon dioxide as well as supercritical water. Initial numerical simulations were performed to determine the approximate parameters that could induce flow oscillations. This thesis is structured into six chapters, including the introduction chapter.

Chapter 2 covers the literature review on some of the previous research studies performed in the field of instabilities including natural circulation loops, two-phase flows and supercritical flows.

Chapter 3 discusses the project management aspects and difficulties overcome during the course of constructing the supercritical flow experimental facility.

Chapter 4 outlines the construction and design details of the supercritical flow experimental facility, pre-experimental procedures and safety features of the experimental facility.

Chapter 5 discusses the pre-experimental procedures followed after the construction of the supercritical flow experimental facility construction, which would prepare the facility to conduct experiments using carbon dioxide.

Chapter 6 summarizes the numerical simulations of the supercritical flow facility using the SPORTS code with carbon dioxide as the working fluid. This numerical information could be useful for conducting experiments on the experimental facility.

The final chapter 7 presents the conclusion and scope for future experimental work to be carried out on the experimental facility.

CHAPTER 2

LITERATURE REVIEW

Numerous experimental and analytical studies have been carried out by researchers in single-phase and two-phase natural circulation systems. They have focused on various aspects such as heat transfer, pressure drop, flow stability and other flow dynamics. In this chapter a review of experimental natural-circulation works carried out by various researchers is presented. In addition, a review of relevant work carried out by various researchers on supercritical flow is also presented.

2.1 Experimental Work (Subcritical Flow)

Natural circulation loops are thermosyphons in which the fluid flow occurs due to buoyancy forces caused by the difference in densities between the heated and cooled portions of the loop. Usually, in a natural circulation loop, the sink is located at a higher elevation than the heating source to enhance fluid circulation rates. These loops have been used in emergency reactor cooling systems, solar heating and cooling systems, geothermal power systems and many other energy conversion systems.

Research has been carried out in subcritical flow to understand these natural circulation loops in view of their importance. It has been observed that these subcritical natural circulation loops can exhibit oscillatory modes of flow, which may lead to flow instabilities and flow reversals (Zvirin, 1981). Some of the experimental natural circulation loops that were studied by various researchers for subcritical and two-phase flow are listed in Figure 2.1.

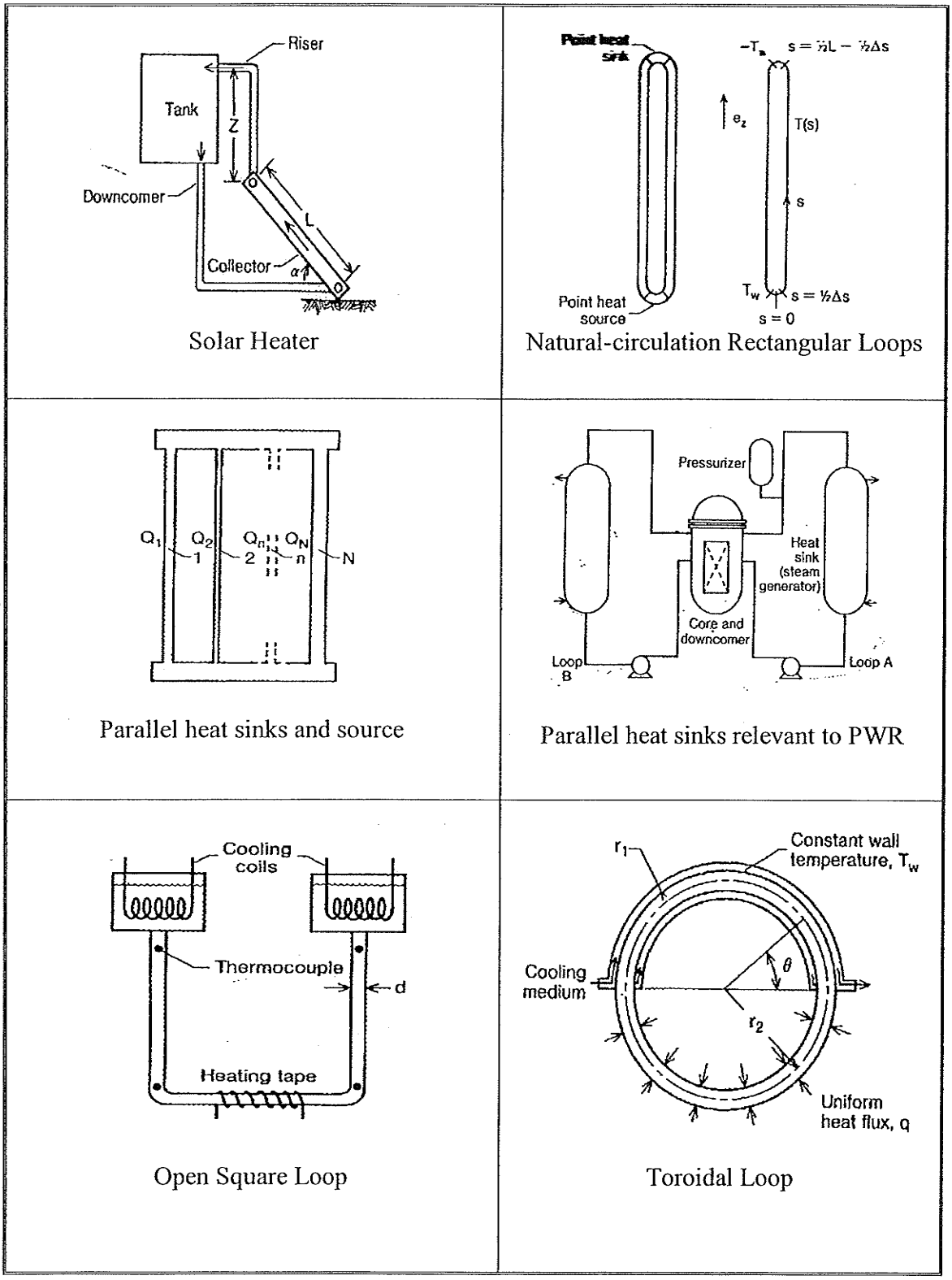

Figure 2.1: Schematic drawings of various natural circulation loops (Zvirin, 1981).

Zvirin (1981), Kakac and Veziroglu (1983), Mertol and Greif (1985), Misale and Tagliafico (1987) and Greif (1988) have extensively reviewed various subcritical natural circulation loops. They have also reviewed theoretical works carried out by researchers.

Hallinan and Viskanta (1986) constructed a simple natural-circulation loop with tube bundles in two vertical legs. The experimental facility operated at atmospheric pressure, with water as the working fluid. They also developed a dynamic one-dimensional analytical model of the experimental facility. At steady-state conditions, parameters like temperature, fluid mass flow rate were measured and compared with the predictions of the theoretical model. Relatively good agreement was observed between experiments and theory.

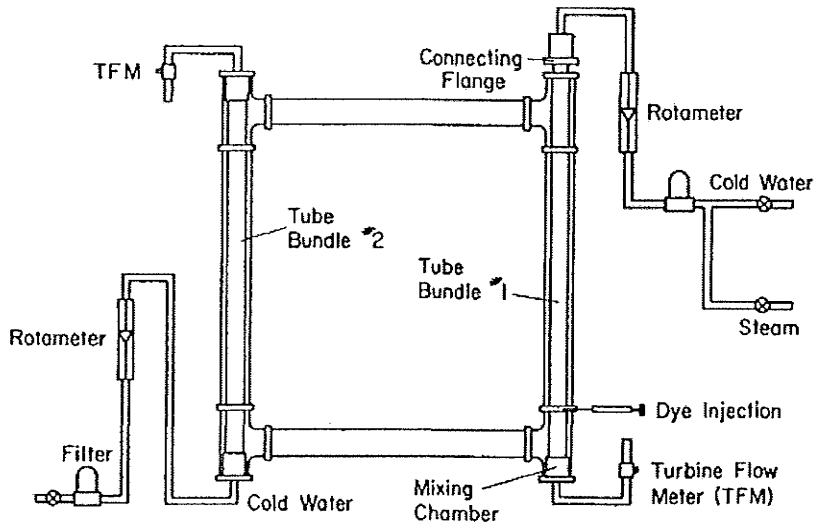

Figure 2.2: Schematic drawing of the experimental natural circulation loop (Hallinan and Viskanta, 1986).

Vijayan and Date (1992) conducted both experimental and theoretical (linear, non-linear) investigations on the stability of a natural-circulation loop with a throughflow in a figure-of-eight loop (a configuration employed in the pressure tube type heavy water

reactors). Through their study, limits of stable and unstable regimes as well as limits of conditionally stable regimes were identified. Contrary to previous studies, they noticed that the stable range decreases with an increase in the throughflow rate, signifying that the geometry of the loop can have an important bearing on the stability berhaviour.

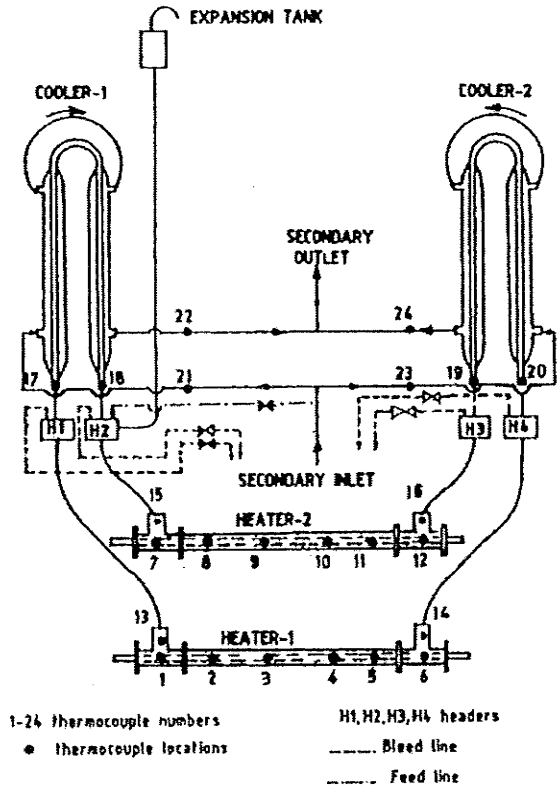

Fig. 1. Experimental loop.

Figure 2.3: Single-phase natural circulation figure-of-eight loop

(Vijayan and Date, 1992).

Vijayan (2002) developed an experimental facility to study steady-state flow in uniform and non-uniform diameter single-phase natural circulation loops. He concluded that the stability behaviour of uniform and non-uniform diameter loops can be expressed by a single non-dimensional parameters. Testing of the conventional laminar flow

correlation showed very good agreement with the data from both uniform and non-uniform diameter loops.

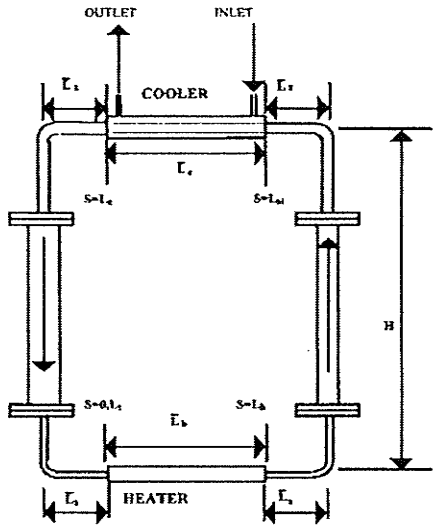

Figure 2.4: Schematic drawing of a non-uniform diameter natural circulation loop (Vijayan, 2002).

Guanghui et al. (2002) conducted experimental and theoretical studies on density wave oscillations in a natural circulation loop. The influence of mass flow rate, pressure, inlet subcooling, heat flux and exit quality on density wave oscillations were analyzed.

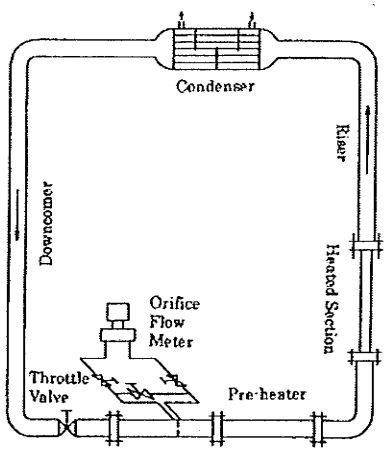

Figure 2.5: The natural circulation loop (Guanghui et al., 2002).

Jiang and Shoji (2003) studied the change of flow stability due to variation of tube wall thermal conductivity. They performed experiments in three different natural-circulation loops each one using a different piping material. The materials were copper tube, top copper tube half and bottom glass half, glass tube. Otherwise the same shape and same boundary conditions were used. Experimental results concluded that the thermal disturbance could be easily introduced and removed by a tube material with higher thermal conductivity. They also proposed a nonlinear model to formulate the wall effects.

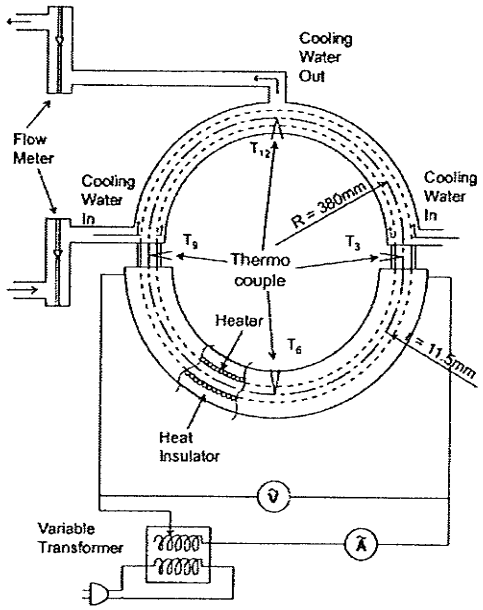

Figure 2.6: Schematic configuration of the experimental setup (Jiang and Shoji, 2003).

2.2 Supercritical Flow Studies

Supercritical water reactor is being considered as one of the next generation nuclear reactor after LWR and HWR. The supercritical water reactor would operate at 25 MPa pressure and would have a high thermal and electrical efficiency. However, the large

temperature change across the supercritical water reactor core (280 °C at the inlet to 500 °C at the exit) leads to a large density change (780 kg/m^3 to 90 kg/m^3) across the core. This gives rise to concern about supercritical flow instabilities in the SCWR.

Harden and Boggs (1964) investigated the transient behavior of a closed natural circulation system experimentally and analytically using Freon-114 as the working fluid. They observed rapid fluctuations in flow and pressure as the fluid is heated to the critical region. The frequencies of these fluctuations were in the range of 10 to 20 cycles per second, and were independent of heating rate. They also noted that the loop could be maintained in stable condition as long as the fluid was not in the thermodynamic region characterized by a maximum in the density-enthalpy product versus temperature plot.

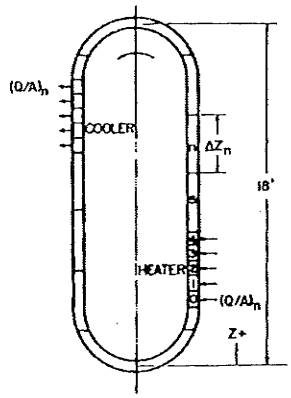

Figure 2.7: Schematic drawing of natural circulation loop (Harden and Boggs, 1964).

Cornelius and Parker (1965) conducted heat transfer studies in natural-and forced-convection loops, and reported heat transfer instabilities near the critical point. They also observed that flow instabilities were strongly damped during forced convection and reported two different types of flow oscillations during the test.

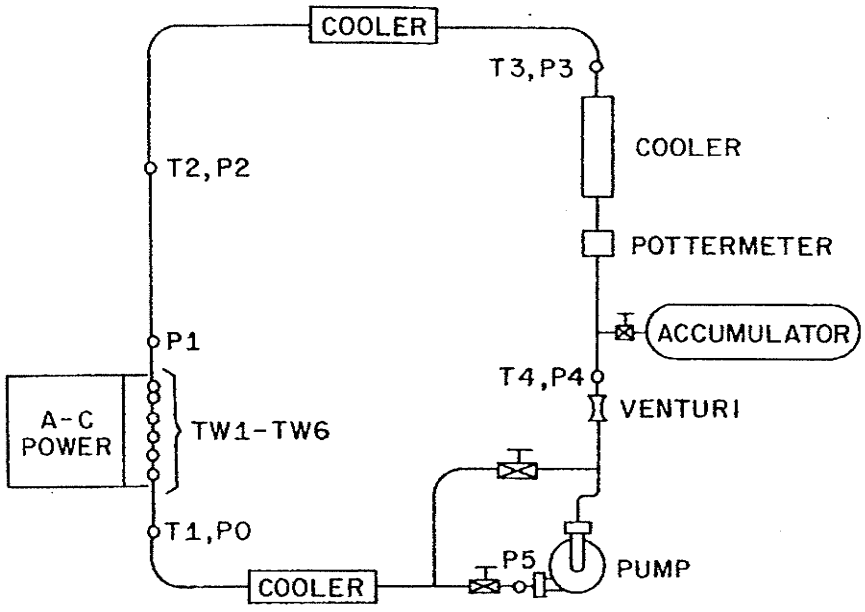

Figure 2.8: Schematic diagram of heat transfer loop (Cornelius and Parker, 1965).

Yamagata (1972) conducted experiments to study supercritical water flowing in horizontal and vertical tubes. He observed severe pressure and flow oscillations while recording heat transfer data but they did not analyze these instabilities. Research was also focused on instabilities associated with cryogenic fluids at supercritical pressure. Later Fukuda et al. (1992) experimentally investigated the instabilities in supercritical helium. Experimental set consists of a liquid helium tank, inlet and outlet plenum, pressurizer and a test section. Three different types of instabilities were observed their mechanisms were also explained. One type of instability was Helmholtz, which was caused by acoustic resonance and other two types of instabilities were found to be density wave instabilities caused by density wave resonance.

Lomperski et al. (2004) conducted experiments in a natural-circulation loop using supercritical carbon dioxide. However, no flow instabilities were observed, in contrast to the numerical predictions as suggested by Chatoorgoon (2001). Jain (2005)

performed stability analysis of a natural-circulation loop by means of experiments and numerical simulations. Her studies concluded that the numerical model predicts instabilities in supercritical water as well as in supercritical carbon dioxide loops and agrees with Chatoorgoon (2001).

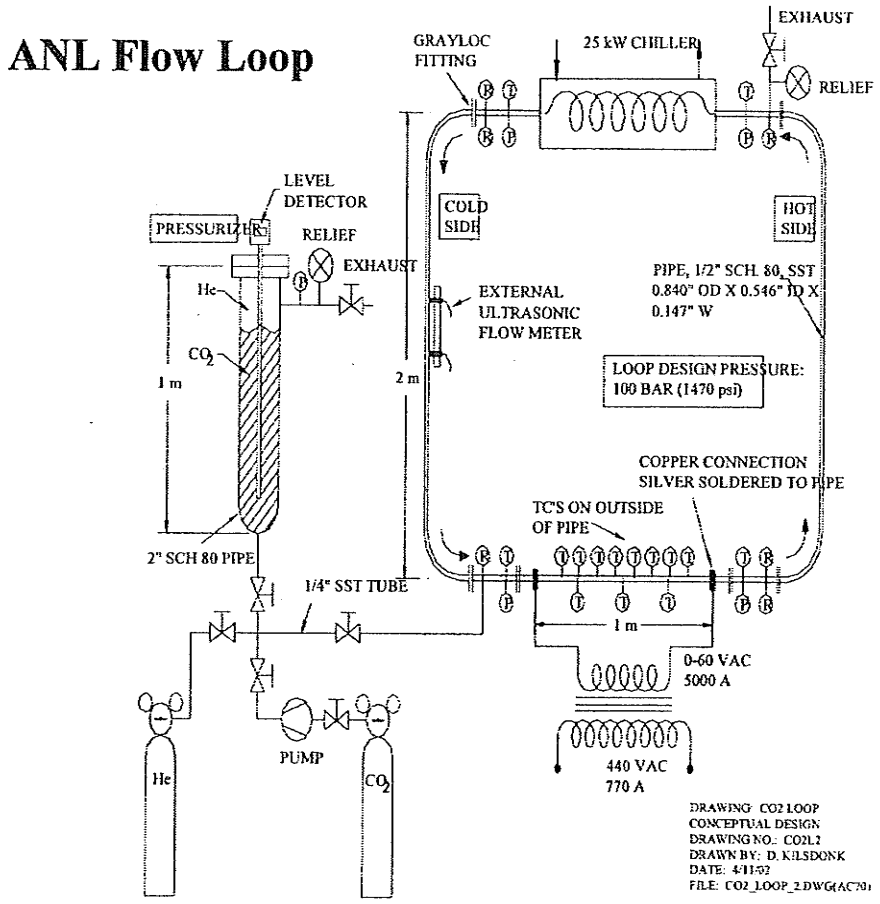

Figure 2.9: Schematic drawing of supercritical carbon dioxide loop (Jain, 2005).

Jain and Corradini (2005) conducted experiments in a rectangular natural circulation loop using carbon dioxide and water as working fluids, to verify stability margin suggested by previous investigators. A linear stability analysis was also conducted and which concluded the presence of instabilities. However, experimental results showed stable behavior.

Yoshikawa et al. (2005) developed a closed loop natural-circulation system for supercritical fluids that operates on the principle of density difference. They have also developed a technique to measure average CO_2 flow velocity in the circulation loop by using a chemical tracer and a UV absorbance optical cell. Their experimental setup finds use in fluid extraction, sample preparation and in precision cleaning techniques. Mignot et al. (2007) studied the behavior of supercritical fluid during a blowdown or depressurization processes.

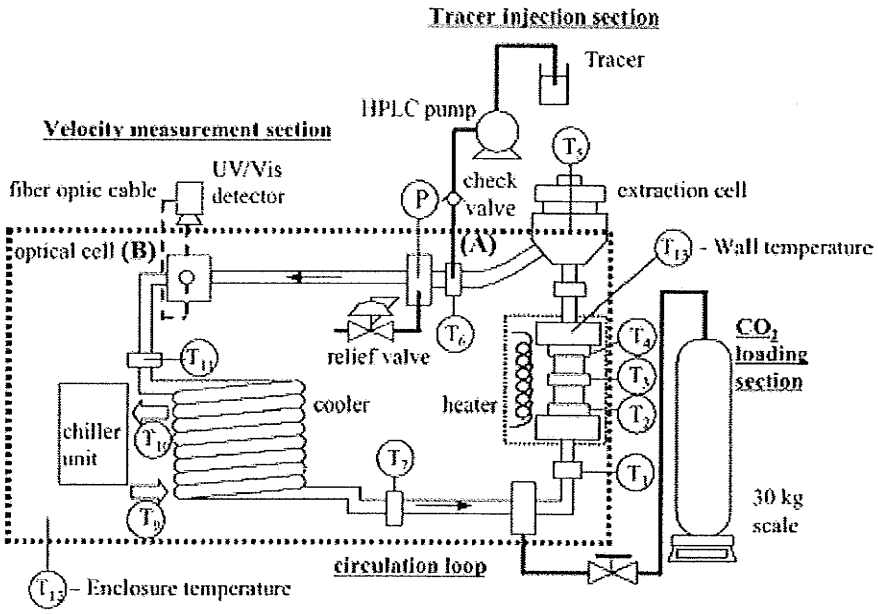

Figure 2.10: Natural convection supercritical circulation apparatus (Yoshikawa et al., 2005).

2.3 Review of Supercritical Fluids in New Generation Nuclear Reactors

Some of designers of new generation nuclear reactors have two design ideas in common. The first idea is to use supercritical fluid as a coolant and as a moderator in place of light water and second idea is to use natural convention as the mode of energy transfer to

eliminate the need for jet pumps, steam separators and other auxiliary systems (that come with two-phase fluid flow design).

Tom and Hauptmann (1979) conducted a feasibility study of cooling heavy water reactors (CANDU type reactors) with supercritical carbon dioxide. A new dual reheat cycle was proposed with an ideal overall plant efficiency of 33%. He also suggested that by using carbon dioxide there would be substantial economic advantage over heavy water. Yoshiaki and Koshizuka (1993) proposed a new concept and design of a supercritical pressure direct cycle light water reactor. The proposed reactor was aimed at increasing the thermal efficiency by 19% over the PWR. The SCLWR does not need a recirculation system, steam separators, dryers, thus simplifying the reactor design.

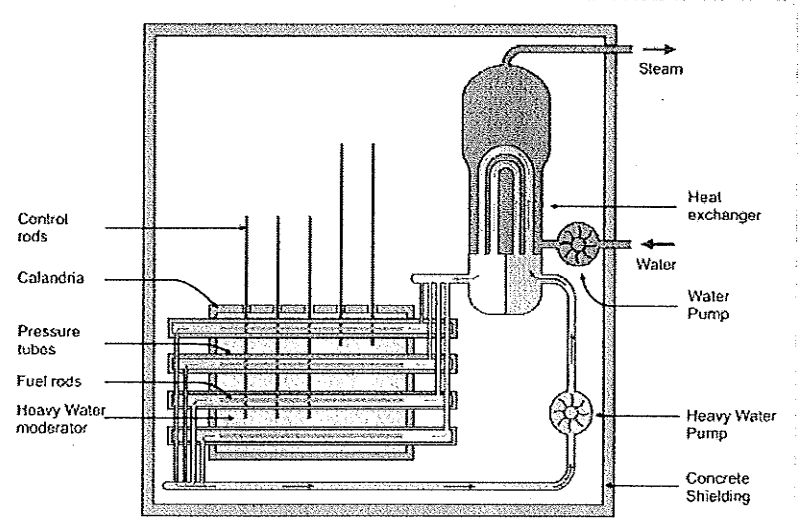

Figure 2.11: Schematic diagram of CANDU reactor (wikipedia.org).

In 1998, Dimmick et al. has also proposed an advanced CANDU reactor concept which would use supercritical steam as coolant. The conceptual reactor works at supercritical conditions and designed to eliminate problems (fuel-dryout and flow

instabilities) associated with two-phase flow fluids. This new reactor concept will have higher thermal efficiency and reduced coolant density. Driscoll et al. (2002) has proposed a gas cooled fast reactor (GFR) which uses supercritical carbon dioxide as a coolant at a pressure of about 19.8MPa.

Sienicki et al. (2003) analyzed and demonstrated the benefits of coupling the STAR-LM natural circulation lead reactor to a supercritical carbon dioxide Brayton cycle. By using a plant conceptual design analysis computer code they have calculated the cycle efficiency to be 44% and consists of fewer, simpler, and smaller-sized components that significantly reduce the footprint of the plant and offers the prospect of significantly reduced operating costs.

Khartabil (2003) has described how CANDU SCWCR is advantageous over the typical CANDU reactors. He described the features of CANDU SCWCR design that contribute to enhance passive safety of the reactor. By separating the high pressure coolant and low pressure moderator, the moderator can be used as an additional heat sink to supplement the emergency core cooling system during some postulated accidents. The second feature is advanced fuel channel design that allows the moderator to operate at much higher temperatures during normal reactor operating conditions.

Zhao et al. (2004) have studied one dimensional thermal hydraulic stability analysis of supercritical fluid cooled reactors (SCWR and GFR supercritical water reactor and Gas cooled fast reactor). His investigation aimed at studying possible occurrence of density-wave instabilities in both the reactors. The affect of orifice coefficient on the SCWR stability at operating power is also studied. He suggested that detailed 3-D studies with neutronic feedback, be carried out for SCWR design because of its sensitivity to

various important parameters. For the gas cooled fast reactor considered in the paper, he concluded that the coolant density change is not large and is comparable to that in a PWR. The rector design should have no flow instabilities at full power normal operating conditions. Zhao et al. (2005) has performed a stability analysis of a supercritical water-cooled reactor during steady-state and sliding pressure start up.

CHAPTER 3

PROJECT MANAGEMENT

3.1 Background

Earlier project coordinators of University of Manitoba's supercritical flow experimental facility had procured some of the major components required for the construction of the experimental facility. The materials procured include piping, accumulator, pressure control system, chiller, heat removal control system, heat exchanger and electro-pneumatic valves. The test section was designed and constructed by Stern Laboratories. Stern Laboratories has provided us with the initial design drawings of the experimental facility.

3.2 Project Implementation

During the implementation of the project, various difficulties were encountered and were resolved during the project. Some of the difficulties overcome during the project were those with the amenities in the laboratory space, power supply, technical support and budgeting constrains of the project.

Earlier in February 2004, laboratory space was allotted for the purpose of constructing the experimental facility. However, the laboratory space needed major renovation works before the experimental facility could be constructed. Air conditioning, heating, fire extinguishers, power supply, carbon dioxide and carbon monoxide gas detectors were some of the amenities provided to the laboratory after meetings and frequent follow up with the physical plant department of the University of Manitoba.

Construction of the experimental facility started only after finding a certified high-pressure stainless steel welder which took place under the supervision of the author.

The electrical wiring provided for the purpose of the experimental facility in the laboratory space was different from the actual requirements and so an external electrical contractor was hired through the physical plant department of the University of Manitoba. Electrical contractors took more than ten months to complete the electrical power requirements in the laboratory space. Their work includes providing proper electrical terminals for chiller, air compressor, wiring for AC-DC rectifier and wiring between breaker circuit and heated channels of the test section.

The experimental facility operates under high-pressure conditions and support from technicians was necessary for conducting various preliminary tests. However, because of other constrains, technicianl support was not available to the extent that was required. On an average technical support of 10 to 15 hours per week was only provided towards the construction of the experimental facility.

The air-cooled chiller for the experimental facility was installed by authorized personnel as per the provincial government regulations. Flexible ducting was also provided from the chiller exhaust duct to dissipate the heat from the air-cooled chiller.

Considerable amount of time and afford was contributed by the author towards obtaining quotations for various products and services, follow up with various companies regarding delivery of material, understanding the working principles of various components of the experimental facility, organizing meeting with department officials and company representatives to advise on various components used. A brief list of the components purchased by the author is provided in the Appendix A. Author has

organized with various trades personnel (welding, ducting, cleaning, electrical etc.,) inorder to obtain specific tasks with regard to the experimental facility.

Author was also involved in budgeting and financial issues of the project. Processing purchase requisitions and follows up with the financial services of University of Manitoba, with regard to the purchase orders were performed constantly during this project. Occasionally attended meeting with officials at purchasing department to clarify issues relating to purchases and budget accounts.

A safety shield was designed and constructed out of steel frames and polycarbonate sheets to protect against accidental rupture/explosion of the experimental facility during experiments. Apart from acting as a protective shield, the safety shield supported major instrumentation for the experimental facility.

Author has contributed equal amount of time and afford as with the technicians in constructing the safety shield and during other preliminary tests performed on the experimental facility. Swagelok compression fittings were used extensively in the construction of the experimental facility and hence, the author took Swagelok installation training for better understanding of these compression fittings.

3.3 Project Management

This work mainly involved project management and design of the supercritical flow experimental facility. Some of the specific tasks performed as part of work were:

- Designed and prepared necessary drawings for the construction of experimental facility. Some of the major design tasks performed includes, support structure for assembling electro-pneumatic valves, purging and evacuation system, inlet

settling chamber, pneumatic supply to electro-pneumatic valves and gas booster, supply gas connections to accumulator and carbon dioxide gas supply system.

- Prepared bill of materials and obtained quotations for various required materials and services. (Some of the external services obtained to complete construction of the experimental facility were stainless steel welding, chiller installation, chiller exhaust ducting, power supply installation, chemical cleaning, pressure testing and Swagelok fittings installations).
- Obtained approvals and processed purchase orders through the university financial services.
- Communicated with suppliers to schedule the shipment of materials and obtained relevant documentation (milltest reports, M.S.D.S, certificates etc.,) for various materials purchased.
- Planned and scheduled various tasks involving technicians, contractors, and trades personnel to complete construction of the experimental facility
- Organized meetings with various departmental people, technicians and with supervisor regarding construction of the experimental facility.
- Scheduled and organized meetings with technicians and with representatives/officers involved in the construction of the experimental facility.
- Prepared progress reports and budget estimates with regard to the project.
- Prepared necessary documentation for the experimental facility including necessary operational manuals, certificates, catalogues and reports (milltest reports, certificates, MSDS etc.,)

CHAPTER 4

EXPERIMENTAL FACILITY

In view of the decision to build a supercritical water reactor in Canada, construction of a supercritical flow experimental facility was initiated at the University of Manitoba to understand the behavior of supercritical flow. The experimental facility designed for supercritical carbon dioxide and supercritical water experiments is a simple rectangular natural circulation loop with three heated horizontal parallel channels. Experimental facility was initially designed for supercritical water experiments but because of budgetary constrains, facility was then designed and constructed for carbon dioxide (working fluid) experiments. By replacing few components (refer section 4.14) of the experimental facility, the facility can be employed to use for supercritical water experiments.

4.0 Supercritical Flow Experimental Facility

The various systems involved in the supercritical flow test facility are as follows:

1. Loop piping
2. Test Section
3. Heat Removal Control System
4. Pressure Control System
5. Inlet Assembly
6. Evacuation System
7. Carbon dioxide Supply

8. Electro-Pneumatic Valves
9. Data Acquisition System and Instrumentation
10. Power Supply
11. Support Structure
12. Safety Features
13. Miscellaneous Devices

4.1 Loop Piping

The experimental facility (loop) design, sizing of the test section and piping were deduced from SPORTS code simulations[1] and other considerations. With few modifications (section 4.14) to the present experimental facility, the facility can be employed for water (working fluid, critical pressure: 22.06 MPa, critical temperature: 373.95 °C) experiments. Presently the experimental facility is designed and constructed to operate with supercritical carbon dioxide (critical pressure: 7.37 MPa, critical temperature: 30.98 °C). Except for a few components of the present experimental facility, the entire loop is designed to withstand 400 °C temperature and 24.13 MPa pressure. Piping made of 31.75 mm XXH stainless steel 316L pipe with dimensions of 42.16 mm O.D. and 22.61mm I.D was used in construction of the facility. Stainless steel 316L elbow joints with 90° are used on the corners of the experimental facility. Stainless steel flanges (XXH, 31.75mm size) were used to join various components of the loop, making it easy to dismantle when required.

[1] Bo Huang, "Calculation of heat flux and bounding power for single-channel loop" September 2002, Internal Report, Mechanical and Manufacturing Department, University of Manitoba.

The experimental facility has an overall flow path length of 16.5 m and a volume of 0.0785 cubic meters. Flexitalic gaskets of 31.75 mm size are used between the stainless steel flanges in order to make the facility pressure tight and leak proof. The ASME Code Section VIII Division 1 was used for calculating the torque required to load the flanges and to maintain the required pressure rating (calculations provided in the Appendix A). A typical flange and gasket assembly is shown in Figure 4.1. A certified high pressure stainless steel welder was hired to perform the welding of the experimental facility. To minimize the heat loss from the piping, the entire loop will be insulated with M Board® insulation sheets. Brief operating instructions of the experimental facility are provided in Appendix A.

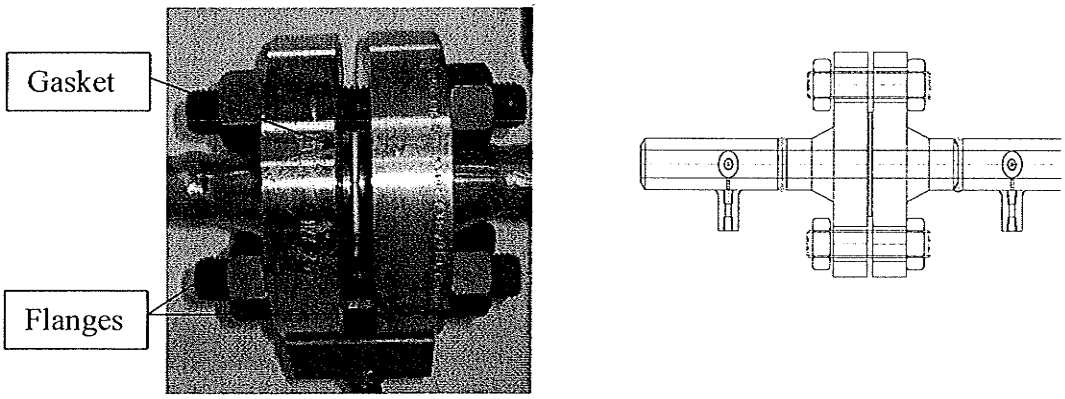

Figure 4.1: Typical flange and gasket assembly.

4.2 Test Section

The horizontal test section was designed and fabricated by Stern Laboratories in accordance with ASME Code[2], with 398.89 °C (750 °F) and 24.13 MPa (3500 psig) as

[2]ASME B31.1- 2001 Edition, Power Piping.

the design temperature and pressure. The test section consists of three Inconel-625 tubes (19.05 mm I.D. and 12.9 mm thick); each tube is of 2.5 m long. Inconel-625 tube was chosen because of its good electrical and thermal conducting properties. These three channels are connected to a common inlet and common outlet headers (316 SS XXH pipe with 58.42 mm I.D) by means of Swagelok® fittings[3], gasket and flange joints. The distance between these two headers is 4.647m. The headers have internal flow dispensers, to help ensure that the flow is evenly distributed between the three channels. Insulating gaskets (0.3175 mm thick phenolic sheet) between the flanges and insulating sleeves (25.4 mm glass filled teflon) around the connecting bolts are employed to electrically isolate the test section from the rest of the facility. Detailed drawings of the test section and its associated components are provided in Appendix C. The detailed schematic drawing of the test section and header assembly is shown in Figure 4.2.

An electro-pneumatic valve (31.5 mm size) was assembled before the inlet header and after the outlet header. Electro-pneumatic valves of the size 19.05 mm are assembled at the inlet and outlet of the three channels. Each electro-pneumatic valve assembly consists of a valve, pneumatically controlled actuator and a position controlling transducer. Complete details of the electro-pneumatic valves are provided in section 4.8. Swagelok® compression fittings were used in connecting these valves to the header and channel assembly. On the downstream side of the three channels, a rupture disk assembly is provided as a safety feature. This is discussed in detail in section 4.12.1.

The fluid passing through the channels is heated by means of direct electric current through the channels. The test section is rested on support stands situated on the

[3]Guidelines from Swagelok Tube Fitter's Manual are followed in assembling the Swagelok fittings.

concrete floor. The top of the support stands are covered with insulating material to prevent any DC current flowing through the support structure. The test section was hydrostatically pressure tested by Stern Laboratories to a pressure of 37.23 MPa at room temperature. Later, the test section was assembled for supercritical carbon dioxide experiments and was hydrostatically pressure tested at 15.85 MPa. A schematic drawing of the supercritical flow experimental facility is shown in Figure 4.3. Figure 4.4 shows the actual supercritical flow test facility assembled in the laboratory (more pictures of the experimental facility are provided in Appendix A).

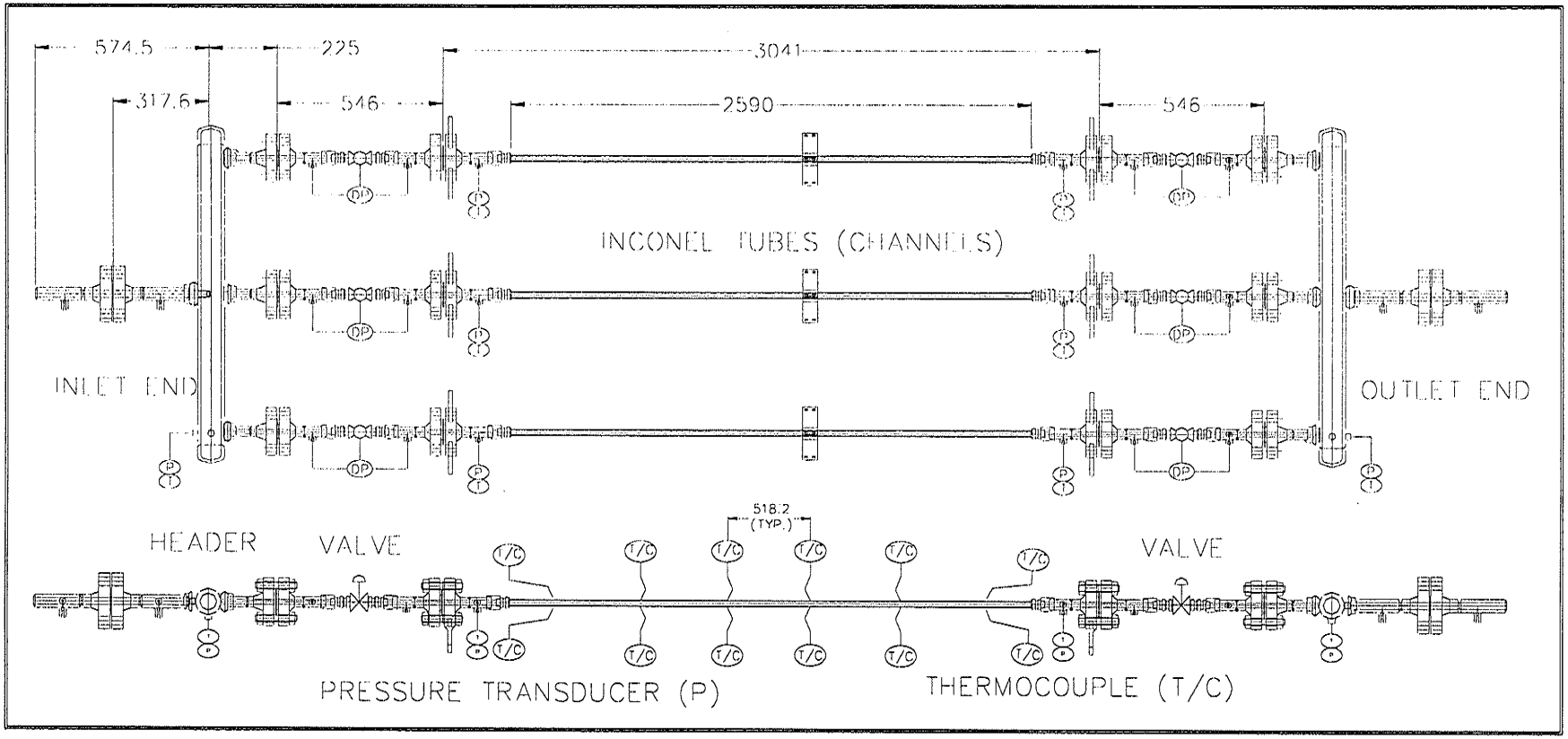

Figure 4.2: Test section of supercritical flow experimental facility.

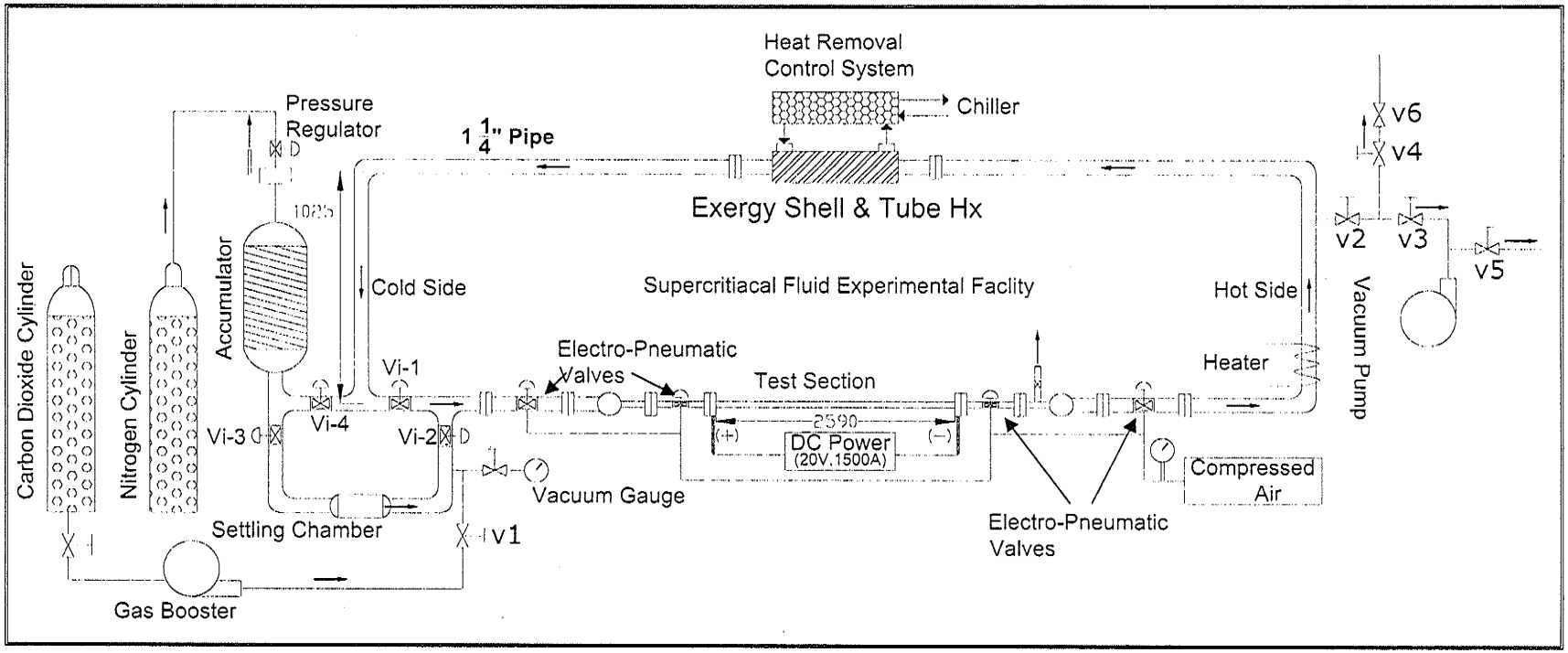

Figure 4.3: Schematic drawing of supercritical flow experimental facility.

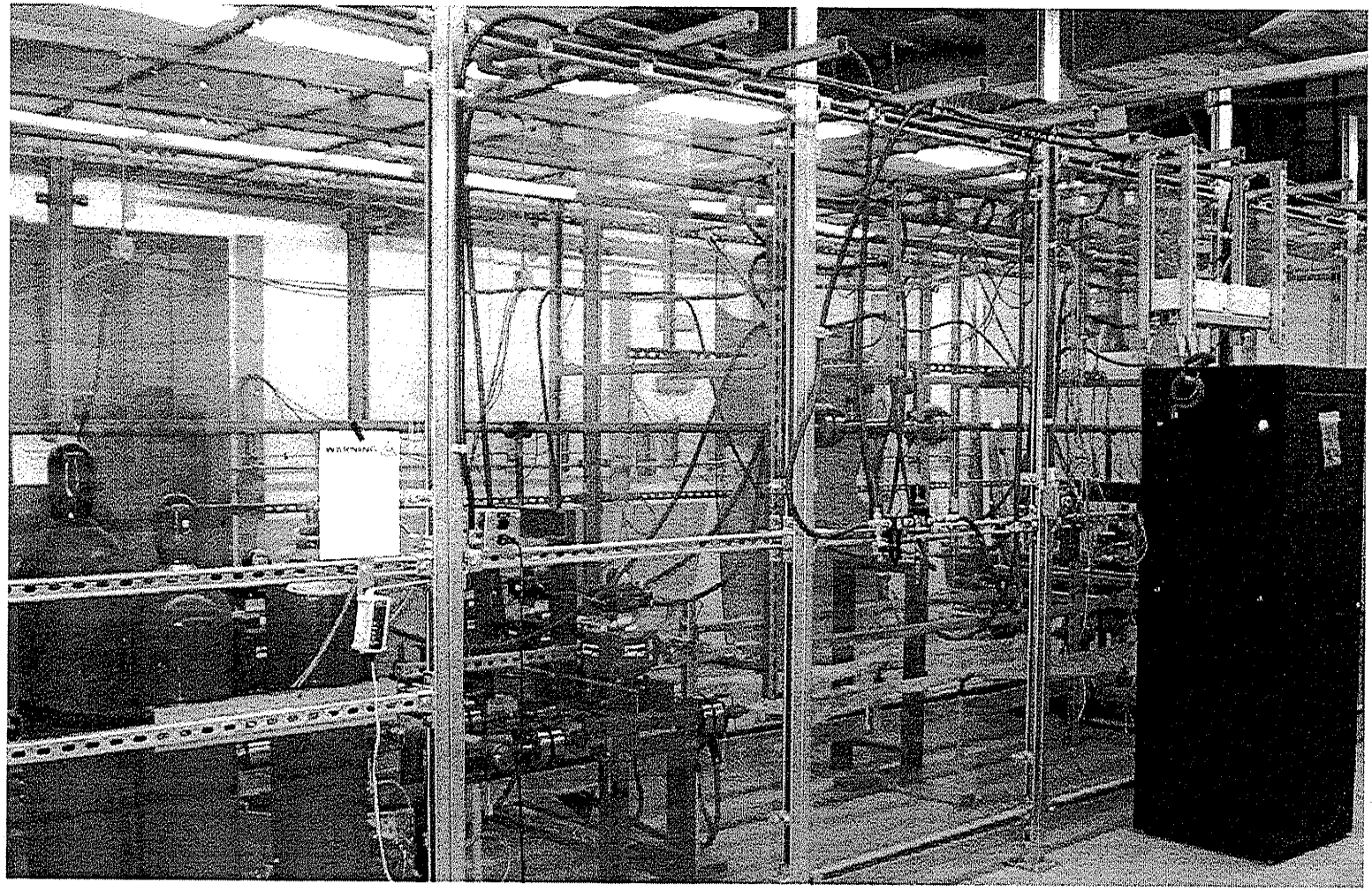

Figure 4.4: Supercritical flow experimental facility.

4.3 Heat Removal Control System

To remove a constant amount of heat from the working fluid, a control system which includes a shell and tube heat exchanger and a chiller was designed. The control system, which was designed by International Cooling Systems (ICS), regulates the amount of heat to be removed from the test facility (by means of heat exchanger) at any given time. The heat removal control system was assembled as per the ICS design; operating and maintenance instructions can be found in their respective documents[4]. Figure 4.5 shows the schematic drawing of the heat removal control system.

4.3.1 Shell and Tube Heat Exchanger

An Exergy® 54 series shell and tube miniature heat exchanger was chosen for carbon dioxide experiments. This heat exchanger consists of 127 stainless steel tubes (3.2mm OD, 0.32mm thick) and is rated for 16.54 MPa on tube side (and 9.65 MPa on shell side). The heat exchanger is having a cross sectional area of $6.5369 \times 10^{-4} m^2$ and a K factor[5] of 5.97. The heat exchanger was custom manufactured with 31.75 mm size stainless steel stubs at the ends. These stubs were welded to stainless steel flanges and were assembled to the facility by means of flexitalic gaskets and mating flanges. Figure 4.3 shows a schematic drawing of the supercritical flow experimental facility with the heat exchanger assembled on top of the facility. A detailed schematic drawing of the shell and tube heat exchanger is provided in Figure 4.6. When conducting experiments using supercritical water (critical pressure: 22.1 MPa, critical temperature: 374.1 ^{o}C), the temperature

[4] a) International Cooling Systems manual for air cooled package unit.
b) International Cooling Systems manual for heat removal system.
c) Supercritical flow experimental facility manual.

[5] Heat exchanger K factor calculations are provided in Appendix B.

difference across the heat exchanger is high ($\Delta T \approx 150\ ^{o}C$) hence the present heat exchanger would not be suitable. A different heat exchanger would need to be designed for this purpose.

4.3.2 Chiller

International Cooling Systems® Indoor air cooled chiller capable of removing up to 25 kW of heat energy is coupled with the shell and tube heat exchanger. The chiller has optional settings of either working with water or with a glycol and water mixture. Chiller water outlet temperature can be controlled by adjusting the thermostat and can supply water at $5^{o}C$ (minimum temperature when using water). This chiller water outlet temperature can be reduced further below $5\ ^{o}C$ by using a glycol and water mixture. Flexible ducting is provided to carry away hot air from the chiller exhaust.

4.3.3 Control System

The programmable control system (PLC) supplied by International Cooling Systems uses a three-way diverting valve to control the heat load that has to be removed via the heat exchanger. Thermocouples measure the inlet and outlet temperatures of the chilled water entering and leaving the heat exchanger. With these measured temperatures and with a inbuilt program, the control system regulates the three-way valve. Thus a constant amount of heat is removed from the supercritical fluid via the shell and tube heat exchanger.

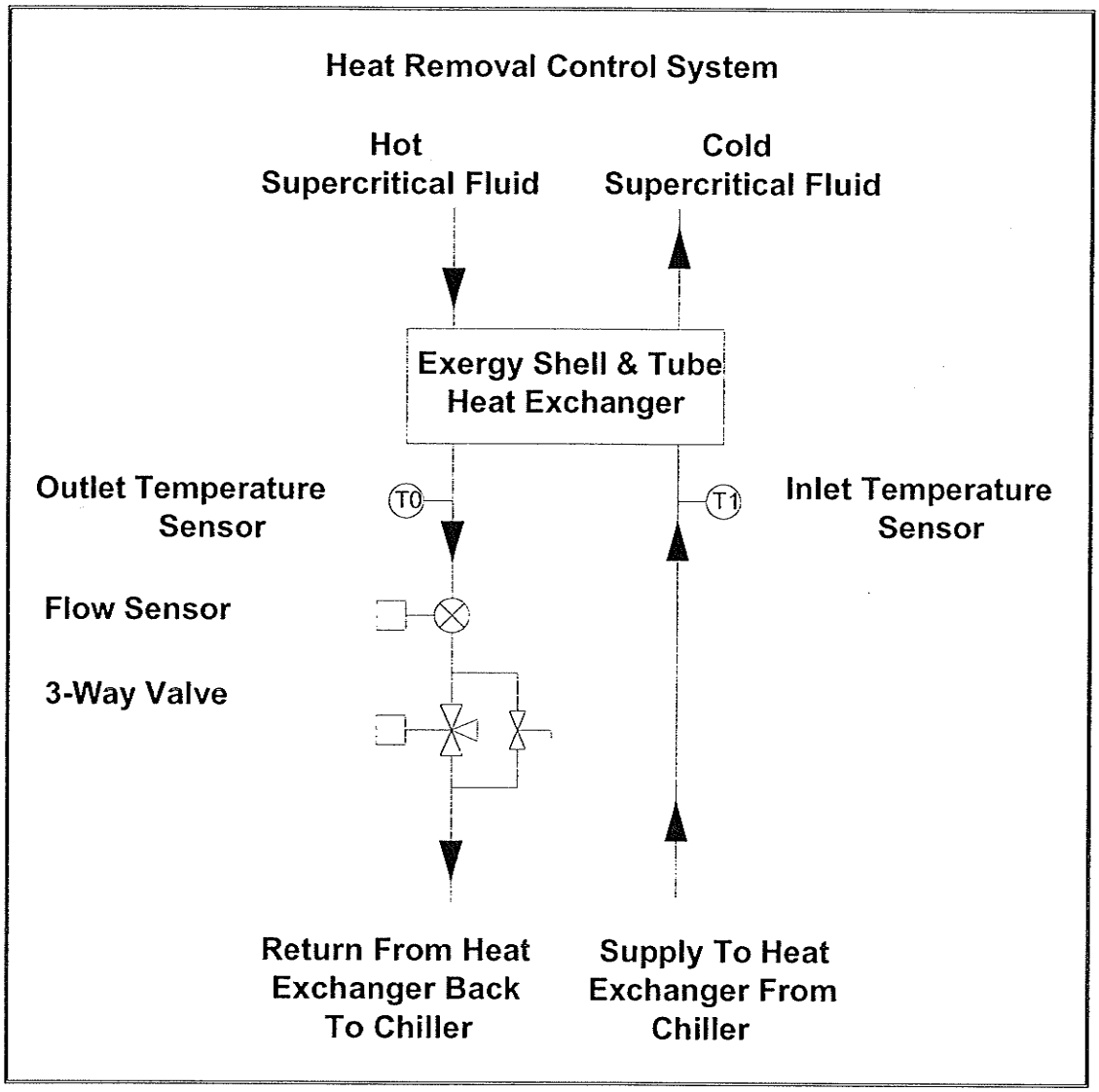

Figure 4.5: Schematic drawing of heat removal control system.

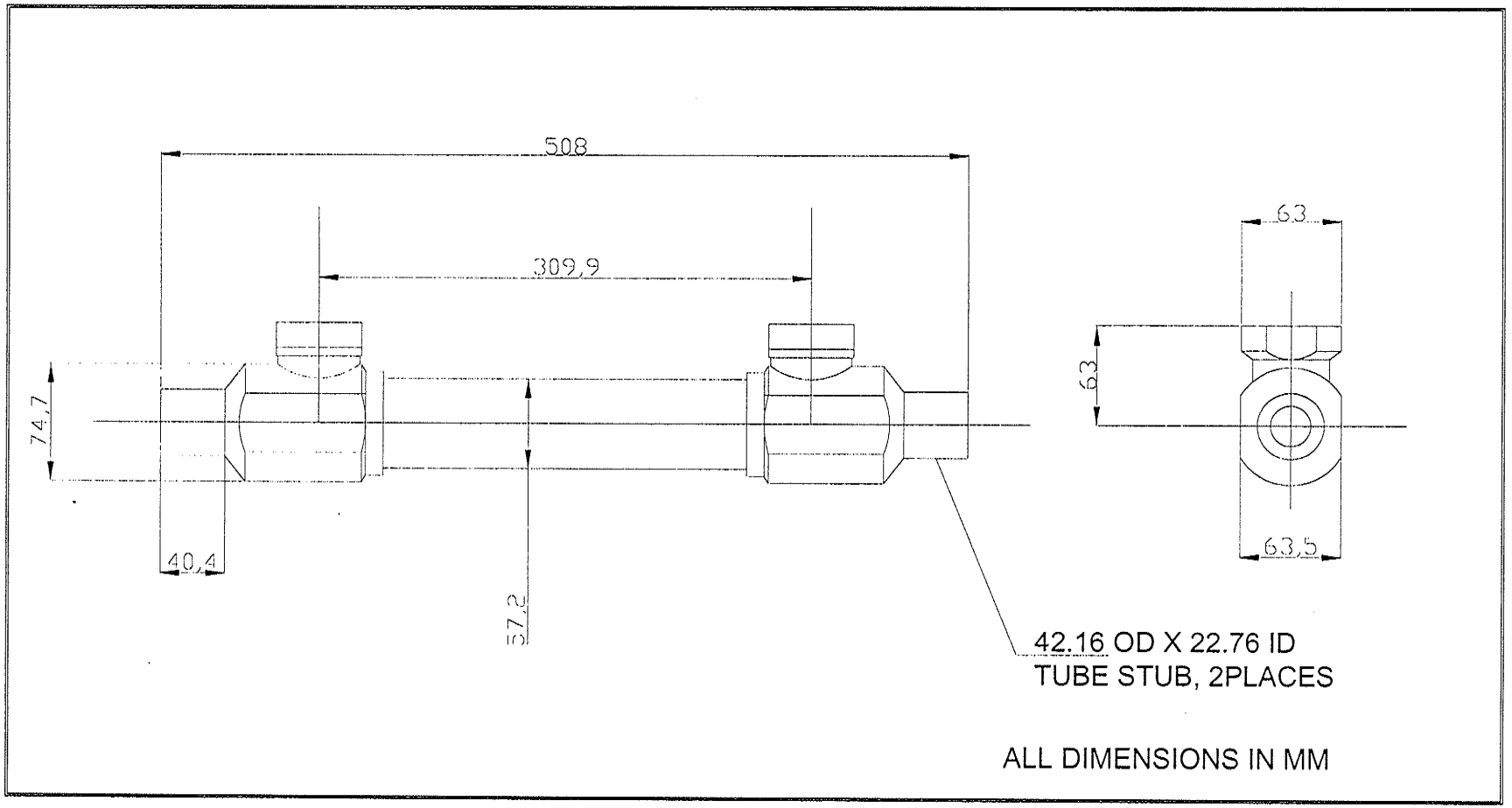

Figure 4.6: Schematic drawing of shell and tube heat exchanger.

4.4 Pressure Control System

A pressure control system was designed to regulate the pressure inside the experimental facility. The system consists of a single stage pressure regulator (PR-57 series, GO Regulator®) connected to a nitrogen gas bottle and to a accumulator (Hydac bladder accumulator).

A precision pressure regulator was installed on the accumulator. This can safely maintain inlet pressures up to 68.94 MPa and has a flow coefficient of 0.05. The regulator can be adjusted to have an outlet pressure in the range of 0 to 27.57 MPa. Figure 4.7 shows the schematic drawing of the pressure regulator. A grade 4.0 nitrogen gas cylinder (T style) at 13.79 MPa pressure, supplied by Praxair® was connected to the regulator which, in turn, was assembled to the accumulator. Nitrogen cylinders come with CGA-580 connections and are suitable for connecting with the pressure regulator through a flexible hose (high pressure flexible metal hose braided with stainless steel, 28.26 MPa working pressure). Depending on the usage, nitrogen cylinders can be ganged together by means of a manifold, or a different nitrogen gas bottle can be used (Style 4K nitrogen gas cylinder by Praxair has twice the capacity of T style nitrogen cylinder). Figure 4.8 shows the pressure control system as assembled in the supercritical flow experimental facility.

The bladder accumulator (11.0Lts, Hydac®) consists of a fluid section (working fluid) and a gas (nitrogen gas) section where the bladder acts as a gas-proof screen in the accumulator. The fluid around the bladder is connected with the fluid in the loop. When the pressure inside the experimental facility drops below a set limit, the compressed gas expands and forces the stored fluid into the loop. The pressure regulator helps to maintain a predetermined set pressure. Excess nitrogen gas from the pressure regulator is released

into atmosphere. Swagelok pre-swaged fittings were used in assembling the accumulator to the experimental facility.

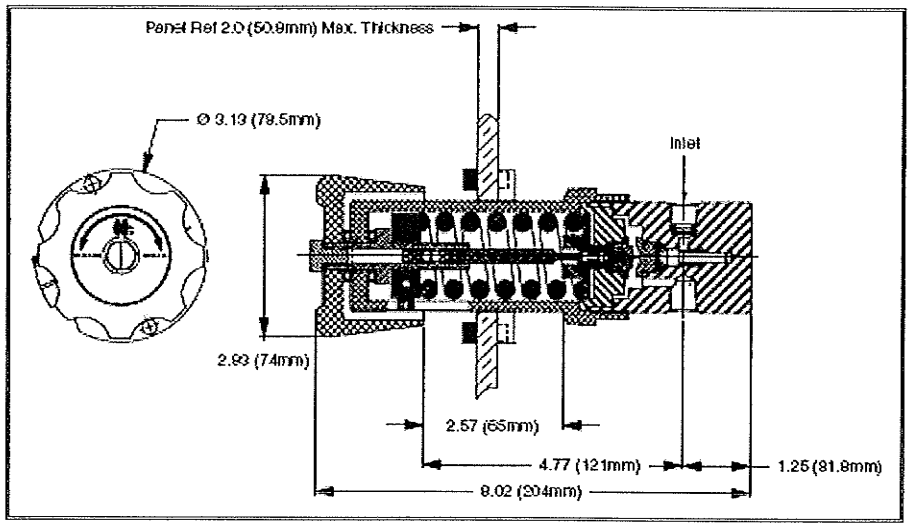

Figure 4.7: Schematic drawing of pressure regulator.

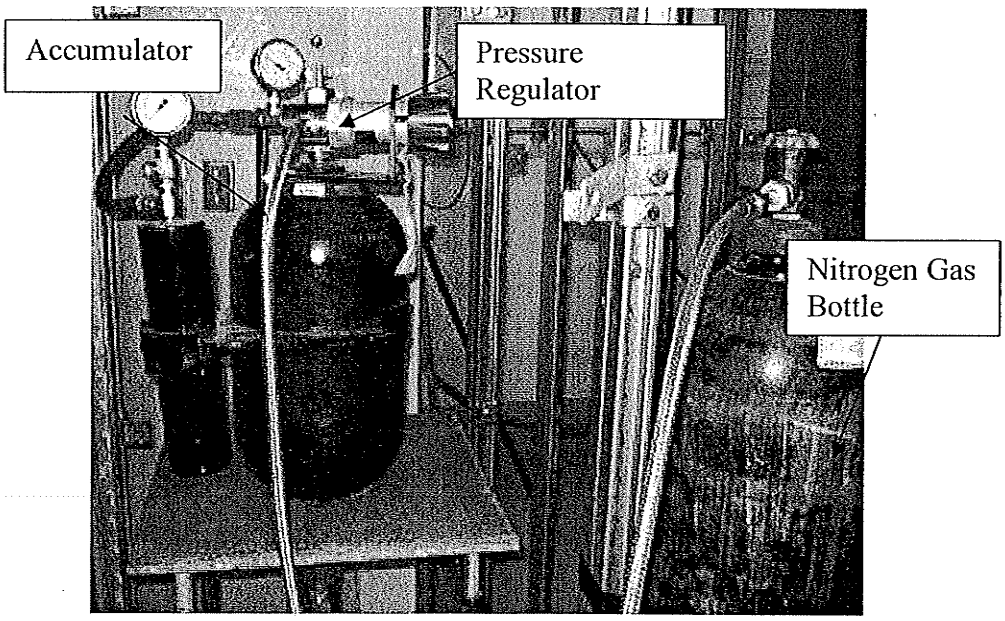

Figure 4.8: Pressure control system.

4.5 Inlet Assembly

The inlet assembly mainly comprises of the settling chamber, ball valves and piping. A schematic drawing of the inlet assembly is shown in Figure 4.11.

4.5.1 Settling Chamber

A gas bottle supplied by Parker® was chosen as a settling chamber, it is intended to reduce temperature fluctuations at the inlet. This settling chamber is a certified cylindrical vessel made out of carbon steel with a total internal volume of 56 liters (approximately three times the volume of the entire loop) and designed to withstand 20.68 MPa pressure at 93.33 °C. This settling chamber was coupled to the experimental facility by means of code 62-O' ring head adapter fittings as shown in Figure 4.9.

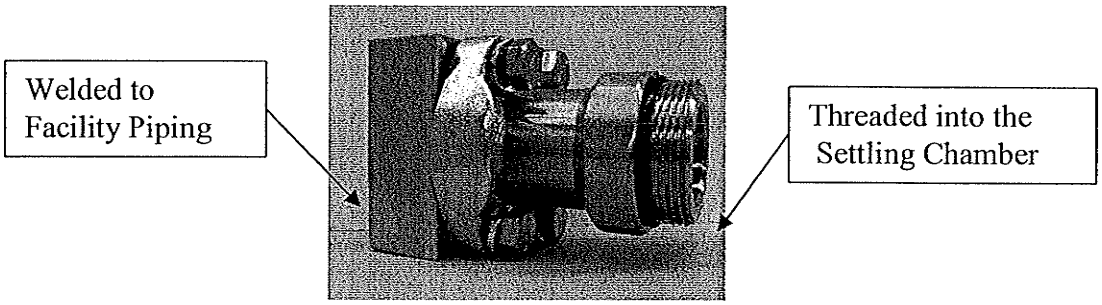

Figure 4.9: Code 62- O' ring adapter fittings.

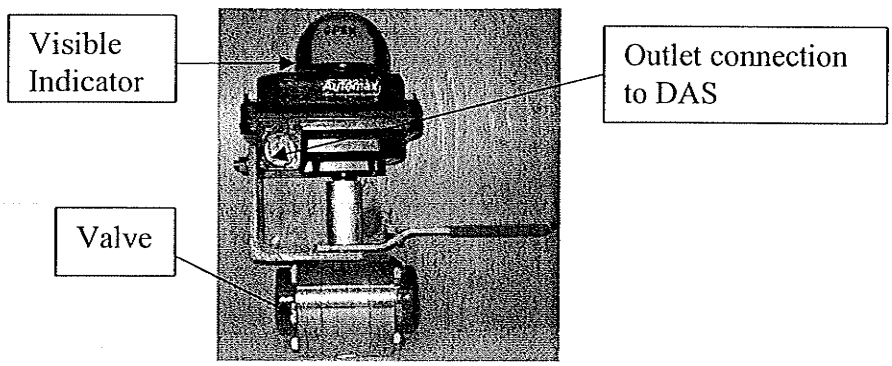

Figure 4.10: Flow regulating ball valves (On/Off type).

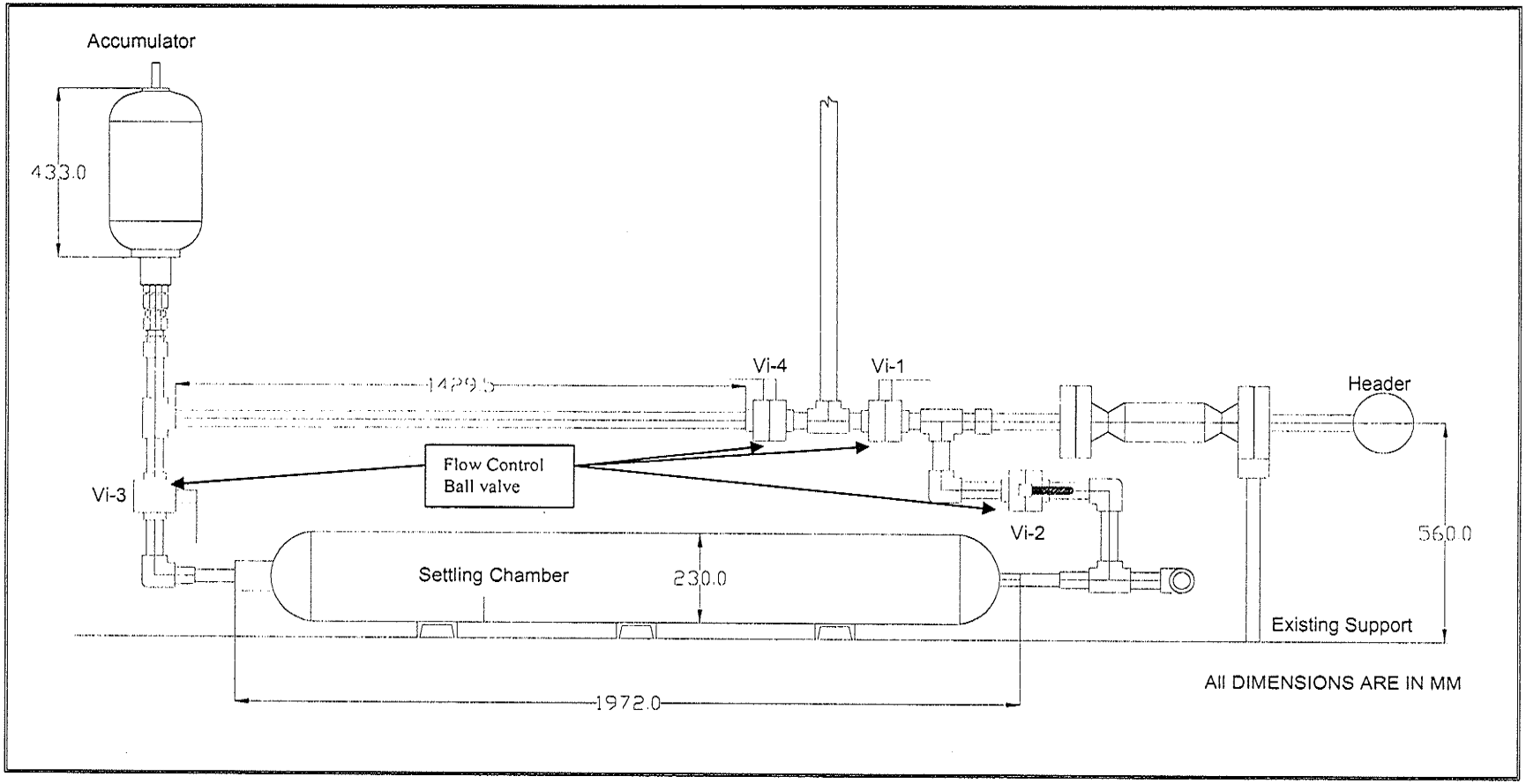

Figure 4.11: Schematic drawing showing the settling chamber assembly.

4.5.2 Flow Control Valves

Four H27 series Habonim® ball valves[6] (Vi-1, Vi-2, Vi-3 and Vi-4) were welded[7] to the loop as show in the Figures 4.10 and 4.11. These valves are provided with limit switches and visible indicators (red for closed and green for open), status of these valves is monitored by the data acquisition system. By controlling these valves various flow configurations can be obtained during experiments.

a) Zero Loop Configuration: In this configuration, valves Vi-4, Vi-2 are in the closed position and Vi-1 is in open position, thus eliminating the accumulator from the experiment.

b) Non-Zero Loop Configuration with settling chamber: In this configuration, valves Vi-1 is in closed condition and valves Vi-2, Vi-3 and Vi-4 are in open position.

c) Non-zero Loop Configuration without settling chamber: In this configuration, valves Vi-1, Vi-4 are in open position and valves Vi-2, Vi-3 are in the closed position.

4.6 Evacuation System

The experimental facility was designed to permit purging and evacuation procedures. The test facility was chemically cleaned and purged with working fluid (carbon dioxide) and evacuated to eliminate impurities (air) from the loop. A detailed description of the purging and evacuation procedures is discussed in section 5.3. A vacuum pump (RB series, Busch®) capable of achieving 29.8 inHg vacuum was selected for this purpose. Stainless steel tubing and compression fittings were used in purging system design.

---

[6]For operation and maintenance instructions refer to a) H27 Series High Pressure Ball Valves, bulletin A-106, b) Flowserve®, Automax® valve automation systems, Installation, operation and maintenance instructions.

[7]Habonim® valves are welded as per guidelines given in "HABONIM Welding Instructions of valve to pipe line".

Figure 4.12 shows the schematic drawing of the purging and evacuation scheme. (Stainless steel is the primary construction material for vacuum systems, particularly for ultra high vacuum systems, owing to its low permeability to hydrogen, resistance to corrosion and ease of breakout).

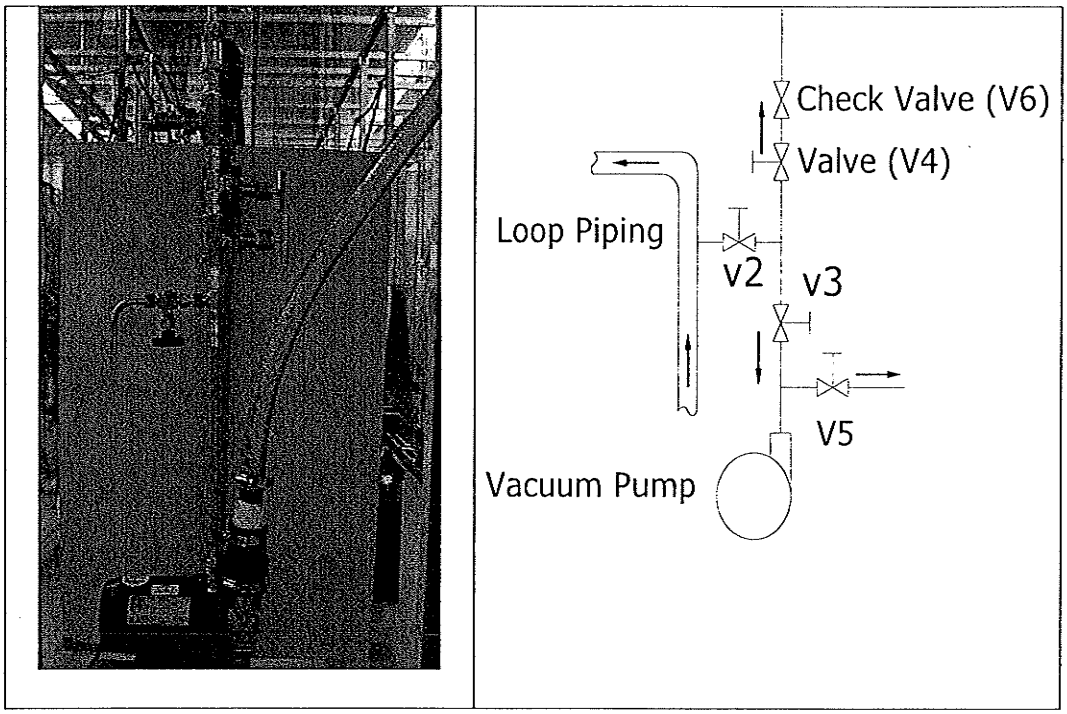

Figure 4.12: Schematic drawing of the purging and evacuation system.

4.7 Carbon dioxide Supply

Standard commercial carbon dioxide cylinders are available at 5.86 MPa pressure but they are not suitable to build up the required pressure (max.10 MPa) inside the experimental facility. Hence, these gas cylinders cannot be used directly to pressurize the loop. To attain the required carbon dioxide pressure in the loop, a gas booster was selected. The gas booster will raise the pressure of the carbon dioxide gas from the cylinder to 10 MPa pressure inside the experimental facility.

4.7.1 Carbon dioxide Gas

Grade 4.0 carbon dioxide supplied by Praxair® was used in filling the loop to the required pressure after repeated purging and evacuation procedures (detailed instructions of pressurizing the facility with carbon dioxide is provided in Appendix A). Instrument grade carbon dioxide which is of 99.99% pure contains less than 15 ppm of oxygen and less than 10 ppm of water (other grades including CD 5.0SE – 99.999 %, CD 4.8SC – 99.998%, CD 4.8RS – 99.998%). Some researchers have conducted similar experiments using carbon dioxide whose purity range lies between 95 % and 99.98 % (Pioro and Duffy, 2003). Using Praxair carbon dioxide grade 4.0, which is of 99.99% pure, will give relatively good results even if there are traces of impurity left behind after the chemical cleaning of the experimental facility. The carbon dioxide cylinders are supplied with standard CGA 320 connections and are stored as per safety regulations in the laboratory.

4.7.2 Gas Booster

A Maxpro® gas booster is an excellent alternative to using a high pressure stationary compressor. The gas booster was chosen for building the required pressure inside the experimental facility. The single acting, single stage gas booster has a compression ratio of 20:1 and is capable of generating up to a maximum pressure of 31.30 MPa. This lightweight gas booster (DLE30-1) requires compressed air to boost the pressure of the carbon dioxide. The gas booster works with compressed air at 620.52 kPa at 16cfm flow rate. Figure 4.13 shows the schematic drawing of the pneumatic connections for the gas booster. The gas booster is connected to the standard gas cylinder using stainless steel braided flexible hose and Swagelok fittings.

In the case of experiments using water as the working fluid, the gas supply connections (flexible hose, gas cylinder) can be removed completely from the loop. The Swagelok connection (Figure 5.1) can be closed using a Swagelok plug. As liquid water is essentially incompressible, the loop can be completely filled with water and when it is heated in the test section, the required supercritical pressure can be obtained.

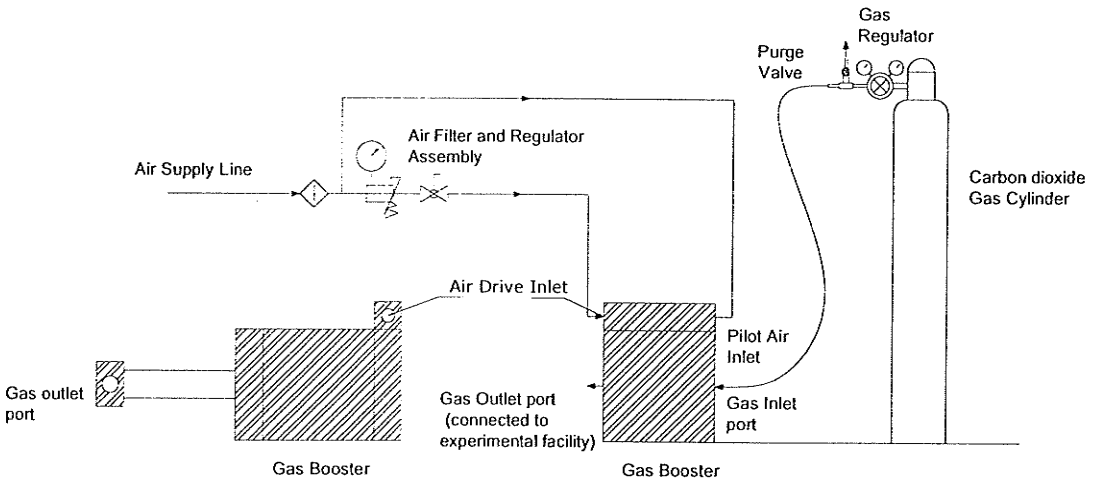

Figure 4.13: Schematic diagram of gas booster and carbon dioxide cylinder assembly.

4.8 Electro-Pneumatic Valves

Eight electro-pneumatic valves were assembled on the experimental facility as shown in the Figure 4.3 and Figure 4.4. Two electro-pneumatic valves (31.5 mm size) were installed on the facility; one is located upstream of the inlet header, while the other was located downstream of the outlet header. These two electro-pneumatic valves are intended to regulate the flow in the loop. Six electro-pneumatic valves (19 mm size) were installed upstream and downstream of the three channels, between the inlet and outlet headers. These six valves are to be used to control the pressure drop of each channel and there by altering each channels stability characteristic of the system.

Each of these electro-pneumatic valve assemblies consists of a valve (Jarecki®), an actuator (Habonim®) and a position controlling transducer (Flowserve®), which are discussed in detail below.

4.8.1 Valve and Actuator Assembly

The Jerecki® valves along with the Habonim® actuators are the main components of the electro-pneumatic valves, which are shown in Figure 4.14. The actuator transforms the linear motion of its pneumatic pistons into rotary motion via gear and racks that than drive the central pinion. The actuator receives its pneumatic signal from the transducer assembly on top of it. Table 4.1 presents the C_v values for corresponding percentage opening of valves.

Table 4.1: C_v values for corresponding percentage opening of electro-pneumatic valves.

Valve Percentage Opening (%)	0	10	20	30	40	50	60	70	80	90	100
C_v	0	0.21	0.43	0.70	1.05	1.62	2.64	4.00	6.40	9.60	12

Restriction coefficient (K) can be calculated from equation $K = 894 \times (D^2 / C_v)^2$

Where C_v is valve flow coefficient in gpm/psi differential and

D is diameter of the valve in inches.

4.8.2 Transducer / Positioner

The Apex® 5000 transducers were used to rotate the valve actuators in proportion to a given input signal. The input signal is a pneumatic supply at a pressure of 689 kPa (100 psi) and an electric signal (4 to 20 mA). The supply pressure is directed to the actuator through a precision spool valve. The transducer and actuator assembly is calibrated for the 4 -20 mA input signal. With a pneumatic input signal of 690 kPa (100 psi) and a 4mA signal, the valve is completely closed; and for an input signal of 690 kPa (100 psi) supply pressure and a 20mA signal, the valve is completely open.

Supply air pressure to the valves must be limited to 817.37 KPa (120 psi) and the electrical signal to 4 to 20 mA of input transducer signal to control these valves. The supply air should be clean, dry, and oil free, and of instrument quality in accordance with ISA S7.3 specifications (dew point less than 18 degrees below ambient temperature, particle size less than 5 microns, oil content less than 1ppm). These valves are also provided with visible indicators a red colour for closed and a green colour for open. This feature is useful for local position determination.

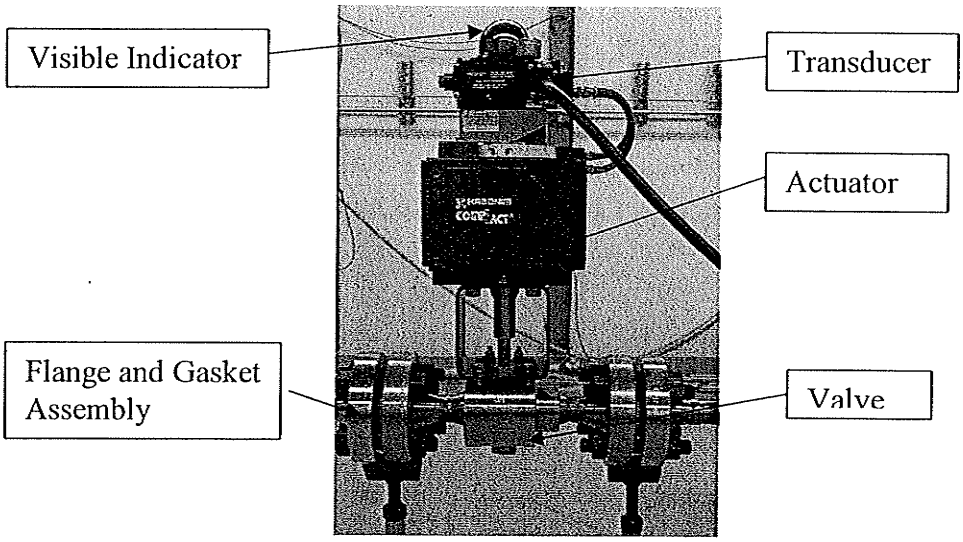

Figure 4.14: Electro-pneumatic valve.

4.8.3 Pneumatic Supply

A single cylinder air compressor (Princess Auto®) with a 60-gallon capacity, ASME certified, was chosen for the purpose of operating the electro-pneumatic valves and the gas booster. The vertical automatic cut-off air compressor is rated for 5 HP and can supply compressed air at 18.5 cfm at 689.47 MPa supply air pressure. A pressure switch available with the compressor can be varied from 790 kPa to 960 kPa. The switch is currently set at 960 kPa cut-off pressure.

A pneumatic distribution system was designed with a coalescing filter and flow regulator to meet the pneumatic supply requirements of the experimental facility (Figure 4.15). Swagelok compression fittings were used in assembling these components. An extra pneumatic supply port was made available for future needs. The variable flow regulator (Praxair® model no. 07R215AC) controls the air flow between 0 to 1.72 MPa. The coalescing filter (Praxair model no.15F2PEA) separates liquid aerosols and droplets of water from the air. The fine filter element of grade 6.0 present inside the coalescing filter restricts the aerosol particles to 0.75 micron size. Figure 4.16 shows the pneumatic hose connections to the electro-pneumatic valves.

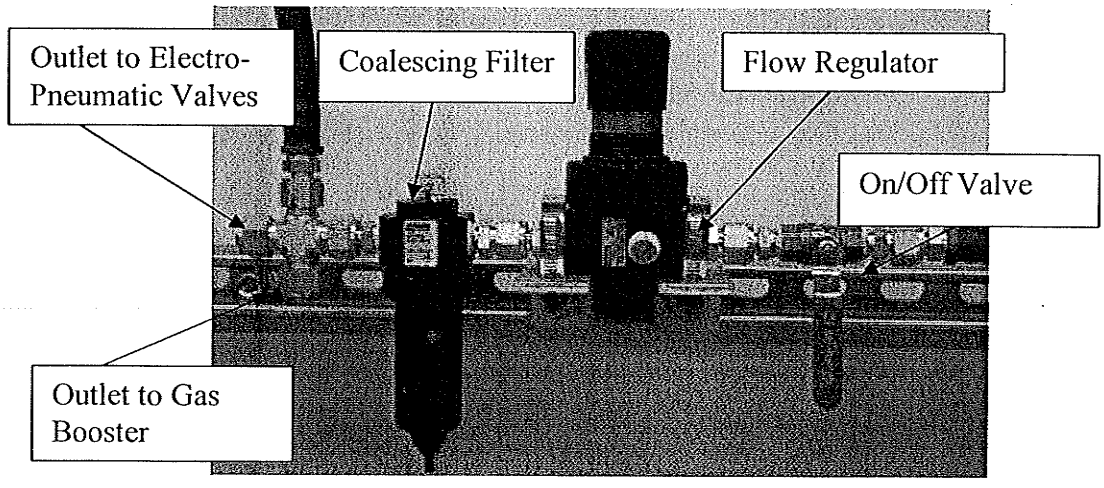

Figure 4.15: Pneumatic distribution system with filter and regulator assembly.

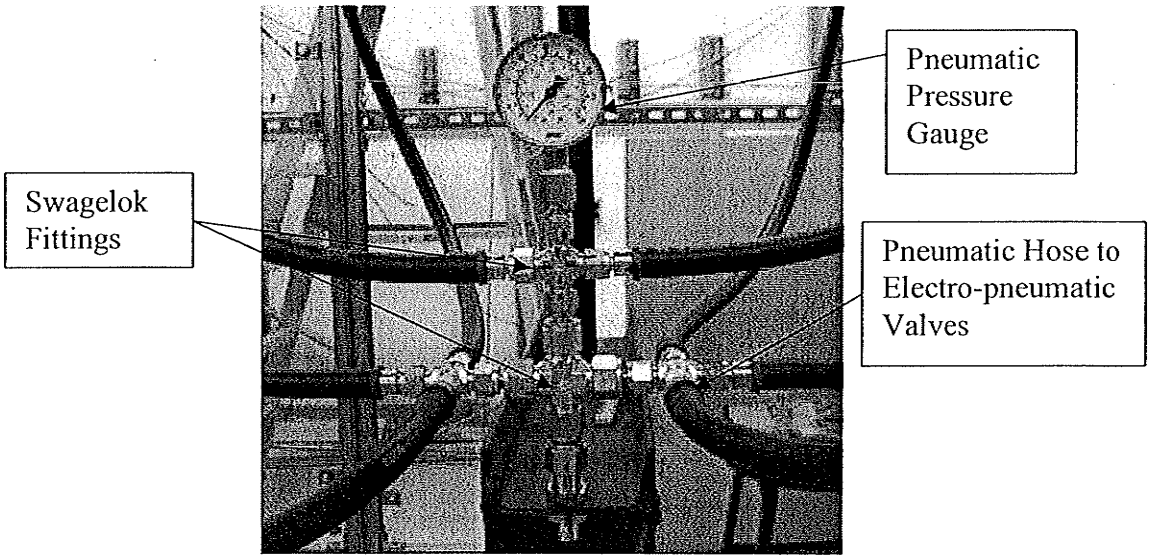

Figure 4.16: Pneumatic connections for the electro-pneumatic valves.

4.9 Data Acquisition System and Instrumentation

The data acquisition system (DAS) was designed and constructed by AECL. It is the key operating system in controlling the experimental facility and in preventing possible operational errors during the experiments. The electro-pneumatic valves (8 nos.), which requires a 4 to 20 mA input signal to control the percentage opening, is fed through the data acquisition system. Flow regulating ball valves (On/Off valves, Habonim®, Figure 4.10, 4.11) and the open and closed positions are also monitored by the DAS. Temperature and pressure measurements, power input to the channels are recorded at pre-determined regular time intervals by the data acquisition system. The DAS also incorporates some of the safety features that would shut down the experimental facility (power supply) in the case of an excess pressure build-up during experiments, or if the temperature of the working fluid exceeds the preset safe limit.

4.9.1 Thermocouples and Pressure Transducer

Temperature measurements can be recorded at various locations using surface thermocouples and fluid thermocouples assembled on the facility. Twelve surface thermocouples (0.040 O.D.x12. LG, Type K, Delta M®) aree assembled on the outer surface of the each channel. Ten fluid thermocouples (3.175 mm O.D x 304.8 mm, LG, Type K, DeltaM Corporation®) were also installed at various locations on the experimental facility to measure bulk fluid temperatures. Boundary layer effects were considered in assembling the fluid thermocouples and they were placed in such a way that the thermocouples tip lies in the center of the flow. DP 363 (Validyne®) differential pressure transducers were used to measure the pressure drop across the eight electro-pneumatic valves and DP 303 (Validyne®) transducers are used to measure the pressure drop across the two headers, across the three channels and across the heat exchanger. These pressure transducers were calibrated and results are traceable to national standards. Three GP-50 (Dycor Technologies®) absolute pressure transducers were used to measure the absolute pressure inside the accumulator and in the two headers of the test section. These absolute pressure transducers were also calibrated by the manufacturer. Swagelok compression fittings were used in assembling all thermocouples and pressure transducers.

4.10 Power Supply

An AC to DC converter (124KVA/600V/3ϕ rectifier, EMHP Power Supply®) is used to supply DC power to heat the test section by electrical induction. The output current (0 to 1500 Amps) and voltage (0 to 20 Volts) from the power source can be continuously varied during the experiments and the amount of energy supplied to the test section

channels can be monitored continuously. The unit is rated to hold current fluctuations to with in 0.1 % of the full load current for the line voltage variations of 0.1%. A maximum of 10 kW per channel can be supplied from the power supply source. Circuit breakers rated at 1500 Amps were installed between the power supply and test section as per the electrical code. Using the control panel the power supplied to the three channels is controlled. The test facility is electrically isolated from the test section by using glass filled teflon® glass gaskets between the stainless steel flanges and insulating sleeves to the flange bolts. These insulating measures are taken on the upstream side of the test section. As the voltage drops to zero (approximately), from the front end to back end of the test section, it is safe from any risk of electrical shock and so the down stream side of the test section is not electrically insulated. (Precession shunt circuits may be installed to measure precise and accurate power measurements on each of the three channels if required in a later stage of the experiments).

4.11 Support Structure

The support structure for the test facility was designed to withstand the complete weight of the test section including the valves and piping, which are part of the test facility. The support structure has adjustable screws and this feature helps to maintain the horizontal orientation of the facility. Any minor adjustments in height can easily performed by adjusting the screws. The test section was supported on a flat C channel which allows minor thermal expansion of the test section channels without creating any stress on the heated tubes (channels). These support structures have to be modified to include rollers,

which would allow for thermal expansion when doing experiments using supercritical water.

4.12 Safety Features

The experimental facility was designed to operate at 24 MPa pressure and 400 °C temperature and so it is necessary that safety measures be taken well in advance to eliminate any damage and personal injury in case of an accidental explosion of any part of the test facility. As part of the safety requirements, the test facility was designed with a rupture disk assembly, safety shield and carbon dioxide gas detection system.

4.12.1 Rupture Disk Assembly

On each of the three channels, a 12.7 mm size rupture disk assembly was installed through a common union outlet, which was then vented to a safe area using Swagelok fittings and tubing. Depending on the working fluid requirements (carbon dioxide or water) the rupture disk holders can be assembled with rupture disks rated for 10.61 MPa (1540 psi in case of CO_2 experiments) or 24.13 MPa (3500 psi in case of water experiments) which will prevent the facility from getting damaged in the case of excess pressure build-up during experiments. Presently, the experimental facility is equipped with 12.7 mm size PB series inconnel rupture disks rated for 10.61 MPa pressure at 93 °C, which is suitable for carbon dioxide experiments. Figure 4.17 shows the rupture disk assembly over the three channels of the test section. Swagelok and Parker tube fitting were used in this assembly. The outlet tube (19.05 mm) from these 12.7 mm

rupture disk tubes was routed away from the experimental facility and directed into a safe zone.

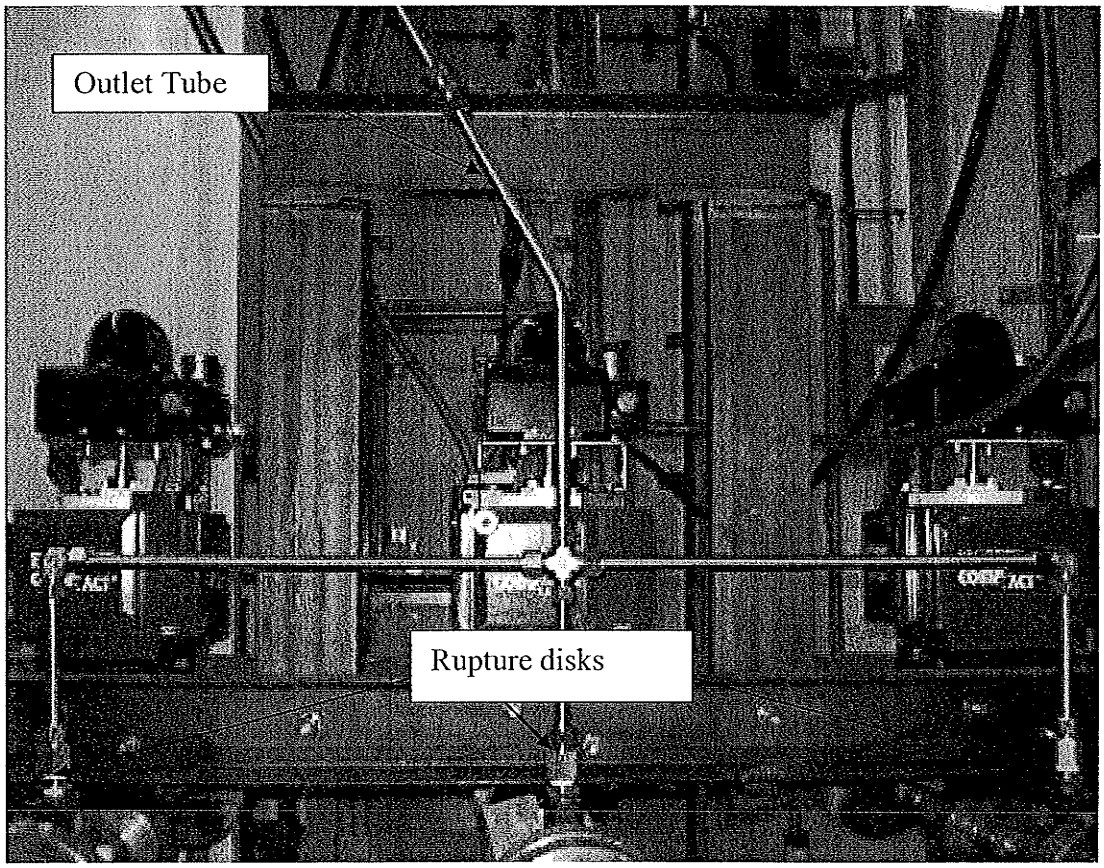

Figure 4.17: Rupture disk assembly over the three channels of test section.

4.12.2 Safety Shield

A protective safety shield was constructed around the experimental facility as a safety measure to protect against any accidental failure. The support structure of the safety shield also acts as a frame to hold the control panel of the heat removal system, the pneumatic distribution system and for supporting other auxiliary items such as gas cylinders. Transparent polycarbonate sheets of thickness 9 mm and 6 mm were used for

this purpose. Figure 4.18 shows the schematic drawing of the safety shield enclosure provided around the experimental facility.

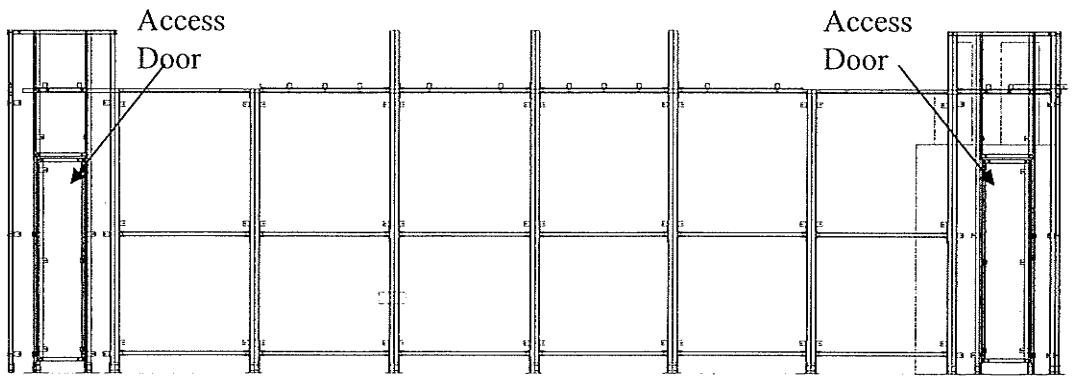

Figure 4.18: Schematic drawing of the safety shield enclosure for the supercritical flow experimental facility.

4.12.3 Carbon dioxide Detection System

Carbon dioxide levels in the laboratory must be monitored continuously to ensure they are always within the safe limits. In the case of a leak from the test facility, carbon dioxide will occupy the entire room and may be unsafe. Large amounts of carbon dioxide (78 liters) at high pressure pose a high risk if it leaks from the experimental facility. In order to overcome this danger and to monitor the carbon dioxide levels in the laboratory a carbon dioxide detection system was incorporated.

An Analox 50™ carbon dioxide gas analyzer with audio and visual alarms was employed to detect and monitor carbon dioxide levels in the laboratory. The analyzer consists of a main powered sensor unit and a repeater. The sensor unit is mounted on the test facility safety shield, 450 mm from the floor level and as close as possible to the test

facility. The repeater was installed at eye level outside the entrance door which will indicate the safety level before an operator enters the laboratory. The analyzer is set at 0.5% and if an excess level of carbon dioxide is detected, then an alarm signal will be triggered. At dangerous levels, a second alarm warns of the need for immediate evacuation from the laboratory and cannot be entered until the monitor returns to safe mode. Exhaust fan (5000 cfm) employed in the laboratory would remove the carbon dioxide from the laboratory in the case of a leak. Figure 4.19 shows the schematic drawing of the carbon dioxide detection system.

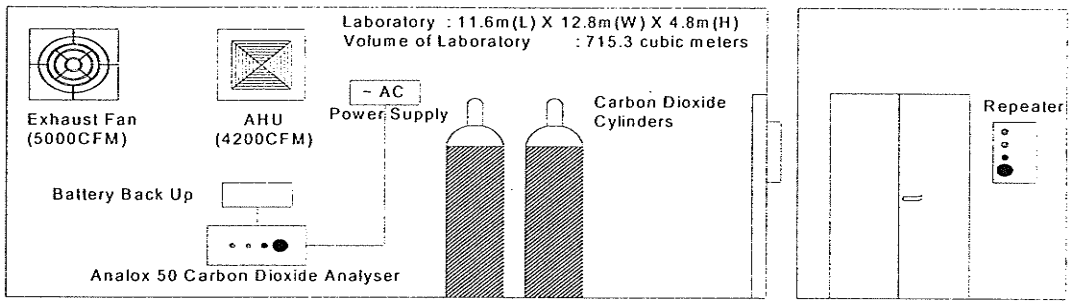

Figure 4.19: Schematic drawing of carbon dioxide detection system.

4.12.4 Emergency Power Shutdown Switches

Emergency power shutdown switches were also incorporated into the experimental facility safety features. These switches will shut down the power supply to the experimental facility when activated. One of these switches (Fig 4.20.a) is located near the data acquisition system, and the operator. In case of emergency shut down of the experimental facility, this switch can be activated just by pressing the emergency shutdown switch (panic switch) and can be deactivated just by turning clockwise. Other emergency power shutdown switches (Fig 4.20.b) can be operated with a key. Two more power shutdown switches (Fig 4.20.c) were also assembled on the facility access doors,

which would be activated upon opening these doors. Figure 4.20 (a, b, c) shows the emergency power shutdown switches assembled on the experimental facility.

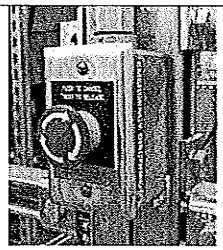
Fig 4.20.a

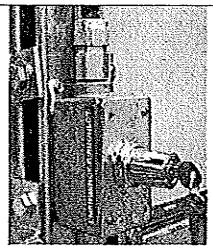
Fig 4.20.b

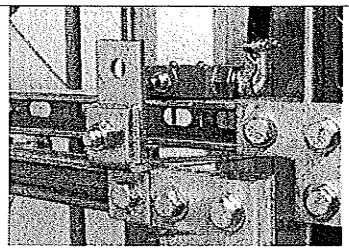
Fig 4.20.c

Figure 4.20: Emergency power shutdown switches.

4.13 Miscellaneous Devices

4.13.1 Heating Tape

The test section is positioned horizontally and when the fluid is heated, the fluid flow could take any one of the two directions. In order to direct the fluid in a desired direction (counter-clock wise direction) a flexible heating tape can be used to initially heat the fluid on the vertical hot leg side of the test facility. As the fluid is heated, the fluid flows in the loop due to natural convection. Omega flexible heating tape (HTWC102-008) of 25.4 mm wide and 2.44 m is wounded on the hot leg of the test facility. With the percentage controller available with the heating tape the amount of heating can be varied up to maximum of 576 Watts.

4.13.2 Flow Meter

An Ultrasonic flow meter manufactured by GE Panametrics (GC 868) was recommended for measuring supercritical fluid flow velocity. The device does not interrupt the flow physically and has no wetted or moving parts and hence there is no pressure drop to

account for. The device uses a Transit-Time flow measuring technique to accurately measure the flow rate. This flow meter is recommended to be installed on the test facility to measure the fluid flow rates during experiments.

4.14 Changes for Experimental Facility When Using Water (working fluid)

The following table gives the list of all the components that need to be replaced/ modified for the supercritical water experimental facility.

Table 3.2: Suggested changes for supercritical water experimental facility.

Component	Suggestions	Description
Constant pressure control system (Pressure regulator, stainless steel cylinder hose, CAG 580 adapter)	No change is required	Pressure regulator is be restored to 24 MPa (operating pressure) set pressure.
Accumulator	Design a system that will ensure water entering to the accumulator is less than 94^0C.	Accumulator can withstand temperature up to 94 °C.
Inlet Settling Chamber	Design fluid chamber (settling chamber)	Chamber which can withstand 300 °C is recommended.
Flow regulating ball valves (Habonim H27 series valves) 4 Nos.	Change the body seal and steam thrust seal for high temperature operation.	Body seal and thrust seal of PEEK as recommended by Habonim® for high temperature operation.
Channel rupture disks	Rupture disc with 25 MPa pressure rating.	This is a necessary change Presently rupture disks rated for 10.61 MPa pressure.
Heat Exchanger	Different heat removal system has to be designed.	Present heat exchanger operating limits are 16.54 MPa (tube side).
Support structure	Roller supports	Roller supports allow thermal expansion of the test section.
Absolute pressure transducers	Replace absolute pressure transducer that can measure 25 MPa of pressure.	Current pressure transducers can measure only up to 10 MPa.
Differential pressure transducers	Change the diaphragms of the each pressure transducers suitable for supercritical water.	Mount them on long tubes and properly cool the tubes, so that temp. of fluid in contact with sensors is less than 170 °C.

CHAPTER 5

PRE–EXPERIMENTAL PROCEDURES

After completion of the supercritical flow experimental facility construction, the following pre-experimental procedures were followed.

5.1 Chemical Cleaning

The supercritical flow experimental facility was constructed using factory-shipped materials and some of the stainless steel piping and tubing may have collected dust and other debris during the course of time; hence chemical cleaning was a necessary procedure to be followed before conducting any experiments. The ASTM (A380–99) standard was taken as a guideline in conducting the chemical cleaning. As a first step, all flow regulating valves (8 nos.) were opened manually by connecting the proper fittings (12.7 mm JIC union and Swagelok female connector) and by supplying compressed air at 690 kPa pressure (the complete step-by-step procedure for manual opening of the electro-pneumatic valves is described in Appendix A). The settling chamber, which was previously cleaned by the supplier, was temporarily disconnected from the experimental facility. The facility was then completely sealed by using a stainless steel plate and a teflon sheet (detailed description of disconnecting the settling chamber is provided in Appendix A).

A pressure test was conducted using compressed air at 690 kPa pressure to detect any possible leaks from the facility. A Swagelok tube fitting (Figure 5.1) provided for

this purpose was used in connecting the pneumatic air supply and gas supply during the pressure testing and chemical cleaning.

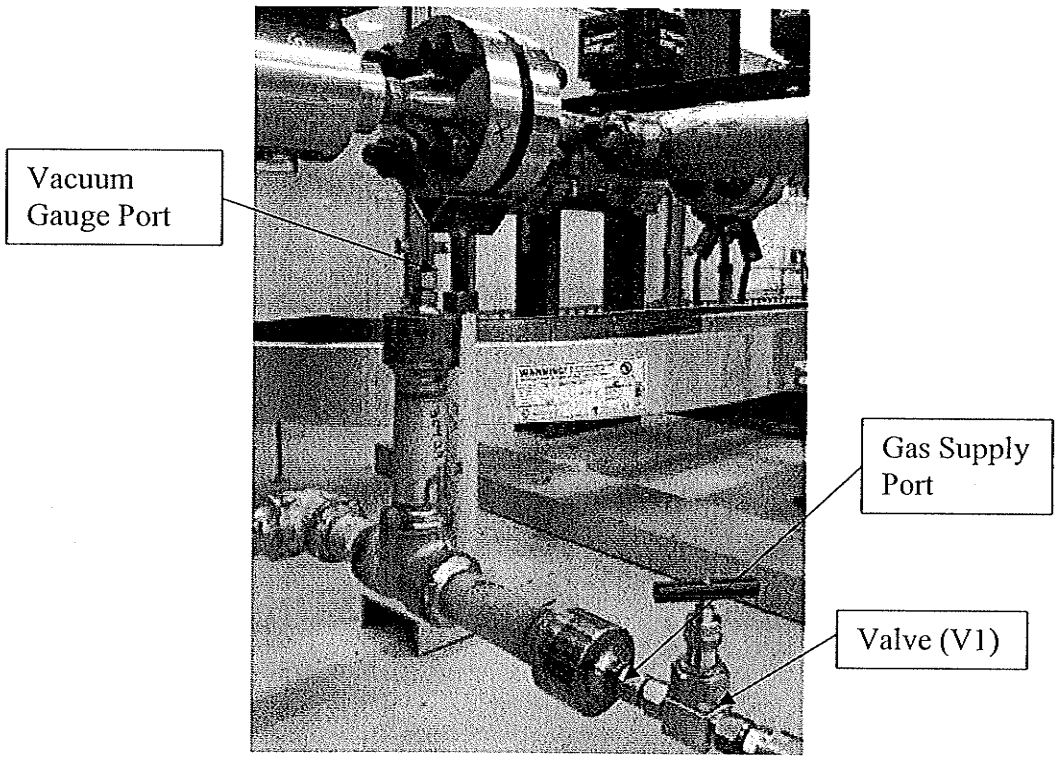

Figure 5.1: Photograph showing the 12.7 mm port with Swagelok fitting, used in connecting the pneumatic hose during the pressure tests.

The accumulator was disconnected from the experimental facility and a circulation pump was assembled in its place. Diluted Carbochlor® solution (1:5 ratio) was pumped into the experimental facility up to a pressure of 689.5 kPa. Sufficient care was taken to ensure that the trapped air was removed from the system. After soaking the facility for two hours with the chemical solution, the solution was then drained out. The experimental facility was again filled with the chemical solution and circulated in alternate directions for 20 minutes, by closing and opening the flow control valves (Vi-1 and Vi-2, Figure 4.11). This procedure of circulating the solution through the facility in

different directions was repeated three times; and each time the solution was drained completely. Later the facility was filled with water and circulated in different directions and was then drained from the system. Water was also circulated three times through the system to ensure that no trace of the chemical solution was left. The experimental facility was then dried by blowing compressed air (689.47 kPa) through the system.

5.2 Pressure Testing

The experimental facility was pressure tested to ensure that it had no leaks and could withstand 10.34 MPa pressure during experiments. The ASTM (F 2164-02) standard was taken as a guideline in conducting the pressure test. After the chemical cleaning, the experimental facility was completely dried out and the settling chamber was reassembled in its place. All Swagelok fittings were thoroughly checked and tightened to ensure that the facility was completely sealed. The accumulator was also assembled back in its place and was connected to the nitrogen gas cylinder (size-T, cylinder pressure: 18.02 MPa, Praxair®) to test the performance of pressure control system. A pressure gauge (pressure range: 0 to 34.47 MPa) was assembled on the test section header to monitor pressure inside the facility during the tests (Figure 5.2).

A nitrogen gas cylinder (Size-4K, cylinder pressure: 31.02 MPa, Praxair®) was connected to the experimental facility using flexible hose and a pressure regulator assembly. The experimental facility was then pressurized in three stages (3.10 MPa, 5.17 MPa, and 10.34 MPa) and at each stage, a leak detection procedure were followed. Swagelok Snoop® liquid leak detector solution was used on the external surfaces of the fittings; if there is a leak, gas bubbles buildup on the surface of the fittings. In each stage

of the pressurization test, the facility was left pressurized for 45 minutes and the pressure inside the facility was monitored for possible pressure drop over long time intervals. The facility was finally pressurized to 10.34 MPa pressure and the supply regulator valve was completely closed. At this stage the facility was left pressurized for about 18 hours (the rupture disk assembly on the test section is rated for 10.61 MPa pressure). A small decrease in pressure was observed after an 18 hour time span. After a thorough search for leaks, a leak was discovered from one of the Swagelok fittings, which was used in assembling the accumulator. This particular Swagelok fitting was removed and reassembled to fix the leak. A possible reason for the leak could be insufficient tightening of the fitting. The experimental facility was then left pressurized (at 9.65 MPa) for 21 days and no pressure drop was observed with the system.

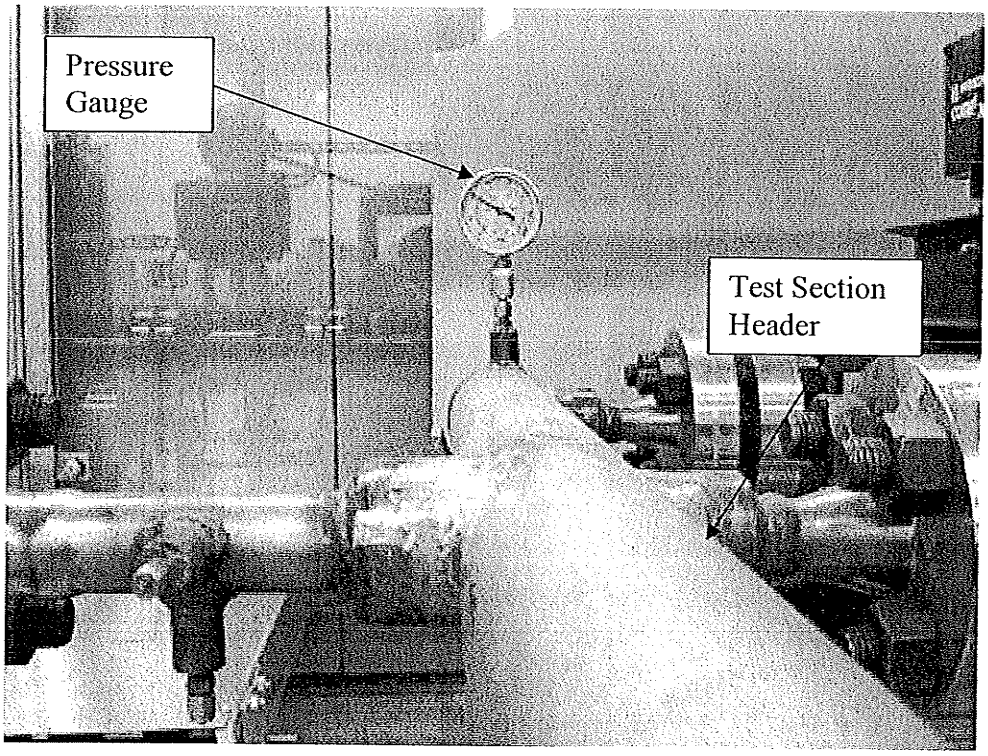

Figure 5.2: Pressure gauge assembled on the test section header.

5.3 Evacuation and Purging

In order to ensure that the experimental facility is free from air and moisture, the facility was purged with carbon dioxide (grade 4.0, 99.99 %, Praxair). The carbon dioxide cylinder was connected through a Swagelok fitting, on the experimental facility (Figure 5.1). A vacuum gauge (range: -30 in Hg to 206.84 kPa) was assembled near to the settling chamber to monitor the pressure during the evacuation and purging tasks. A Schematic drawing of the purging and evacuation system, which includes the valves and vacuum pump, is shown in Figure 5.3. Valves that are to be operated during the purging and evacuation procedures are as follows:

V1 - valve connected to carbon dioxide supply line (Figure 5.1)

V2 - valve connected to the vacuum pump and purge valve junction

V3 - valve (Needle valve)

V4 - valve (Needle valve)

V5 - valve (Quarter turn valve)

V6 - check valve (non – return valve)

Steps for purging and evacuation of the facility:

1. Close valves (V1, V2, V3, V4, V5)
2. Open valve V1 and supply carbon dioxide gas into the loop (at a pressure less than 200 KPa).
3. Open valve V2 and V4 and let carbon dioxide gas pass through the facility (purging) for five minutes.
4. Close valve V4.
5. Close valve V1.

6. Open valve V3 and operate the vacuum pump to evacuate the loop (monitor the vacuum gauge).
7. Close valve V3.
8. Close valve V2.
9. Open valve V5 This will release the vacuum pump from negative pressure and it prevents the possibility of vacuum pump oil flowing back into the system (as recommended by the vacuum pump manufacturer).
10. Repeat steps 2 to 7, for 4 times (cycles) to ensure that the facility is relatively free from air and moisture.

This procedure is to be followed each time purging and evacuation is performed on the facility.

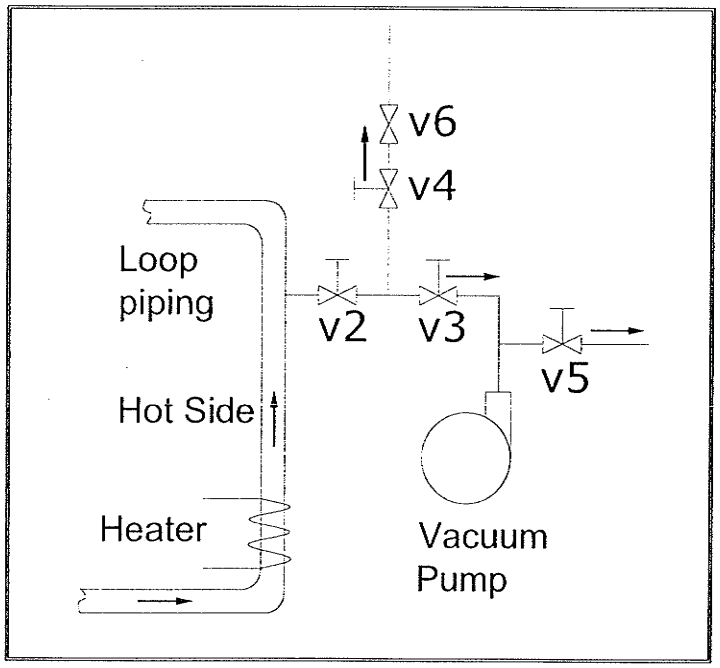

Figure 5.3: Schematic drawing showing vacuum pump and the valve scheme used for purging and evacuation of the experimental facility.

CHAPTER 6

NUMERICAL SIMULATIONS

The following chapter discusses the numerical simulations carried out using the SPORTS numerical simulation code for the present supercritical flow experimental facility configuration and using carbon dioxide as the working fluid.

6.1 Background

Chatoorgoon (2001) has conducted numerical and analytical analysis of flow stability inside a natural circulation loop for supercritical water at 25 MPa pressure and 350 °C temperature using the SPORTS code. From his analysis he concluded that the instability boundary may lie near the peak of flow-power characteristic. He also pointed out that this may be a new type of instability.

6.2 SPORTS Code

Chatoorgoon (1986) has developed a simple non-linear thermalhydraulic stability code (SPORTS code), which was initially developed to investigate the stability of flows at low pressure due to subcooled boiling and to perform transient simulations of thermalhydraulic and neutron coupled dynamics. Later Voodi (2004) has modified the SPORTS code to make it suitable to apply for different fluids (including carbon dioxide). The mathematics involved in the SPORTS code is beyond the scope of the present work and the can refer to Chatoorgoon (1986) and Voodi (2004) for further details.

6.3 Parametric Analysis

The objective of the numerical simulations work is to understand the influence of various parameters on the steady-state numerical simulations were conducted by changing each parameter and keeping other parameters constant. The parameters that were studied in this work are:

- Inlet Temperature
- Pressure
- Channel Inlet K Factor
- Channel Outlet K Factor

The present supercritical flow experimental facility's dimensions were entered as input data into the SPORTS input file. The Input file was also modified to simulate carbon dioxide fluid flowing through a single heated channel. The K-factor (5.97) for the heat exchanger was calculated from data provided by the manufacturer and is provided in Appendix B. During the numerical simulations, the power (heating) to the channel was limited to 15 kW as the experimental facility has limitations on the maximum amount of DC power supplied to each channel (10 kW per channel).

The ITR factor in the SPORTS input file can be either 0 or 1. For the present steady-state runs, the ITR value was set equal to zero, (if ITR is set equal to one, then the input file is set to simulate a transient run). Other input parameters like inlet temperature (TIN), pressure (PIN, PEX) are modified according to the simulation performed. Sixty steady-state simulations were carried out by varying the above mentioned parameters (Inlet Temperature, Pressure, Channel Inlet K factor, Channel outlet K factor) and are listed in Table 6.1. For the present study, the SPORTS code was modified to generate an

output file with power and its corresponding flow rate in the experimental facility during the simulation. A sample SPORTS code input and output files are provided in Appendix B.

Table 6.1: Numerical simulations for carbon dioxide using SPORTS code.

Cases	Pressure	Temperature	Channel Inlet K-factor	Channel Outlet K-factor
Unit	(MPa)	(°C)		
Cases 1 to 10	7.5	25	0,0,0,0,0, 2,5,8,10,13	2,5,8,10,13, 0,0,0,0,0
Cases 11 to 20	7.5	28	0,0,0,0,0, 2,5,8,10,13	2,5,8,10,13, 0,0,0,0,0
Cases 21 to 30	7.5	31	0,0,0,0,0, 2,5,8,10,13	2,5,8,10,13, 0,0,0,0,0
Cases 31 to 40	9.5	27	0,0,0,0,0, 2,5,8,10,13	2,5,8,10,13, 0,0,0,0,0
Cases 41 to 50	9.5	30	0,0,0,0,0, 2,5,8,10,13	2,5,8,10,13, 0,0,0,0,0
Cases 51 to 60	9.5	32	0,0,0,0,0, 2,5,8,10,13	2,5,8,10,13, 0,0,0,0,0

6.4 Discussion of Results

In this analysis Inlet temperature, pressure, channel inlet K factor and channel outlet K factor were the parameters studied. These simulations are helpful for better understanding of the experimental facility and will help in conducting experiments. Results of the steady-state simulations are presented in Appendix B. The steady-state profiles obtained from analysis of the different parameters is presented in the figures (6.1, 6.2, 6.3, 6.4, 6.5, and 6.6) that follow.

Channel inlet K factor was studied for two different pressures 7.5 MPa and 9.5 MPa and by varying the inlet temperature between 25 °C and 31 °C. The steady-state

profiles obtained from the analysis of these cases are presented in Figure 6.1 and Figure 6.2. From the plots it was observed that for a given temperature and pressure the steady-state profiles having high channel inlet K factor (13) has low peak power than for the cases with low channel inlet K factor (2).

Influence of the channel outlet K factor on the system was also studied at 7.5 MPa and 9.5 MPa pressures and by varying the inlet temperature between 25 °C to 31 °C. The steady-state profiles obtained from the analysis are plotted in Figure 6.3 and Figure 6.4. From the analysis, it was noticed that for a given temperature and pressure the steady-state profiles having high channel outlet K factor (13) has high peak power than for the cases with low channel outlet K factor (2).

The effect of the temperature was plotted in Figures 6.5 and 6.6. It was observed that the steady-state profile having high inlet temperature has low peak power than for the case with low inlet temperature and other factors (pressure, channel inlet K factor and channel outlet K factor) remaining constant.

These simulations are helpful in understanding the behavior of the system or the experimental facility under various conditions. From the simulations it is suggested to conduct experiment with channel outlet K factor (13), channel inlet K factor (0), inlet temperature (31 °C) and pressure (7.5 MPa). This particular case has a low peak power (5 kW) from the steady-state profile.

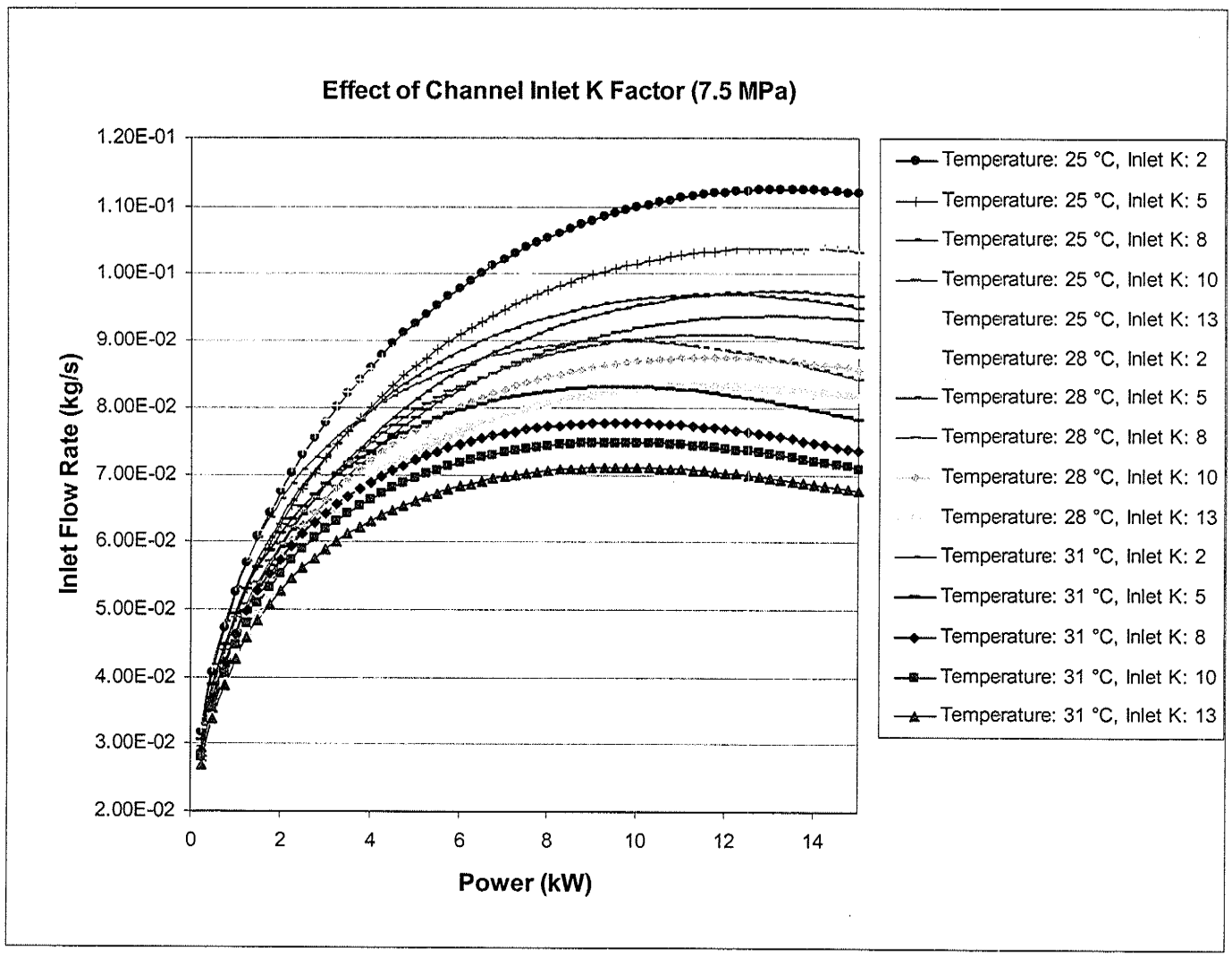

Figure 6.1: Steady-state profiles at 7.5 MPa pressure and zero channel outlet K factor.

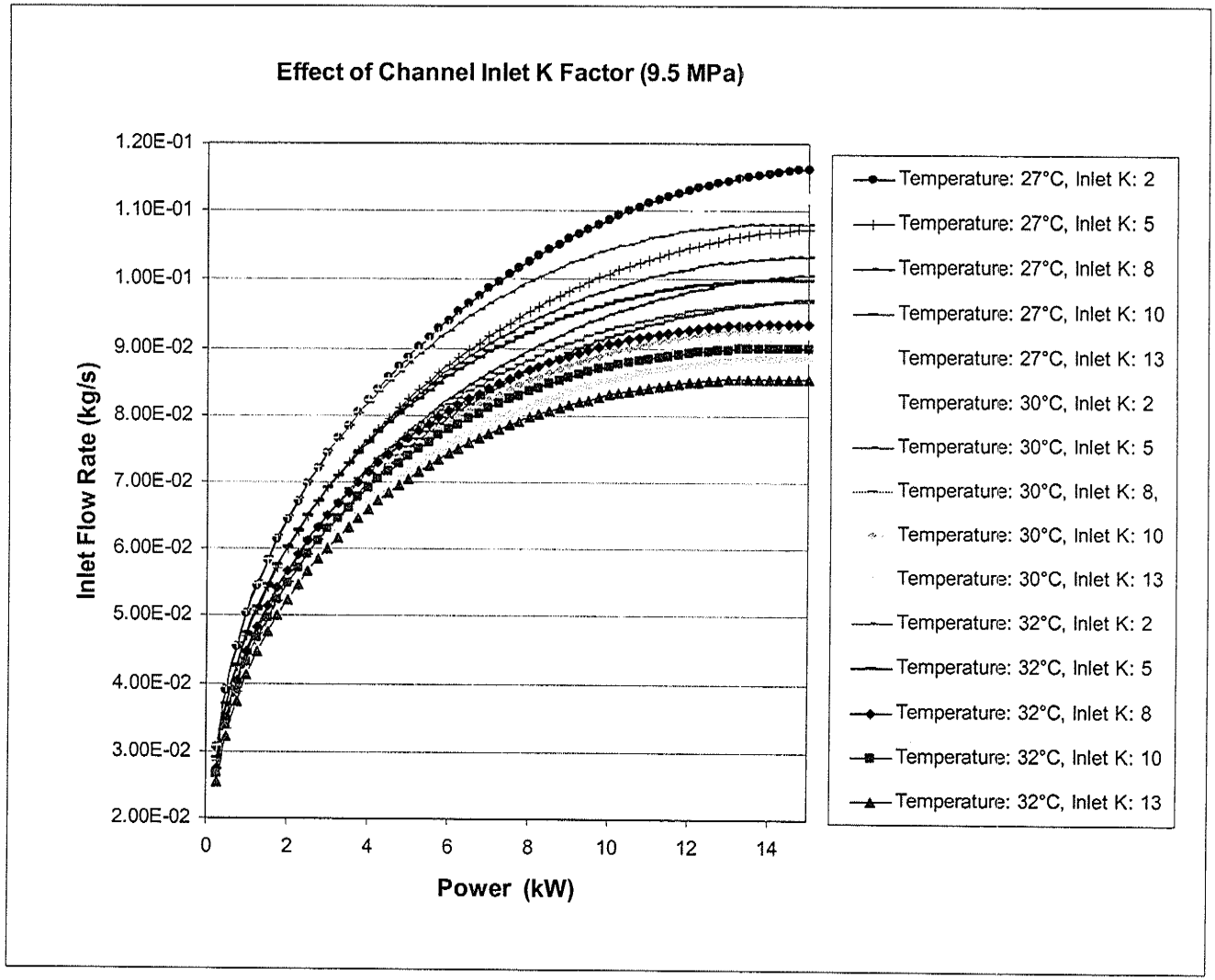

Fig 6.2: Steady-state profiles at 9.5 MPa pressure and zero channel outlet K factor.

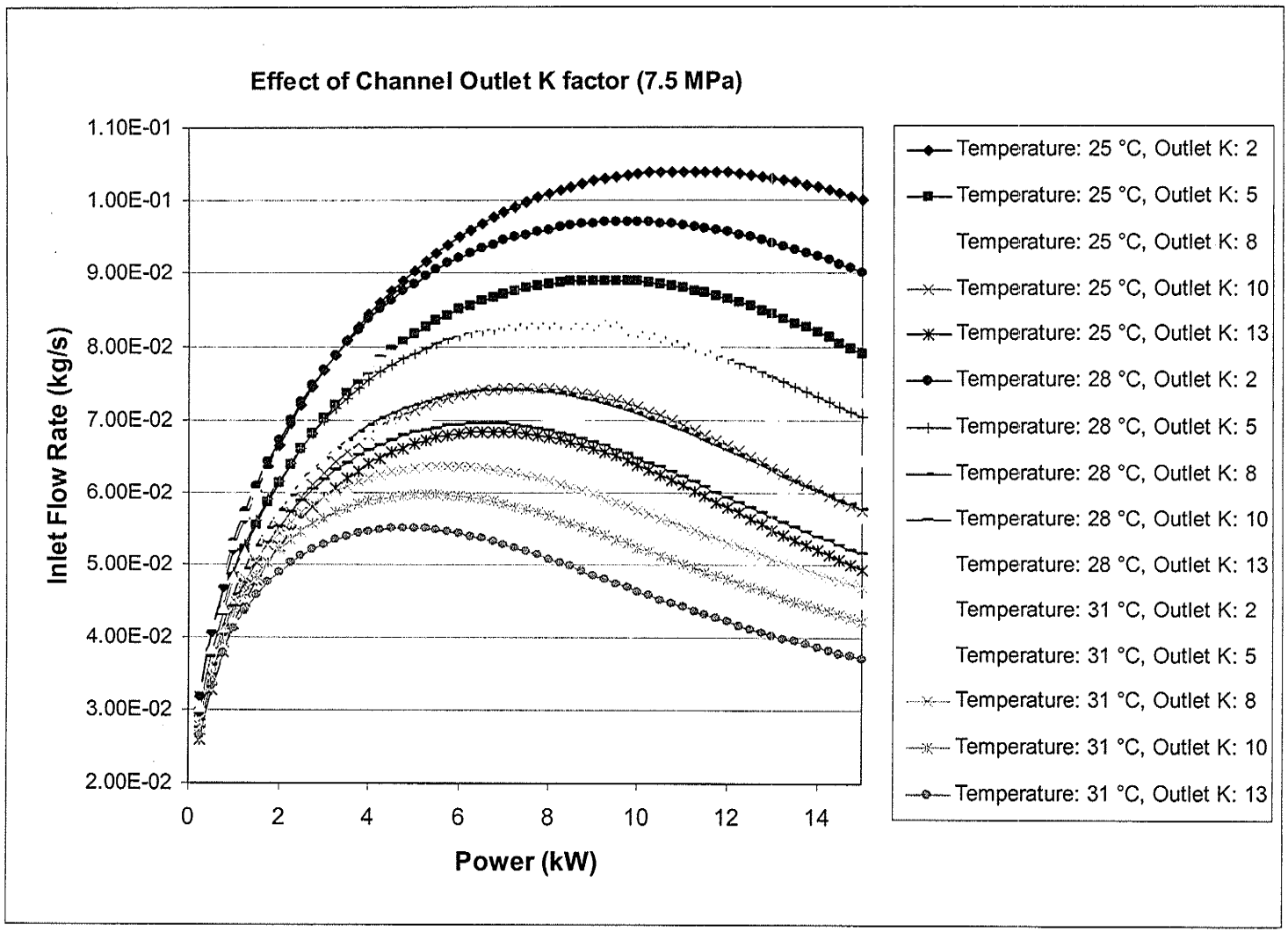

Figure 6.3: Steady-state profiles at 7.5 MPa pressure and zero channel inlet K factor.

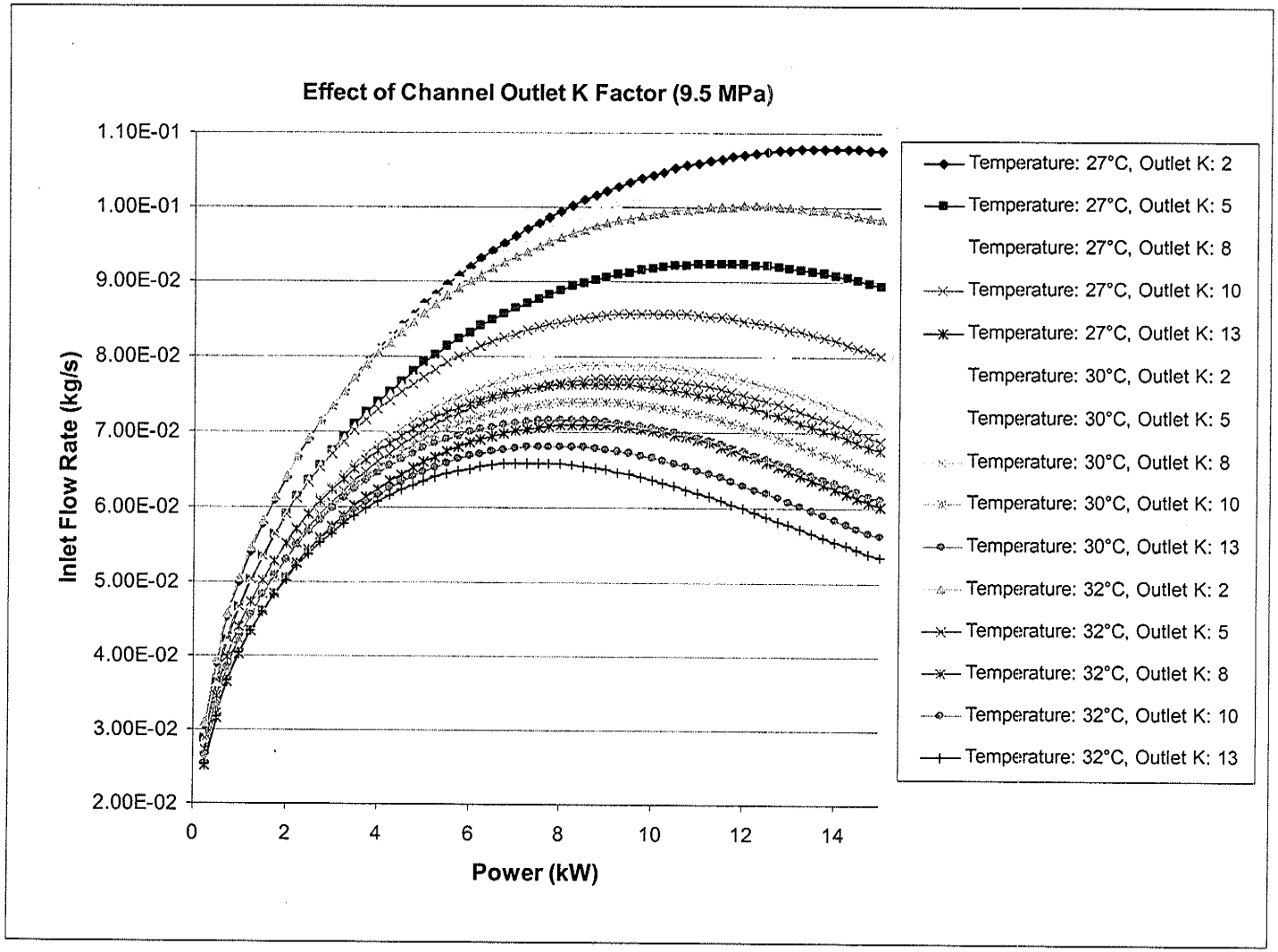

Fig 6.4: Steady-state profiles at 9.5 MPa pressure and zero channel inlet K factor.

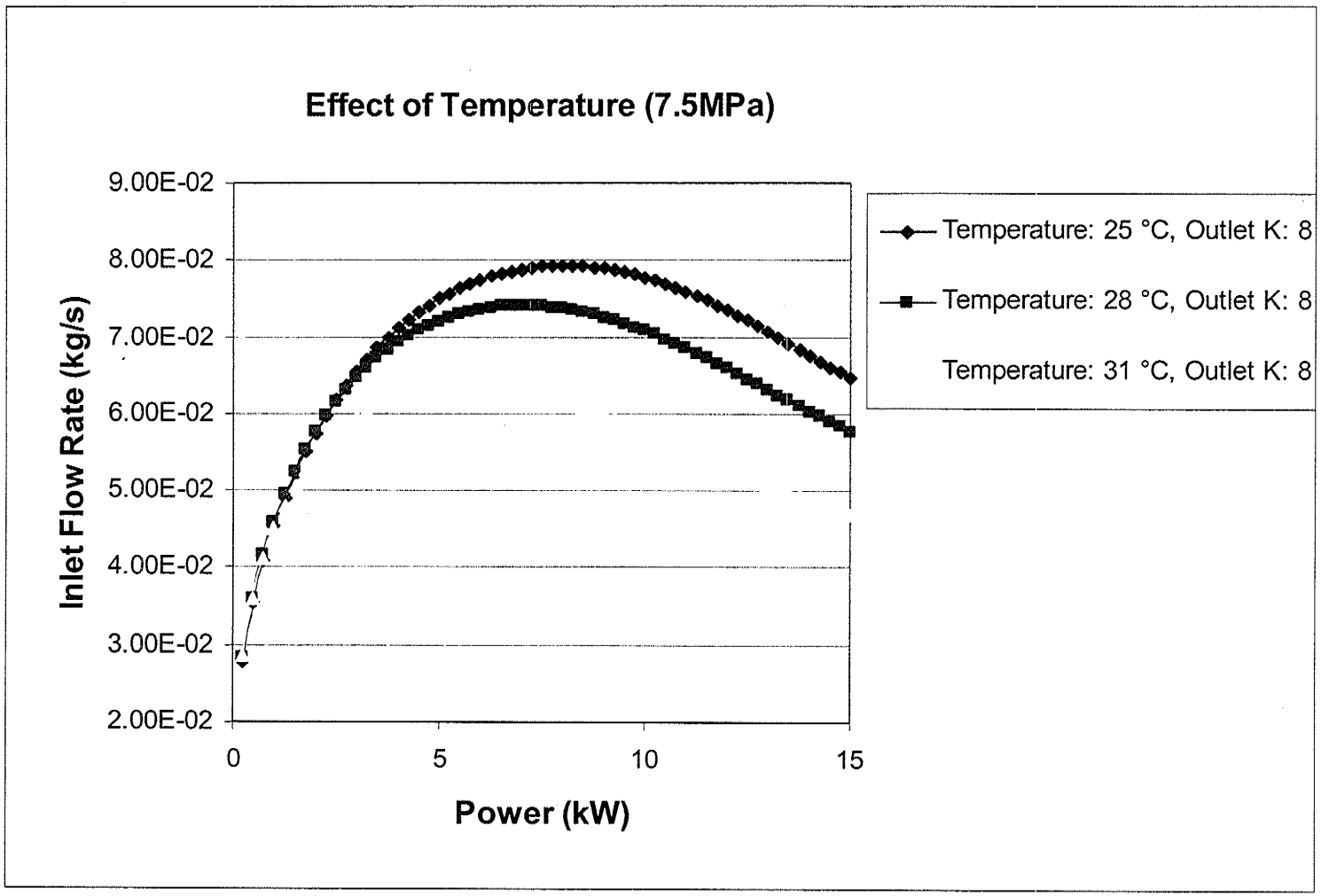

Figure 6.5: Steady-state profiles at 7.5 MPa pressure and zero channel inlet K factor.

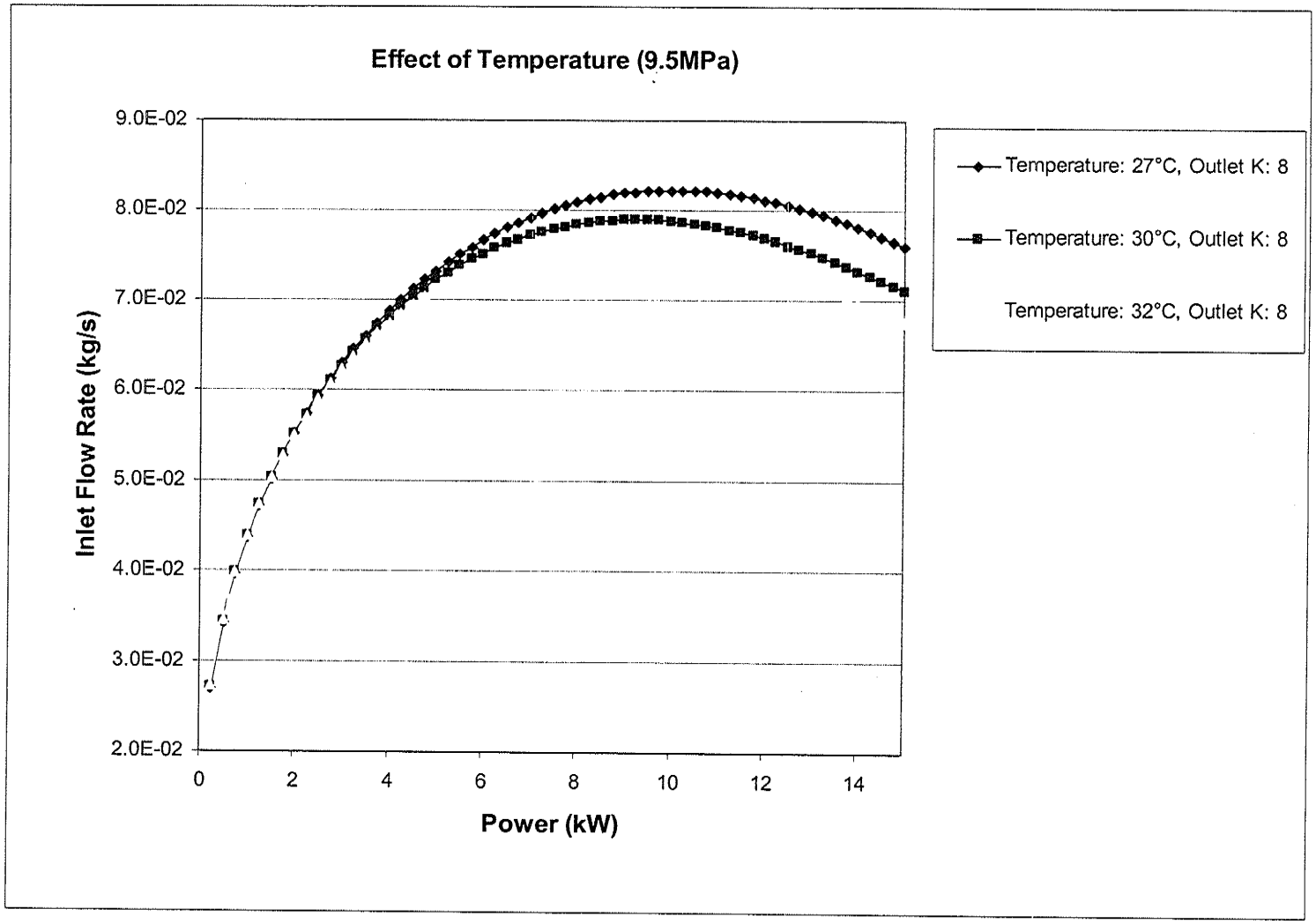

Figure 6.6: Steady-state profiles at 9.5 MPa pressure and zero channel inlet K factor.

CHAPTER 7

CONCLUSION AND RECOMMENDATIONS

7.1 Conclusion

In this work, an experimental facility was designed and constructed for studying the behavior of supercritical fluids. Pre-experimental procedures such as chemical cleaning and leak tests were performed. Pressure testing was also conducted to verify the pressure rating (10 MPa) of the facility for future carbon dioxide experiments. With the modifications suggested in section 4.14, the current experimental facility can also be employed to conduct experiments using water as the working fluid at supercritical condition.

Using the SPORTS code, sixty numerical simulations were conducted. The code was set up to simulate the experimental facility using carbon dioxide as the working fluid flowing in a single channel distributed heat system. The channel inlet K factor, channel outlet K factor, inlet temperature and pressure were studied.

7.2 Recommendations

Preliminary testing of the individual systems heat removal system, pressure control system, and data acquisition system has to be performed before conducting full scale experiments. After fine tuning of the experimental facility, insulation has to be provided to prevent heat loss from the experimental facility. Extension of the numerical simulations, a complete stability analysis may be conducted to better understand the

stability of the system using the SPORTS code. Numerical simulations can be further extended to study water as a working fluid.

7.3 Future work

The present supercritical flow experimental facility can be employed to conduct a wide range of experiments apart from stability studies. The supercritical flow experimental facility may be modified to conduct heat transfer and pressure drop characteristics, flow-field mapping and water corrosion studies.

REFERENCES

[1] Buongiorno, J., Corwin, W., MacDonald, P., Mansur, L., Nanstad, R., Swindeman, R., Rowcliffe, A., Was, G., Wilson, D., Wright, I., Supercritical Water Reactor (SCWR), 2003, "Survey of Materials Experience and R&D Needs to Assess Viability, INEEL/EXT-03-00693 (Rev. 1)," Idaho National Engineering and Environmental Laboratory.

[2] Callahan, F. J., 1998, "Swagelok tube fitter's manual".

[3] Chatoorgoon, V., 1986, "SPORTS-A Simple non-linear thermalhydraulic stability code," Nuclear Engineering and Design, Vol.93, pp.51-67.

[4] Chatoorgoon, V., 2001, "Stability of supercritical fluid flow in a single-channel natural-convection loop," International Journal of Heat and Mass Transfer, Vol.44, pp.1963-1972.

[5] Cornelius, A. J., and Parker, J. D., 1965, "Heat transfer instabilities near the thermodynamic critical point" proceedings of Heat Transfer and Fluid Mechanics Institute, pp.317-329.

[6] Duffey, R. B., and Pioro, I. L., 2005, "Experimental heat transfer of supercritical carbon dioxide flowing inside channels (survey)," Nuclear Engineering and Design, Vol.235, pp.913-924.

[7] Dimmick, G. R., Spinks, N. J., and Duffy, R., 1998, "An advanced CANDU reactor with supercritical water coolant: conceptual design features," proceeding of Pacific Basin Nuclear Conference, pp.1211-1218.

[8] Fukuda, K., Hasegawa, S., Kondoh, T., Nozaki, F., and Nagayoshi, T., 1992, "Instability of supercritical helium flow," Journal of Heat Transfer: Japanese Research, Vol.21, no: 2, pp.177-186.

[9] Greif, R., 1988, "Natural Circulation Loops," Journal of Heat Transfer, Vol.110, pp.1243-1258.

[10] Guanghui, S., Dounan, J., Fukuda, K., and Yujun, G., 2002, "Theoretical and experimental study on density wave oscillation of two-phase natural circulation of low equilibrium quality," Nuclear Engineering and Design, Vol.215, pp.187-198.

[11] Hallinan, K. P., and Viskanta. R., 1986, "Dynamics of a Natural Circulation Loop," Journal of Analysis and Experiments Heat Transfer Engineering, Vol.7, pp.3-4.

[12] Harden, D. G., and Boggs, J. H., 1964, "Transient flow characteristics of a natural-circulation loop operated in the critical region," proceedings of the Heat Transfer and Fluid Mechanics Institute, Stanford University Press, pp.38-50.

[13] Jain, R., 2005, "Thermal-hydraulic instabilities in natural circulation flow loops under supercritical conditions," doctoral dissertation, the University of Wisconsin, Madison, USA.

[14] Jain, R., and Corradini, M. L., 2005, "A linear stability analysis for natural-circulation loops under supercritical conditions," Thermal Hydraulics, Vol.155, pp.312-323.

[15] Jiang, Y. Y., and Shoji, M., 2003, "Flow stability in a natural circulation loop: influence of wall thermal conductivity," Nuclear Engineering and Design, Vol.222, pp.16-28.

[16] Kakac and Veziroglu, T. N., 1983, "Review of two-phase flow instabilities," NATO Advanced study institutes series, series E: Applied sciences, no.64, pp.577-677.

[17] Kang, L. J., 2007, January 6th, "Supercritical Fluid Extraction of Natural Products," Retrieved from http://www.andrew.cmu.edu/user/jitkangl/SFE/Supercritical%20Fluid%20Extraction%20of%20Natural%20Product.htm.

[18] Khartabil, H. F., 2003, "Enhanced passive safety for pressure tube reactors cooled with supercritical water," proceeding of Global 2003, pp.1791-1795.

[19] Lomperski, S., Cho, D., Jain, R., and Corradini, M. L., 2004, "Stability of a natural circulation loop with a fluid heated through the thermodynamic pseudocritical point," proceeding of International Congress on Advances in Nuclear Power Plant, pp.1736-1741.

[20] Mertol, A., and Greif, R., 1985, "A Review of Natural Circulation Loops," proceedings of conference, Natural Convection: Fundamentals and Applications, pp.1033-1071.

[21] Mignot, G., Anderson, M., Corradini, M., 2007, "Critical flow experimental and analysis for supercritical fluid," 3rd International symposium on SCWR design and technology, paper no. SCWR2007-P047, pp.438 - 446.

[22] Misale, M., and Tagliafico L., 1987, "The transient and stability behaviour of single-phase natural circulation loops," Heat and Technology, Vol.5, No.1-2, pp.101-116.

[23] Pioro, I.L., and Duffey, R. B., 2003, "Literature Survey of Heat Transfer and Hydraulic Resistance of Water, Carbon Dioxide, Helium and Other Fluids at

Supercritical and Near-Critical Pressures," Chalk River Laboratories Chalk River, Ontario, Canada.

[24] Pioro, I, L., Khartabil, H, F., and Duffey, R, B., 2004, "Heat transfer to supercritical fluids flowing in channels – empirical correlations (survey)," Nuclear Engineering and Design, Vol.230, pp.69-91.

[25] Pioro, I. L., and Khartabil, H, F., 2005, "Experimental study on heat transfer to supercritical carbon dioxide flowing upward in a vertical tube," 13th International conference on Nuclear Engineering, ICONE13-50118.

[26] Roelofs, F., 2004, "CFD Analyses of heat transfer to supercritical water flowing vertically upward in a tube," NRG report 21353/04.60811/P.

[27] Sienicki, J. J., Moisseytsev, A. V., Wade, D. C., Farmer, M. T., Tzanos, C. P., Stillman, J. A., Holland, J. W., Petkov, P. V., Therios, I. U., Kulak, R. F., and Wu, Q., 2003, "The STAR-LM lead cooled closed fuel fast reactor with a supercritical carbon dioxide brayton cycle advanced power converter," proceedings of Global 2003, ANS/ENS International winter meeting, pp.916-926.

[28] Tom S. K. S., and Hauptmann E. G., 1979, "The feasibility of cooling heavy-water reactors with supercritical fluids," Nuclear Engineering and Design, Vol.53, pp.187-196.

[29] Upadhye, P. D., 2007, "Stability studies of supercritical flow in single channel natural convection loops," doctoral dissertation, University of Manitoba, Canada.

[30] Vijayan, P. K., and Date, A. W., 1992, "The limits of conditional stability for single-phase natural circulation with throughflow in a figure-of-eight loop," Journal of Nuclear Engineering and Design, Vol.136, pp.361–380.

[31] Vijayan, P. K., 2002, "Experimental observations on the general trends of the steady state and stability behaviour of single-phase natural circulation loops," Journal of Nuclear Engineering and Design Vol.215, pp.139–152.

[32] Voodi, A. V., 2004, "Analytical study of non-dimensional parameters governing supercritical flow instabilities," dissertation, the University of Manitoba, Canada.

[33] Wikipedia.org, http://en.wikipedia.org/wiki/CANDU_Reactor.

[34] Yamagata, K., Nishikawa, K., Hasegawa, S., Fujii, T., and Yoshida, S., 1972, "Forced convective heat transfer to supercritical water flowing in tubes," International Journal of Heat and Mass Transfer, Vol.15, pp. 2575-2593.

[35] Yoshiaki, O., and Koshizuka, S., 1993, "Concept and design of a supercritical pressure direct cycle light water reactor," Nuclear Technology, Vol.103, pp.295-302.

[36] Yoshikawa, S., Smith Jr, R, L., Inomata, H., Matsumura, Y., Arai, K., 2005, "Performance of a natural convection circulation system for supercritical fluids," Journal of Supercritical Fluids, Vol.36, pp.70-80.

[37] Zhao, J., Saha, P., and Kazimi, M. S., 2004, "One dimensional thermal hydraulic stability analysis of supercritical fluid cooled reactors," Proceeding of International Conference on Nuclear Engineering, pp.259-268.

[38] Zhao, J., Saha, P., and Kazimi, M. S., 2005, "Stability of supercritical water-cooled reactor during steady-state and sliding pressure start-up," proceeding of 11th International Topical Meeting on Nuclear Reactor Thermal-Hydraulics, paper no.106.

[39] Zvirin, Y., 1981, "A review of natural circulation loops in pressurized water reactors and other systems," Nuclear Engineering and Design, Vol.67, pp.203-225.

APPENDIX - A

A.1 Torque Calculations for loading Flanges with Gaskets

The supercritical flow experimental facility was constructed using flange-and-gasket assemblies. Two different size flanges 31.75 mm and 25.4 mm (1.25 in and 1 in) were used with the flexitalic gaskets. The sealing principle common to gaskets is that a material is clamped between two surfaces being sealed. The clamping force (load) is large enough to deform the gasket material and hold it in tight contact even when the pressure attempts to open the gap between the surfaces. The ASME code (ASME Code Section VIII Division I, Appendix 2, Rules for Bolted Flange Connections with Ring Type Gaskets) was used to calculate the amount of torque to be applied to keep the joints leak proof and pressure tight.

Figure A.1 shows the schematic drawing of the gasket used with the 24.5 mm (1in.) flange assemblies. Sample calculations are provided here for loading a 24.5 mm (1in) size flange and gasket assembly rated for 10 MPa pressure. All the factors that are used in the calculation are obtained from the above mentioned reference.

The minimum initial bolt load required is obtained from the formula

$$W_{m2} = 3.14bGy \qquad \text{-------(A)}$$

Where W_{m2} is the minimum required bolt load for gasket seating, lb

b is the effective gasket or joint-contact surface seating width, in

G is the diameter, in.

When $b_0 \leq 1/4$ in., G = mean diameter of gasket contact face, in.

When $b_0 > 1/4$ in., G = outside diameter of gasket contact face less $2b$, in.

Where b_0 is basic gasket seating width, in.

y = gasket or joint-contact surface unit seating load, psi.

The required bolt load for the operating conditions W_{m1} is determined in accordance with the formula $W_{m1} = H + H_p = 0.785G^2P + (2b \times 3.14GmP)$ -------(B)

Where H is the total hydrostatic end force ($0.785G^2P$), lb

H_p is the total joint contact surface compression load ($2bx3.14GmP$) , lb

P is the internal design pressure, psi.

m is the gasket factor

(from Table 2-5.1 of 1989 Section VIII – Division 1, ASME)

For the present design P is 2200 psi (10 MPa x 1.5(factor of safety) = 15 MPa)

G is 0.925 in (23.5mm)

b_0 is 0.1535 in (3.8mm)

m is 2.5 (for spiral wound metal)

Substituting these values into equation (B) we obtain W_{m1}

$\Rightarrow W_{m1} = H + H_p = 0.785G^2P + (2b \times 3.14GmP)$

$\Rightarrow W_{m1} = 0.785(0.925)^2 2300 + (2x0.1535x3.14x0.925x2.5x2300)$

$\Rightarrow W_{m1} = 6671.94lb$ (2.9678×10^4N)

Nominal diameter of the bolt used in loading the gasket and flange assembly is 0.748 in (19mm)

Torque (T) = 6671.94 x 0.748 $lbin$

T = 4,990.61 $lbin$ (563.8124 Nm)

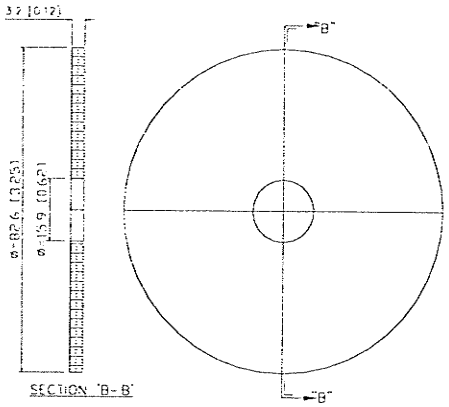

Figure A.1: Schematic drawing of gasket used with 24.5mm (1in.) flange assemblies.

A.2 Manual Opening Procedure for Electro-Pneumatic Valves

The electro pneumatic valves (8 nos.) require a pneumatic supply and 4 to 20 mA of input signal to operate. These valves can also be operated manually in the case the DAS fails to operate them. There are two pneumatic hose connections from the transducer/positioner to the actuator of the flow regulating system which can be connected to a pneumatic supply line inorder to operate them. Figure A.2 shows the pneumatic ports on the actuator and Figure A.3 shows the hose with the JIC fitting used in this process. Following are the steps to be followed in manually operating the electro-pneumatic valves:

1. Disconnect the two pneumatic hose connections from the transducer.
2. Connect the JIC union to the female JIC fitting, which is connected to the actuator.
3. Supply a flow of air at 690 kPa pressure for few seconds.
4. The valve will be opened and the indicator dome on top of the valve assembly turns green indicating that the valve is in open position.
5. Replace the pneumatic hose connections back in their respective locations.

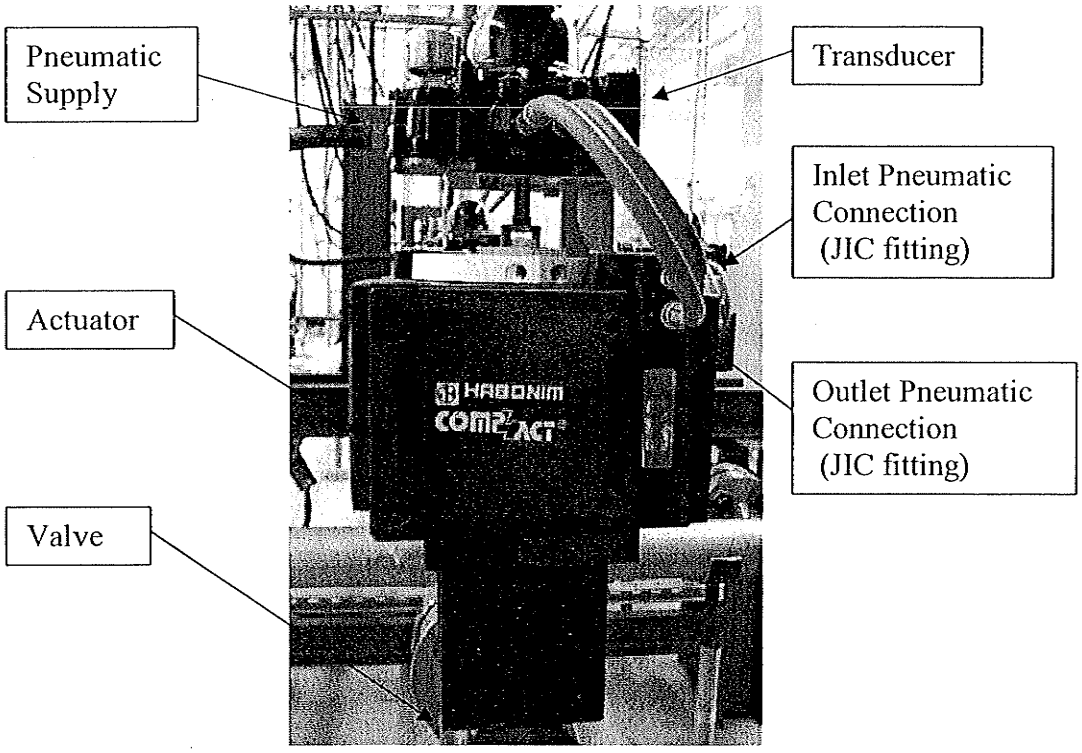

Figure A.2: Pneumatic hose connecting the transducer and the actuator of the flow regulating valves.

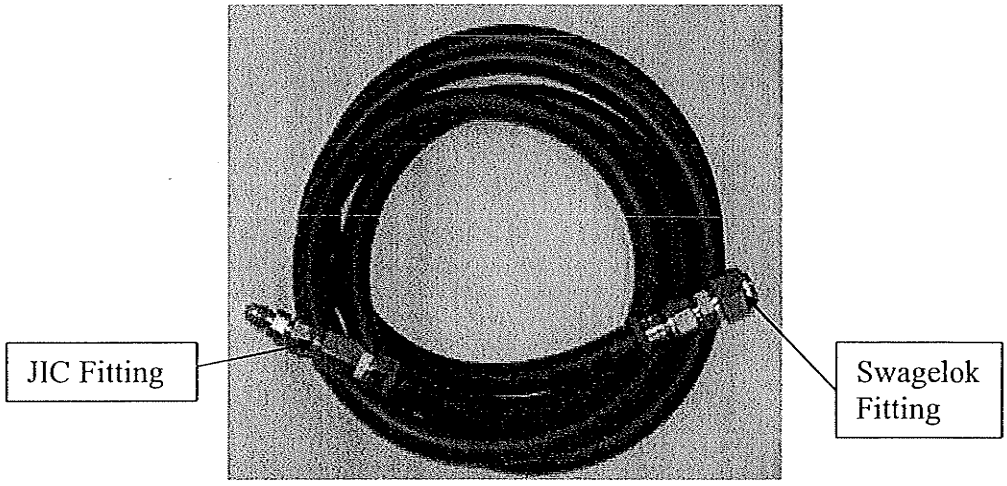

Figure A.3: Pneumatic hose with Swagelok and JIC male union fittings used in manual opening of the flow regulating valves.

A.3 Disconnecting the Settling Chamber from the Experimental Facility

The settling chamber of the experimental facility can be disassembled from the facility by removing the screws from the code 62 fittings. During the chemical cleaning procedure, the settling chamber was removed from the experimental facility and the facility was resealed by using Teflon and stainless steel square strips. The facility was completely sealed by sandwiching teflon strip between the fittings and the stainless steel plate. Figure A.4 shows the disassembled settling chamber from the experimental facility and the facility port sealed, using teflon and stainless steel strips.

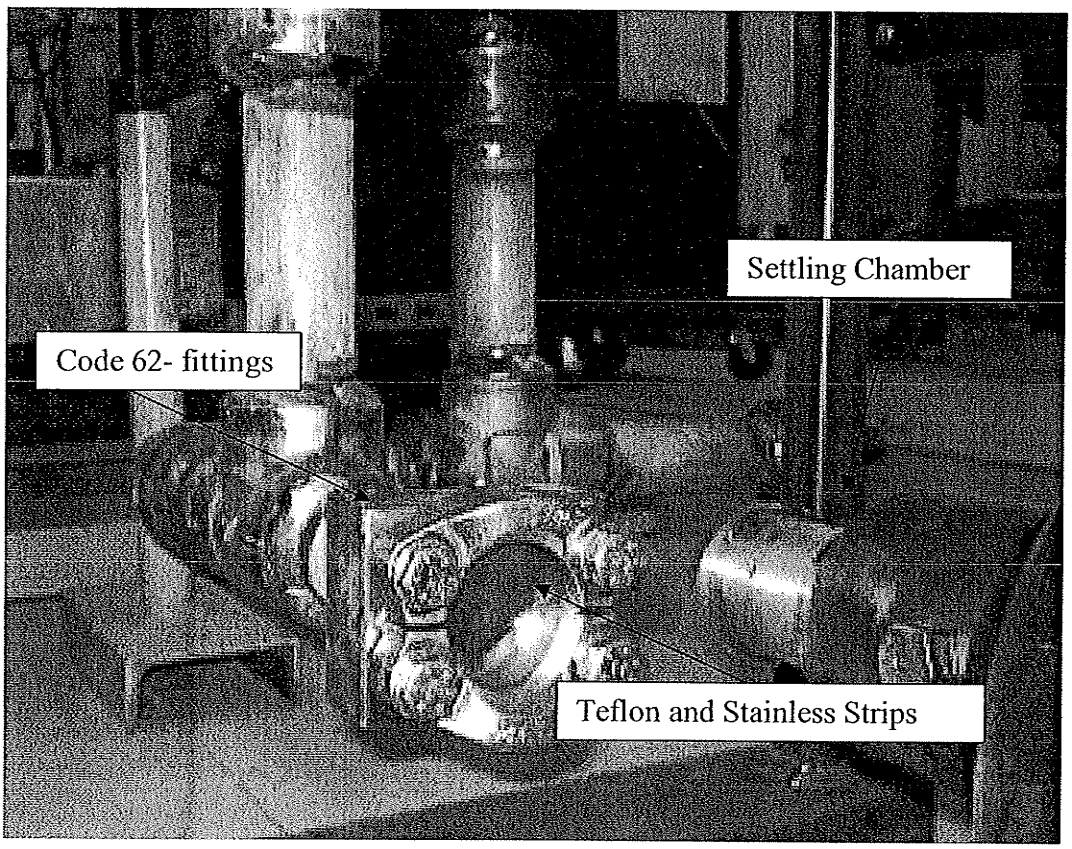

Figure A.4: Picture showing disconnected setting chamber from the experimental facility.

A.4 Supercritical Flow Experimental Facility Operating Instructions

After the chemical cleaning, purging and evacuation procedures are completed, the experimental facility is set to conduct experiments. Any given experiment must be completely designed first before following the facility operating instructions[8].

Experimental facility operating instructions:

Step 1: Switch on the main power supply (Figure.A.5.a) located in the electrical room.

Step 2: Switch on the AC-DC power converter (Figure.A.5.b) and set the power input (0 to 30kW) to the experimental facility. The voltage and current readings can be monitored on this power converter (rectifier).

Step 3: Switch on the main circuit breaker switch (Figure.A.5.c).

Step 4: Switch on the individual circuit breaker for channels (Figure.A.5.d). Either one channel or any two channels or three channels may be switched on as needed.

Step 5: Switch on the power (Figure.A.5.e) to the chiller.

Step 6: Switch on the chiller (Figure.A.5.f) and set the required chill water outlet conditions.

Step 7: Switch on the power to the control panel (Figure.A.5.g) of the heat removal system and program it for the required heat removal rate.

Step 8: Switch on the data acquisition system (Figure.A.5.h) and set the program to record the temperature and pressure readings during the experiment.

Step 9: Switch on the air compressor (Figure.A.5.i) and set the required outlet pressure.

[8] Trouble shooting for any of these control panels and in-depth operating instructions are available in their respective manuals and with supercritical flow experimental facility operational manual.

Step 10: Switch on the test section breaker (Figure.A.5.j) for a corresponding experiment (single channel / double channel / triple channel); any of the three test tubes may be powered.

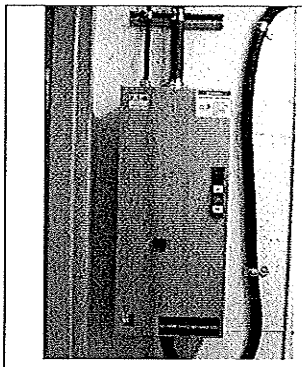

Figure A.5.a

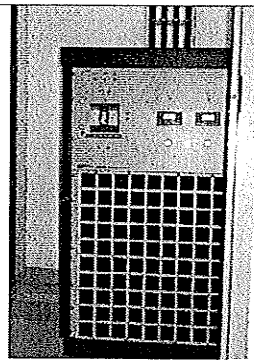

Figure A.5.b

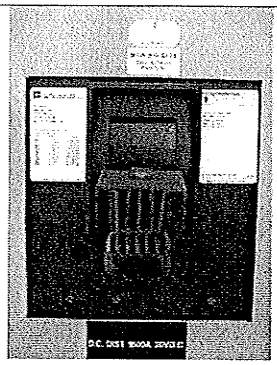

Figure A.5.c

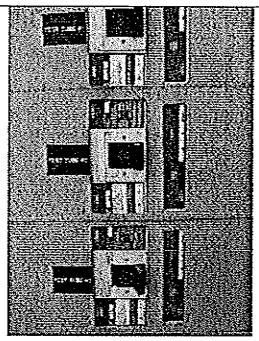

Figure A.5.d

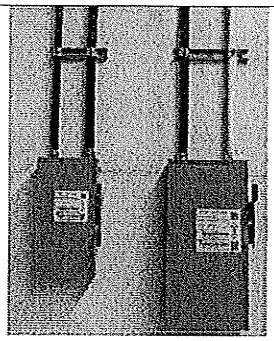

Figure A.5.e

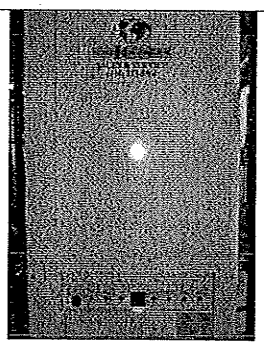

Figure A.5.f

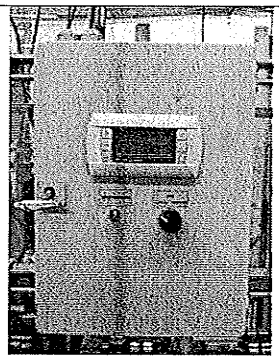

Figure A.5.g

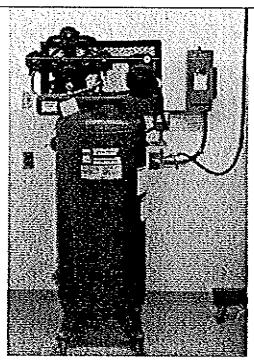

Figure A.5.h

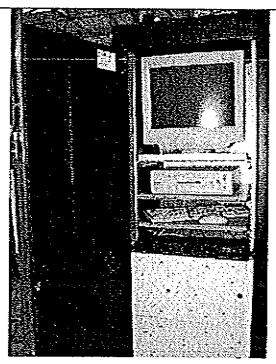

Figure A.5.i

Figure A.5: Various control panels on the supercritical flow experimental facility.

A.5 Pressurizing the Experimental Facility with Carbon dioxide

This section describes the procedures to be followed in pressurizing the experimental facility with carbon dioxide. After pre-experimental procedure the experimental facility was pressurizing with carbon dioxide (working fluid).

The following steps are to be followed when pressurizing the experimental facility with carbon dioxide.

Steps to be followed:

Step 1: Close valve V_2 on the experimental facility (Figure 5.3).

Step 2: Connect gas booster to valve V_1 (Figure 5.1) through a stainless steel braided flexible hose.

Step 3: Connect the pneumatic supply to the gas booster and regulate the supply air pressure as required (620 kPa).

Step 4: Connect the carbon dioxide gas cylinder to the gas booster. Use the gas regulator provided on the cylinder to regulate the gas outlet pressure.

Step 5: Open valve V_1.

Step 6: Purge the gas regulator during changing the gas cylinders. Two gas cylinders (K-size, grade 4.0, Praxair®) are required to fill the experimental facility to 8.2 MPa (1200 psi).

Step 7: Close valve V_1 when designed pressure is achieved within the facility (monitor pressure gauge/absolute pressure gauge on DAS).

Step 7: Disconnect the gas booster assembly from the valve V_1

A.6 Swagelok Tube Fittings

Swagelok compression fittings were used extensively in the construction of the supercritical experimental facility. These fittings were chosen for their wide range of application and easy installation. However proper understanding and installation of these fittings is necessary before selecting and using these compression fittings (the author has successfully completed a Swagelok tube fitting installation[9] training course).

Swagelok tube fitting is a flareless, mechanical-grip fitting consisting of a body, nut, front ferrule and back ferrule. Figure A.6 shows the Swagelok tube fitting (male connector) with tube inserted into the Swagelok nut. Front and back ferrules in the nut compress the tube and provide the necessary mechanical grip and sealing. Further instructions on the usage of various Swagelok fittings and on assembly instructions may be found in the Swagelok tube fitter's manual.

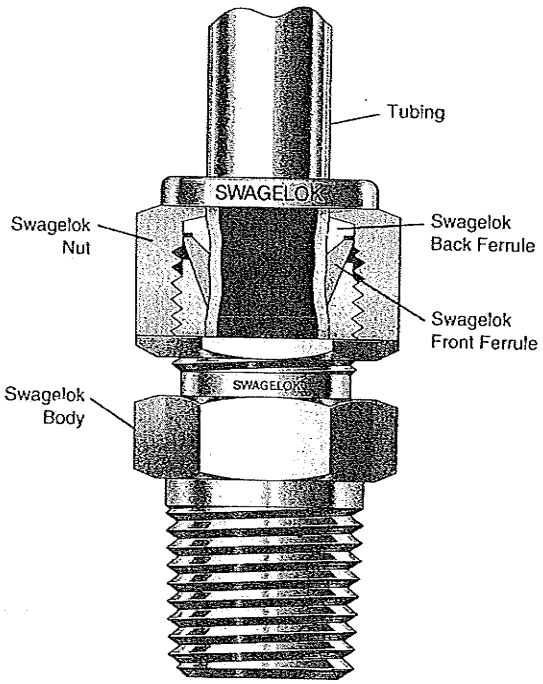

Figure A.6: Schematic drawing of Swagelok tube fitting.

[9] http://www.swagelok.com/FittingInstallVideo.htm.

A.7 Supercritical Flow Experimental Facility Pictures

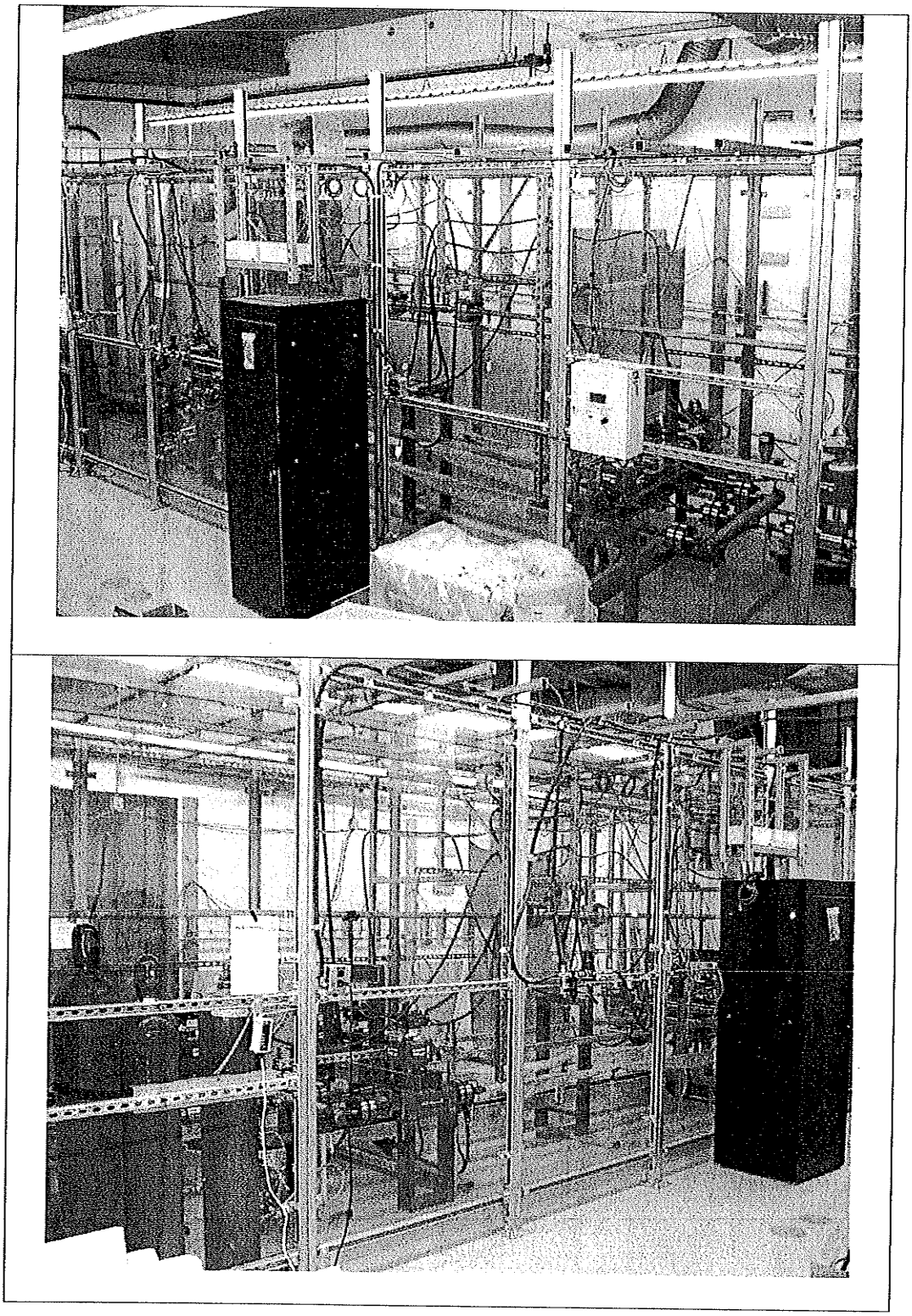

Figure A.7: Photographs of supercritical flow experimental facility (I).

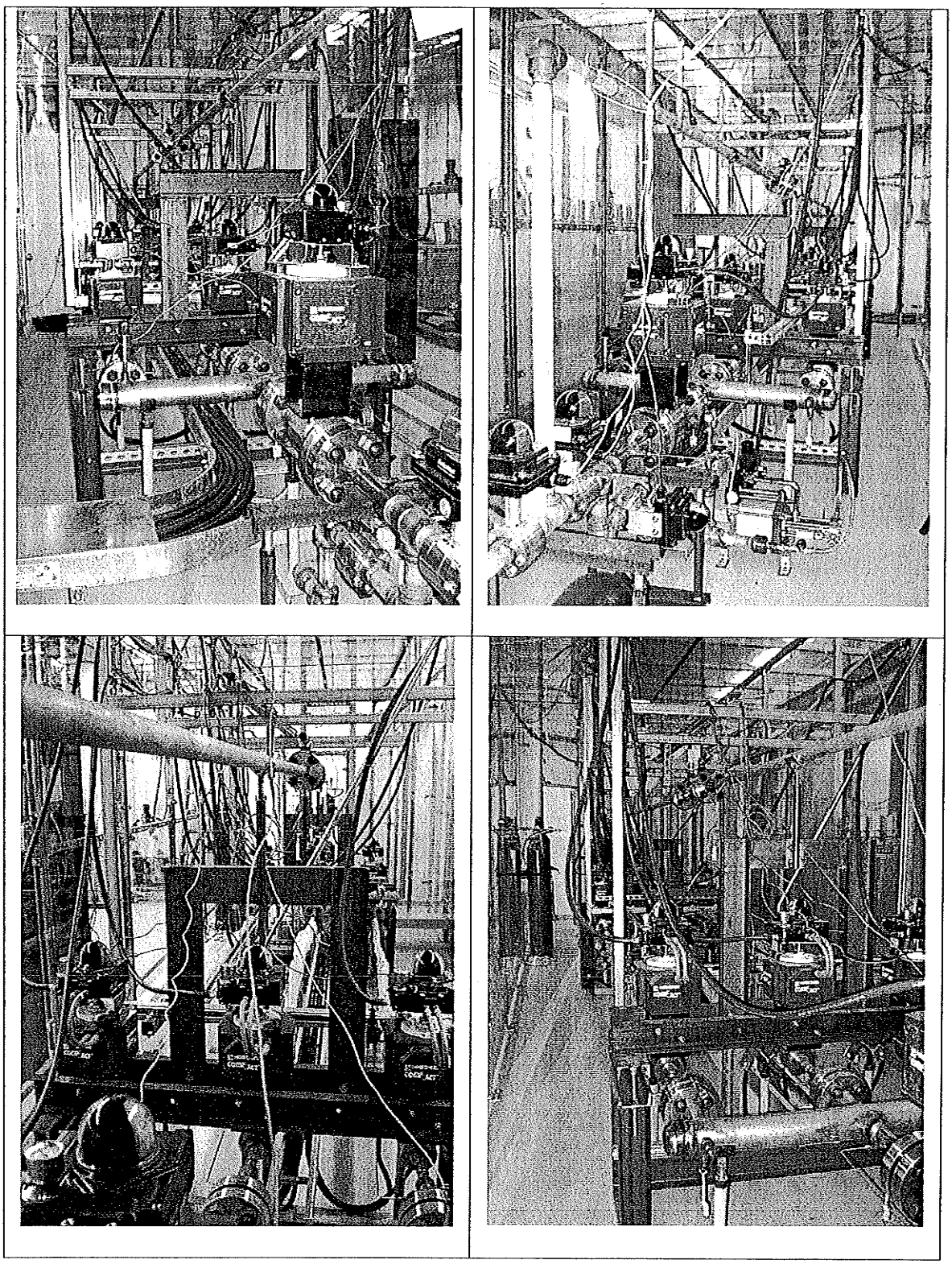

Figure A.8: Photographs of supercritical flow experimental facility (II).

A.8 List of Materials Procured

	Major System	List of material procured by author
1	Loop piping	1 1/4" 316 SS Socket weld elbow joints 1 1/4" 316 SS Socket tee weld joints 1 1/4" x 1/2" 316 SS Socket weld reducing coupling 1 1/4" 316 SS weld neck flanges 1/8" 316 SS Threaded couplings 1/4" 316 SS Threaded couplings 1 1/4" 304 SS Gaskets 1/4" 316 SS Plugs 1/4" 316 SS Nuts 1/4" 316 SS Male adapters 1/4" 316 SS Female connector 1/8" 316 SS Male connectors 1/8" 316 SS Plugs
2	Test Section	1/2" PB Inconel rupture discs 1/2" 316 SS Tube 1/2" 316 SS Elbow tube fittings 1/2" 316 SS Tee tube fitting 1/2" x 3/4" 316 SS Reducer tube fitting 1 1/4" x 1/2" 316 SS Reducing adapter 1/2" 316 SS Plugs 3/4" SS 316 Tube 3/4" SS 316 Elbow tube fitting 1/2" 316 SS Ferrule sets (front and back) 3/4" 316 SS Ferrule sets (front and back) 1/8" 316 SS Plugs 1/8" 316 SS Nuts 1/8" 316 Ferrule sets (front and back) 1/8" 316 SS Tube
3	Heat Removal Control System	Propylene glycol 1 1/4" Rubber hose 1 1/4" 316 SS Male connectors 1 1/4" 316 SS Female connector 1 1/4" 316 SS Union elbow 1 1/4" 304 Coupling

		1 1/4" Hose barb 1 1/4" 304 SS Nipple 1 1/4" 304 SS Hex union
4	Pressure Control System	1/4" 316 SS braided hose CGA 580 Fitting 1/4" Check valve
5	Settling Chamber	Gas bottle 1 1/4" Code 61 fittings sets 1 /14" 316 SS Ball valves
6	Carbon dioxide Supply	CGA 320 Fitting 429 High pressure gas regulator 1/4" Brass Purge valve 1/4" SS Braided hoses 1/4" 316 SS Female connector 9/16"- 18 x 1/4" FNPT adapters Gas Booster 1/4" 316 SS Male connector 1/4" 316 SS Female adapter 1/4" 316 SS Check valve 1/4" 316 SS Needle valve 1/2" x 1/4" 316 SS Reducer
7	Electro-Pneumatic Valves	Air Compressor 3/8" Rubber hose 3/8" Coalescing filter 3/8" Pneumatic regulator 3/8" Brass Tee tube fittings 3/8" Brass Union tube fittings 3/8" Brass Male connectors 3/8" Brass Hose barb fittings 3/8" Brass ball valve 1/4" Pressure gauge
8	Data Acquisition System and Instrumentation	Thermocouple wiring Thermocouple connecting plugs
9	Power Supply	Surge protected extension cords Emergency power shutdown switches

10	Support Structure	C - Channels (carbon steel) 1/2" Threaded rod Fasteners (various general purpose) Poly carbonate sheets Steel channels and struts
11	Evacuation System	1 1/4" x 1/2" 316 SS socket weld adapter 1/2" 316 SS Needle valve 1/2" x 1/4" 316 SS Reducer 1/4" 316 SS Female adapter 1/4" SS Gauge (Vacuum) 1/4" SS Gauge - Pressure 1/2" x 3/8" NPT 316 SS Nipple 3/8" 316 SS Needle valves 3/8" 316 SS Tee fittings 3/8" 316 SS Port connector 3/8" 316 SS Flexible hose 3/8" 316 SS Tube 3/8" 316 SS Check valve 3/8" 316 SS Ferrule set (Front and back) 1/8" x 3/8" 316 SS Reducer
12	Safety Features	Carbon dioxide gas detector
13	Miscellaneous Devices	1 1/4 316 SS Habonim ball valve repair kits 1 1/4 316 SS Habonim ball valves 1/2" Threaded rods Compressor oil Vacuum pump oil Carbon dioxide gas cylinders Nitrogen gas cylinders Heating tape Swagelok and Parker fittings General purpose fasteners
14	Services	Electrical contract works Welding Tube fitting Swagelok fittings installation Pressure transducers calibration

Pressure testing
Chemical cleaning
Chiller Installation
Chiller exhaust duct work
Electrical power exhaust duct work

APPENDIX – B

B.1 Numerical Simulation

Sample Input file used in performing numerical simulations using carbon dioxide and supercritical flow experimental facility configuration.

B.1.1 Input File

```
/----------
/CASE TITLE
/----------
/TITLE   NAME
/    !                                        !
TITLE   Candu-X Stability Assessment
/-----------
/OPTIONS DATA
/-----------
/100       IOUT   IPLOT   IPLOT6   NSUBC    NOSV    NHEAT    ICHF
/    !     !      !       !        !        !       !        !
100         1      1      60       0        0       0        0
/100       ITR    NOPT    IFOPT    NEXP     NRES    IPLT     KOPT
/    !     !      !       !        !        !       !        !
100         0      0       0        0        0       1        0
/101       HC1    HC2     ITYPE    NCH
/          !      !       !        !
101        2.0    3.0     1        1
/------------
/GEOMETRIC DATA (HR geom)
/------------
/200       NREG     CHK
/    !     !        !
200         10      .04
/201(250)    RLEN       A        DE     ANGLE    NSECT
/    !      !         !        !      !        !
201        1.375  4.076e-4   .02278     0       14
201        0.895  1.819e-4   .01522     0       9
201        3.021  1.317e-4   .01295     0       30
201        0.895  1.819e-4   .01522     0       9
201        1.285  4.076e-4   .02278     0       13
201        1.020  4.076e-4   .02278     90.     10
201        3.380  4.076e-4   .02278     0       34
201        .711   8.302e-2   .32512     0       7
201        3.380  4.076e-4   .02278     0       34
201        1.020  4.076e-4   .02278    -90.     10
/299       IRPT     NCOD      TFA      TRK     TRUFF
/    !     !        !         !        !       !
299         8       3        0.0      0       0
299         1       3        0.0      0.      0
299         5       3        0        0       0
299         4       3        0        0       0
299         1       3        0        0.      0
299         4       3        0        0       0
299         30      1        1.0      0       0
299         4       3        0        0       0
299         1       3        0        10.     0
299         4       3        0        0       0
299         4       3        0        0       0
299         1       3        0        0.      0
299         8       3        0        0       0
299         10      3        0.0      0.0     0
299         34      3        0.0      0.0     0
299         7       40      -1.0      0.853   0
299         34      3        0.0      0       0
299         10      3        0.0      0       0
299         0       0        0        0       0       0       0       0       0
299         0       0        0        0       0       0       0       0       0
/------------------
/BOUNDARY CONDITIONS
/------------------
/300       POW      TIN      FLOW     PIN      PEX      ZIN
/    !     !        !        !        !        !        !
300         .25     28.      .08      75.E2    75.E2
/301      RHOFLG    TFLG     PRFLG    N2PH
/    !    !        !        !        !
```

```
301        0.000     0.0     5.0      2
/--------------
/TRANSIENT DATA
/--------------
/                              DELKF/
/400          DT    FSDT     RAMP     FPOW   SHDPOW   SDTDLY  REACTIR   SHDRTY
/    !        !     !        !        !      !        !       !         !
400          .02    75.0        0    8.01
/--------------
/FUEL MODEL DATA
/--------------
/500    NFPINS(TOT)   PINLEN     RADS     RADG     RADF
/    !        !        !        !        !        !
500             1    3.021   .039250   .03925   .03925
/501          CPF     DENF       HG     THCF     THCS   RCTEMP   RFTEMP
/    !        !       !        !        !        !        !
501         450.0   5430.0   1.0E90      152     220.     40.      40.
/--------------------
/NEUTRON KINETIC DATA (SHIM PLATES INSERTED)
/--------------------
```

B.1.2 Output File

```
                    ++++++++++++++++++++++++++++++++++
                    +      SPORTS PACKAGE          +
                    +  COPY OF USER INPUT TO SPORTS  +
                    ++++++++++++++++++++++++++++++++++

 CARD
NUMBER                          CARD IMAGE
     1      10      20      30      40      50      60      70      80      90      100     110
.....V.....V.....V.....V.....V.....V.....V.....V.....V.....V.....V.....V.....V.....V.....V.....
***** /---------
***** /CASE TITLE
***** /---------
***** /TITLE   NAME
***** /      !                                                  !
00001 TITLE    Candu-X Stability Assessment
***** /------------
***** /OPTIONS DATA
***** /------------
***** /100         IOUT    IPLOT   IPLOT6    NSUBC     NOSV    NHEAT     ICHF
***** /     !      !       !       !         !         !       !         !
00002 100           1       1      60        0         0       0         0
***** /100         ITR     NOPT    IFOPT     NEXP      NRES    IPLT      KOPT
***** /     !      !       !       !         !         !       !         !
00003 100           0       0       0        0         0       1         0
***** /101         HC1     HC2     ITYPE     NCH
***** /             !       !       !         !
00004 101          2.0     3.0       1       1
***** /-------------
***** /GEOMETRIC DATA (HR geom)
***** /-------------
***** /200         NREG      CHK
***** /     !      !         !
00005 200           10      .04
***** /201(250)     RLEN      A       DE      ANGLE     NSECT
***** /     !      !         !       !       !         !
00006 201         1.375  4.076e-4   .02278      0        14
00007 201         0.895  1.819e-4   .01522      0         9
00008 201         3.021  1.317e-4   .01295      0        30
00009 201         0.895  1.819e-4   .01522      0         9
00010 201         1.285  4.076e-4   .02278      0        13
00011 201         1.020  4.076e-4   .02278     90.       10
00012 201         3.380  4.076e-4   .02278      0        34
00013 201          .711  8.302e-2   .32512      0         7
00014 201         3.380  4.076e-4   .02278      0        34
00015 201         1.020  4.076e-4   .02278    -90.       10
***** /299         IRPT      NCOD      TFA       TRK      TRUFF
***** /     !      !         !         !         !        !
00016 299           8         3       0.0       0        0
00017 299           1         3       0.0       0.       0
00018 299           5         3         0       0        0
00019 299           4         3         0       0        0
00020 299           1         3         0       0.       0
00021 299           4         3         0       0        0
```

```
00022 299          30     1    1.0     0     0
00023 299          4      3    0       0     0
00024 299          1      3    0       10.   0
00025 299          4      3    0       0     0
00026 299          4      3    0       0     0
00027 299          1      3    0       0.    0
00028 299          8      3    0       0     0
00029 299          10     3    0.0     0.0     0
00030 299          34     3    0.0     0.0     0
00031 299          7      40   -1.0    0.853     0
00032 299          34     3    0.0     0     0
00033 299          10     3    0.0     0     0
00034 299          0      0    0       0     0     0     0     0     0
00035 299          0      0    0       0     0     0     0     0     0
***** /-----------------
***** /BOUNDARY CONDITIONS
***** /------------------
***** /300         POW     TIN     FLOW     PIN     PEX     ZIN
***** /     !     !       !       !        !       !       !
00036 300          .25     28.     .08     75.E2   75.E2
***** /301        RHOFLG    TFLG    PRFLG    N2PH
***** /     !     !       !       !        !
00037 301          0.000     0.0     5.0      2
***** /--------------
***** /TRANSIENT DATA
***** /--------------
***** /                              DELKF/
***** /400          DT     FSDT     RAMP     FPOW    SHDPOW   SDTDLY  REACTIR   SHDRTY
***** /     !      !      !        !        !       !       !       !
00038 400          .02     75.0      0     8.01
***** /---------------
***** /FUEL MODEL DATA
***** /--------------
***** /500    NFPINS(TOT)   PINLEN     RADS     RADG     RADF
***** /     !      !       !        !       !       !
00039 500            1     3.021   .039250   .03925   .03925
***** /501          CPF     DENF      HG      THCF     THCS    RCTEMP   RFTEMP
***** /     !      !       !        !       !       !       !
00040 501          450.0   5430.0   1.0E90     152     220.     40.     40.
***** /-------------------
***** /NEUTRON KINETIC DATA (SHIM PLATES INSERTED)
***** /--------------------
00041
***** WARNING : coefficients and their respective powers (card group 299) records ID only are read
```

SUMMARY OF INPUT DATA : Candu-X Stability Assessment

NODE NUMBER	AREA M2	LENGTH M	POWER DISTRIBUTION	RESTRICTION LOSS COEFF.	GRAVITY INDEX	SECTION CODE	SECTION NAME
00001	0.407600E-03	0.982143E-01	0.000000E+00	0.000000E+00	0.000000E+00	00003	RISER
00002	0.407600E-03	0.982143E-01	0.000000E+00	0.000000E+00	0.000000E+00	00003	RISER
00003	0.407600E-03	0.982143E-01	0.000000E+00	0.000000E+00	0.000000E+00	00003	RISER
00004	0.407600E-03	0.982143E-01	0.000000E+00	0.000000E+00	0.000000E+00	00003	RISER
00005	0.407600E-03	0.982143E-01	0.000000E+00	0.000000E+00	0.000000E+00	00003	RISER
00006	0.407600E-03	0.982143E-01	0.000000E+00	0.000000E+00	0.000000E+00	00003	RISER
00007	0.407600E-03	0.982143E-01	0.000000E+00	0.000000E+00	0.000000E+00	00003	RISER
00008	0.407600E-03	0.982143E-01	0.000000E+00	0.000000E+00	0.000000E+00	00003	RISER
00009	0.407600E-03	0.982143E-01	0.000000E+00	0.000000E+00	0.000000E+00	00003	RISER
00010	0.407600E-03	0.982143E-01	0.000000E+00	0.000000E+00	0.000000E+00	00003	RISER
00011	0.407600E-03	0.982143E-01	0.000000E+00	0.000000E+00	0.000000E+00	00003	RISER
00012	0.407600E-03	0.982143E-01	0.000000E+00	0.000000E+00	0.000000E+00	00003	RISER
00013	0.407600E-03	0.982143E-01	0.000000E+00	0.000000E+00	0.000000E+00	00003	RISER
00014	0.407600E-03	0.982143E-01	0.000000E+00	0.000000E+00	0.000000E+00	00003	RISER
00015	0.407600E-03	0.000000E+00	0.000000E+00	0.000000E+00	0.000000E+00	00002	BOUNDARY
00016	0.181900E-03	0.994444E-01	0.000000E+00	0.000000E+00	0.000000E+00	00003	RISER
00017	0.181900E-03	0.994444E-01	0.000000E+00	0.000000E+00	0.000000E+00	00003	RISER
00018	0.181900E-03	0.994444E-01	0.000000E+00	0.000000E+00	0.000000E+00	00003	RISER
00019	0.181900E-03	0.994444E-01	0.000000E+00	0.000000E+00	0.000000E+00	00003	RISER
00020	0.181900E-03	0.994444E-01	0.000000E+00	0.000000E+00	0.000000E+00	00003	RISER
00021	0.181900E-03	0.994444E-01	0.000000E+00	0.000000E+00	0.000000E+00	00003	RISER
00022	0.181900E-03	0.994444E-01	0.000000E+00	0.000000E+00	0.000000E+00	00003	RISER
00023	0.181900E-03	0.994444E-01	0.000000E+00	0.000000E+00	0.000000E+00	00003	RISER
00024	0.181900E-03	0.994444E-01	0.000000E+00	0.000000E+00	0.000000E+00	00003	RISER
00025	0.181900E-03	0.000000E+00	0.000000E+00	0.000000E+00	0.000000E+00	00002	BOUNDARY
00026	0.131700E-03	0.100700E+00	0.100000E+01	0.000000E+00	0.000000E+00	00001	HEAT.SEC
00027	0.131700E-03	0.100700E+00	0.100000E+01	0.000000E+00	0.000000E+00	00001	HEAT.SEC

00028	0.131700E-03	0.100700E+00	0.100000E+01	0.000000E+00	0.000000E+00	00001	HEAT.SEC
00029	0.131700E-03	0.100700E+00	0.100000E+01	0.000000E+00	0.000000E+00	00001	HEAT.SEC
00030	0.131700E-03	0.100700E+00	0.100000E+01	0.000000E+00	0.000000E+00	00001	HEAT.SEC
00031	0.131700E-03	0.100700E+00	0.100000E+01	0.000000E+00	0.000000E+00	00001	HEAT.SEC
00032	0.131700E-03	0.100700E+00	0.100000E+01	0.000000E+00	0.000000E+00	00001	HEAT.SEC
00033	0.131700E-03	0.100700E+00	0.100000E+01	0.000000E+00	0.000000E+00	00001	HEAT.SEC
00034	0.131700E-03	0.100700E+00	0.100000E+01	0.000000E+00	0.000000E+00	00001	HEAT.SEC
00035	0.131700E-03	0.100700E+00	0.100000E+01	0.000000E+00	0.000000E+00	00001	HEAT.SEC
00036	0.131700E-03	0.100700E+00	0.100000E+01	0.000000E+00	0.000000E+00	00001	HEAT.SEC
00037	0.131700E-03	0.100700E+00	0.100000E+01	0.000000E+00	0.000000E+00	00001	HEAT.SEC
00038	0.131700E-03	0.100700E+00	0.100000E+01	0.000000E+00	0.000000E+00	00001	HEAT.SEC
00039	0.131700E-03	0.100700E+00	0.100000E+01	0.000000E+00	0.000000E+00	00001	HEAT.SEC
00040	0.131700E-03	0.100700E+00	0.100000E+01	0.000000E+00	0.000000E+00	00001	HEAT.SEC
00041	0.131700E-03	0.100700E+00	0.100000E+01	0.000000E+00	0.000000E+00	00001	HEAT.SEC
00042	0.131700E-03	0.100700E+00	0.100000E+01	0.000000E+00	0.000000E+00	00001	HEAT.SEC
00043	0.131700E-03	0.100700E+00	0.100000E+01	0.000000E+00	0.000000E+00	00001	HEAT.SEC
00044	0.131700E-03	0.100700E+00	0.100000E+01	0.000000E+00	0.000000E+00	00001	HEAT.SEC
00045	0.131700E-03	0.100700E+00	0.100000E+01	0.000000E+00	0.000000E+00	00001	HEAT.SEC
00046	0.131700E-03	0.100700E+00	0.100000E+01	0.000000E+00	0.000000E+00	00001	HEAT.SEC
00047	0.131700E-03	0.100700E+00	0.100000E+01	0.000000E+00	0.000000E+00	00001	HEAT.SEC
00048	0.131700E-03	0.100700E+00	0.100000E+01	0.000000E+00	0.000000E+00	00001	HEAT.SEC
00049	0.131700E-03	0.100700E+00	0.100000E+01	0.000000E+00	0.000000E+00	00001	HEAT.SEC
00050	0.131700E-03	0.100700E+00	0.100000E+01	0.000000E+00	0.000000E+00	00001	HEAT.SEC

1

SUMMARY OF INPUT DATA : Candu-X Stability Assessment

NODE NUMBER	AREA M2	LENGTH M	POWER DISTRIBUTION	RESTRICTION LOSS COEFF.	GRAVITY INDEX	SECTION CODE	SECTION NAME
00051	0.131700E-03	0.100700E+00	0.100000E+01	0.000000E+00	0.000000E+00	00001	HEAT.SEC
00052	0.131700E-03	0.100700E+00	0.100000E+01	0.000000E+00	0.000000E+00	00001	HEAT.SEC
00053	0.131700E-03	0.100700E+00	0.100000E+01	0.000000E+00	0.000000E+00	00001	HEAT.SEC
00054	0.131700E-03	0.100700E+00	0.100000E+01	0.000000E+00	0.000000E+00	00001	HEAT.SEC
00055	0.131700E-03	0.100700E+00	0.100000E+01	0.000000E+00	0.000000E+00	00001	HEAT.SEC
00056	0.131700E-03	0.000000E+00	0.000000E+00	0.000000E+00	0.000000E+00	00002	BOUNDARY
00057	0.181900E-03	0.994444E-01	0.000000E+00	0.000000E+00	0.000000E+00	00003	RISER
00058	0.181900E-03	0.994444E-01	0.000000E+00	0.000000E+00	0.000000E+00	00003	RISER
00059	0.181900E-03	0.994444E-01	0.000000E+00	0.000000E+00	0.000000E+00	00003	RISER
00060	0.181900E-03	0.994444E-01	0.000000E+00	0.000000E+00	0.000000E+00	00003	RISER
00061	0.181900E-03	0.994444E-01	0.000000E+00	0.100000E+02	0.000000E+00	00003	RISER
00062	0.181900E-03	0.994444E-01	0.000000E+00	0.000000E+00	0.000000E+00	00003	RISER
00063	0.181900E-03	0.994444E-01	0.000000E+00	0.000000E+00	0.000000E+00	00003	RISER
00064	0.181900E-03	0.994444E-01	0.000000E+00	0.000000E+00	0.000000E+00	00003	RISER
00065	0.181900E-03	0.994444E-01	0.000000E+00	0.000000E+00	0.000000E+00	00003	RISER
00066	0.181900E-03	0.000000E+00	0.000000E+00	0.000000E+00	0.000000E+00	00002	BOUNDARY
00067	0.407600E-03	0.988462E-01	0.000000E+00	0.000000E+00	0.000000E+00	00003	RISER
00068	0.407600E-03	0.988462E-01	0.000000E+00	0.000000E+00	0.000000E+00	00003	RISER
00069	0.407600E-03	0.988462E-01	0.000000E+00	0.000000E+00	0.000000E+00	00003	RISER
00070	0.407600E-03	0.988462E-01	0.000000E+00	0.000000E+00	0.000000E+00	00003	RISER
00071	0.407600E-03	0.988462E-01	0.000000E+00	0.000000E+00	0.000000E+00	00003	RISER
00072	0.407600E-03	0.988462E-01	0.000000E+00	0.000000E+00	0.000000E+00	00003	RISER
00073	0.407600E-03	0.988462E-01	0.000000E+00	0.000000E+00	0.000000E+00	00003	RISER
00074	0.407600E-03	0.988462E-01	0.000000E+00	0.000000E+00	0.000000E+00	00003	RISER
00075	0.407600E-03	0.988462E-01	0.000000E+00	0.000000E+00	0.000000E+00	00003	RISER
00076	0.407600E-03	0.988462E-01	0.000000E+00	0.000000E+00	0.000000E+00	00003	RISER
00077	0.407600E-03	0.988462E-01	0.000000E+00	0.000000E+00	0.000000E+00	00003	RISER
00078	0.407600E-03	0.988462E-01	0.000000E+00	0.000000E+00	0.000000E+00	00003	RISER
00079	0.407600E-03	0.988462E-01	0.000000E+00	0.000000E+00	0.000000E+00	00003	RISER
00080	0.407600E-03	0.102000E+00	0.000000E+00	0.000000E+00	0.100000E+01	00003	RISER
00081	0.407600E-03	0.102000E+00	0.000000E+00	0.000000E+00	0.100000E+01	00003	RISER
00082	0.407600E-03	0.102000E+00	0.000000E+00	0.000000E+00	0.100000E+01	00003	RISER
00083	0.407600E-03	0.102000E+00	0.000000E+00	0.000000E+00	0.100000E+01	00003	RISER
00084	0.407600E-03	0.102000E+00	0.000000E+00	0.000000E+00	0.100000E+01	00003	RISER
00085	0.407600E-03	0.102000E+00	0.000000E+00	0.000000E+00	0.100000E+01	00003	RISER
00086	0.407600E-03	0.102000E+00	0.000000E+00	0.000000E+00	0.100000E+01	00003	RISER
00087	0.407600E-03	0.102000E+00	0.000000E+00	0.000000E+00	0.100000E+01	00003	RISER
00088	0.407600E-03	0.102000E+00	0.000000E+00	0.000000E+00	0.100000E+01	00003	RISER
00089	0.407600E-03	0.102000E+00	0.000000E+00	0.000000E+00	0.100000E+01	00003	RISER
00090	0.407600E-03	0.994118E-01	0.000000E+00	0.000000E+00	0.000000E+00	00003	RISER
00091	0.407600E-03	0.994118E-01	0.000000E+00	0.000000E+00	0.000000E+00	00003	RISER
00092	0.407600E-03	0.994118E-01	0.000000E+00	0.000000E+00	0.000000E+00	00003	RISER
00093	0.407600E-03	0.994118E-01	0.000000E+00	0.000000E+00	0.000000E+00	00003	RISER
00094	0.407600E-03	0.994118E-01	0.000000E+00	0.000000E+00	0.000000E+00	00003	RISER
00095	0.407600E-03	0.994118E-01	0.000000E+00	0.000000E+00	0.000000E+00	00003	RISER
00096	0.407600E-03	0.994118E-01	0.000000E+00	0.000000E+00	0.000000E+00	00003	RISER
00097	0.407600E-03	0.994118E-01	0.000000E+00	0.000000E+00	0.000000E+00	00003	RISER
00098	0.407600E-03	0.994118E-01	0.000000E+00	0.000000E+00	0.000000E+00	00003	RISER

00099	0.407600E-03	0.994118E-01	0.000000E+00	0.000000E+00	0.000000E+00	00003	RISER
00100	0.407600E-03	0.994118E-01	0.000000E+00	0.000000E+00	0.000000E+00	00003	RISER

1

SUMMARY OF INPUT DATA : Candu-X Stability Assessment

NODE NUMBER	AREA M2	LENGTH M	POWER DISTRIBUTION	RESTRICTION LOSS COEFF.	GRAVITY INDEX	SECTION CODE	SECTION NAME
00101	0.407600E-03	0.994118E-01	0.000000E+00	0.000000E+00	0.000000E+00	00003	RISER
00102	0.407600E-03	0.994118E-01	0.000000E+00	0.000000E+00	0.000000E+00	00003	RISER
00103	0.407600E-03	0.994118E-01	0.000000E+00	0.000000E+00	0.000000E+00	00003	RISER
00104	0.407600E-03	0.994118E-01	0.000000E+00	0.000000E+00	0.000000E+00	00003	RISER
00105	0.407600E-03	0.994118E-01	0.000000E+00	0.000000E+00	0.000000E+00	00003	RISER
00106	0.407600E-03	0.994118E-01	0.000000E+00	0.000000E+00	0.000000E+00	00003	RISER
00107	0.407600E-03	0.994118E-01	0.000000E+00	0.000000E+00	0.000000E+00	00003	RISER
00108	0.407600E-03	0.994118E-01	0.000000E+00	0.000000E+00	0.000000E+00	00003	RISER
00109	0.407600E-03	0.994118E-01	0.000000E+00	0.000000E+00	0.000000E+00	00003	RISER
00110	0.407600E-03	0.994118E-01	0.000000E+00	0.000000E+00	0.000000E+00	00003	RISER
00111	0.407600E-03	0.994118E-01	0.000000E+00	0.000000E+00	0.000000E+00	00003	RISER
00112	0.407600E-03	0.994118E-01	0.000000E+00	0.000000E+00	0.000000E+00	00003	RISER
00113	0.407600E-03	0.994118E-01	0.000000E+00	0.000000E+00	0.000000E+00	00003	RISER
00114	0.407600E-03	0.994118E-01	0.000000E+00	0.000000E+00	0.000000E+00	00003	RISER
00115	0.407600E-03	0.994118E-01	0.000000E+00	0.000000E+00	0.000000E+00	00003	RISER
00116	0.407600E-03	0.994118E-01	0.000000E+00	0.000000E+00	0.000000E+00	00003	RISER
00117	0.407600E-03	0.994118E-01	0.000000E+00	0.000000E+00	0.000000E+00	00003	RISER
00118	0.407600E-03	0.994118E-01	0.000000E+00	0.000000E+00	0.000000E+00	00003	RISER
00119	0.407600E-03	0.994118E-01	0.000000E+00	0.000000E+00	0.000000E+00	00003	RISER
00120	0.407600E-03	0.994118E-01	0.000000E+00	0.000000E+00	0.000000E+00	00003	RISER
00121	0.407600E-03	0.994118E-01	0.000000E+00	0.000000E+00	0.000000E+00	00003	RISER
00122	0.407600E-03	0.994118E-01	0.000000E+00	0.000000E+00	0.000000E+00	00003	RISER
00123	0.407600E-03	0.994118E-01	0.000000E+00	0.000000E+00	0.000000E+00	00003	RISER
00124	0.407600E-03	0.000000E+00	0.000000E+00	0.000000E+00	0.000000E+00	00002	BOUNDARY
00125	0.830200E-01	0.101571E+00	-.100000E+01	0.853000E+00	0.000000E+00	00040	HEAT EX.
00126	0.830200E-01	0.101571E+00	-.100000E+01	0.853000E+00	0.000000E+00	00040	HEAT EX.
00127	0.830200E-01	0.101571E+00	-.100000E+01	0.853000E+00	0.000000E+00	00040	HEAT EX.
00128	0.830200E-01	0.101571E+00	-.100000E+01	0.853000E+00	0.000000E+00	00040	HEAT EX.
00129	0.830200E-01	0.101571E+00	-.100000E+01	0.853000E+00	0.000000E+00	00040	HEAT EX.
00130	0.830200E-01	0.101571E+00	-.100000E+01	0.853000E+00	0.000000E+00	00040	HEAT EX.
00131	0.830200E-01	0.101571E+00	-.100000E+01	0.853000E+00	0.000000E+00	00040	HEAT EX.
00132	0.830200E-01	0.000000E+00	0.000000E+00	0.000000E+00	0.000000E+00	00002	BOUNDARY
00133	0.407600E-03	0.994118E-01	0.000000E+00	0.000000E+00	0.000000E+00	00003	RISER
00134	0.407600E-03	0.994118E-01	0.000000E+00	0.000000E+00	0.000000E+00	00003	RISER
00135	0.407600E-03	0.994118E-01	0.000000E+00	0.000000E+00	0.000000E+00	00003	RISER
00136	0.407600E-03	0.994118E-01	0.000000E+00	0.000000E+00	0.000000E+00	00003	RISER
00137	0.407600E-03	0.994118E-01	0.000000E+00	0.000000E+00	0.000000E+00	00003	RISER
00138	0.407600E-03	0.994118E-01	0.000000E+00	0.000000E+00	0.000000E+00	00003	RISER
00139	0.407600E-03	0.994118E-01	0.000000E+00	0.000000E+00	0.000000E+00	00003	RISER
00140	0.407600E-03	0.994118E-01	0.000000E+00	0.000000E+00	0.000000E+00	00003	RISER
00141	0.407600E-03	0.994118E-01	0.000000E+00	0.000000E+00	0.000000E+00	00003	RISER
00142	0.407600E-03	0.994118E-01	0.000000E+00	0.000000E+00	0.000000E+00	00003	RISER
00143	0.407600E-03	0.994118E-01	0.000000E+00	0.000000E+00	0.000000E+00	00003	RISER
00144	0.407600E-03	0.994118E-01	0.000000E+00	0.000000E+00	0.000000E+00	00003	RISER
00145	0.407600E-03	0.994118E-01	0.000000E+00	0.000000E+00	0.000000E+00	00003	RISER
00146	0.407600E-03	0.994118E-01	0.000000E+00	0.000000E+00	0.000000E+00	00003	RISER
00147	0.407600E-03	0.994118E-01	0.000000E+00	0.000000E+00	0.000000E+00	00003	RISER
00148	0.407600E-03	0.994118E-01	0.000000E+00	0.000000E+00	0.000000E+00	00003	RISER
00149	0.407600E-03	0.994118E-01	0.000000E+00	0.000000E+00	0.000000E+00	00003	RISER
00150	0.407600E-03	0.994118E-01	0.000000E+00	0.000000E+00	0.000000E+00	00003	RISER

1

SUMMARY OF INPUT DATA : Candu-X Stability Assessment

NODE NUMBER	AREA M2	LENGTH M	POWER DISTRIBUTION	RESTRICTION LOSS COEFF.	GRAVITY INDEX	SECTION CODE	SECTION NAME
00151	0.407600E-03	0.994118E-01	0.000000E+00	0.000000E+00	0.000000E+00	00003	RISER
00152	0.407600E-03	0.994118E-01	0.000000E+00	0.000000E+00	0.000000E+00	00003	RISER
00153	0.407600E-03	0.994118E-01	0.000000E+00	0.000000E+00	0.000000E+00	00003	RISER
00154	0.407600E-03	0.994118E-01	0.000000E+00	0.000000E+00	0.000000E+00	00003	RISER
00155	0.407600E-03	0.994118E-01	0.000000E+00	0.000000E+00	0.000000E+00	00003	RISER
00156	0.407600E-03	0.994118E-01	0.000000E+00	0.000000E+00	0.000000E+00	00003	RISER
00157	0.407600E-03	0.994118E-01	0.000000E+00	0.000000E+00	0.000000E+00	00003	RISER
00158	0.407600E-03	0.994118E-01	0.000000E+00	0.000000E+00	0.000000E+00	00003	RISER
00159	0.407600E-03	0.994118E-01	0.000000E+00	0.000000E+00	0.000000E+00	00003	RISER
00160	0.407600E-03	0.994118E-01	0.000000E+00	0.000000E+00	0.000000E+00	00003	RISER

```
  00161  0.407600E-03 0.994118E-01 0.000000E+00 0.000000E+00 0.000000E+00   00003     RISER
  00162  0.407600E-03 0.994118E-01 0.000000E+00 0.000000E+00 0.000000E+00   00003     RISER
  00163  0.407600E-03 0.994118E-01 0.000000E+00 0.000000E+00 0.000000E+00   00003     RISER
  00164  0.407600E-03 0.994118E-01 0.000000E+00 0.000000E+00 0.000000E+00   00003     RISER
  00165  0.407600E-03 0.994118E-01 0.000000E+00 0.000000E+00 0.000000E+00   00003     RISER
  00166  0.407600E-03 0.994118E-01 0.000000E+00 0.000000E+00 0.000000E+00   00003     RISER
  00167  0.407600E-03 0.102000E+00 0.000000E+00 0.000000E+00 -.100000E+01   00003     RISER
  00168  0.407600E-03 0.102000E+00 0.000000E+00 0.000000E+00 -.100000E+01   00003     RISER
  00169  0.407600E-03 0.102000E+00 0.000000E+00 0.000000E+00 -.100000E+01   00003     RISER
  00170  0.407600E-03 0.102000E+00 0.000000E+00 0.000000E+00 -.100000E+01   00003     RISER
  00171  0.407600E-03 0.102000E+00 0.000000E+00 0.000000E+00 -.100000E+01   00003     RISER
  00172  0.407600E-03 0.102000E+00 0.000000E+00 0.000000E+00 -.100000E+01   00003     RISER
  00173  0.407600E-03 0.102000E+00 0.000000E+00 0.000000E+00 -.100000E+01   00003     RISER
  00174  0.407600E-03 0.102000E+00 0.000000E+00 0.000000E+00 -.100000E+01   00003     RISER
  00175  0.407600E-03 0.102000E+00 0.000000E+00 0.000000E+00 -.100000E+01   00003     RISER
  00176  0.407600E-03 0.102000E+00 0.000000E+00 0.000000E+00 -.100000E+01   00003     RISER
  00177  0.407600E-03 0.000000E+00 0.000000E+00 0.000000E+00 -.100000E+01   00002    BOUNDARY
1
 Candu-X Stability Assessment

 CASE OPTIONS
 ------------
 SUBCOOLING OPTION              :  0      OSV OPTION              :  0
 TRANSIENT  OPTION              :  0      EXPLICIT SCHEME OPTION  :  0
 NEUTRON KINETIC OPTION         :  0      OUTPUT OPTION           :  1
 PLOT OPTION                    :  1      TYPE OPTION             :  1
 RESTART OPTION                 :  0      WALL-HEAT OPTION        :  0
 HO/SINGLE-PHASE OPTION         :  2      HO/TWO-PHASE OPTION     :  3
 FUEL OPTION                    :  0

 BOUNDARY CONDITIONS :
 --------------------
 AVERAGE POWER              (KW)    :0.250000E+00
 AVERAGE POWER PROFILE FACTOR       :0.100000E+01
 INLET TEMPERATURE          (DEG C) :0.280000E+02
 INLET PRESSURE             (KPA)   :0.750000E+04
 REF. EXT. PRESSURE         (KPA)   :0.750000E+04
 EST. INLET MASS FLOW       (KG/S)  :0.800000E-01


 PUMP MODEL DATA
 ---------------
 PUMP NODE                      :      0

2.747889359508714E-002 0.250000000000000
3.478253174752888E-002 0.500000000000001
4.009407517254048E-002 0.750000000000001
4.418899564012101E-002  1.00000000000000
4.758223033982154E-002  1.25000000000000
5.048763360752775E-002  1.50000000000000
5.302098700101108E-002  1.75000000000001
5.525316924461934E-002  2.00000000000001
5.723049152917027E-002  2.25000000000001
5.898494619465788E-002  2.50000000000001
6.054056113658816E-002  2.75000000000001
6.191743377058645E-002  3.00000000000001
6.313343875281972E-002  3.25000000000002
6.420478781654318E-002  3.50000000000002
6.514613309627204E-002  3.75000000000003
6.596985582467917E-002  4.00000000000003
6.668659982758801E-002  4.25000000000004
6.730572070671005E-002  4.50000000000004
6.783543495923340E-002  4.75000000000004
6.828280227510448E-002  5.00000000000005
6.865368225794576E-002  5.25000000000005
6.895281304413342E-002  5.50000000000006
6.918401690450199E-002  5.75000000000006
6.935040332158837E-002  6.00000000000006
6.945454996530495E-002  6.25000000000007
6.945454996530495E-002  6.50000000000007
6.945454996530495E-002  6.75000000000008
6.945454996530495E-002  7.00000000000008
6.928587847021303E-002  7.25000000000009
6.910655379317393E-002  7.50000000000009
6.887527160677767E-002  7.75000000000010
6.859421231260314E-002  8.00000000000010
6.826524255826125E-002  8.25000000000011
6.789038992418794E-002  8.50000000000012
6.747187799520482E-002  8.75000000000013
6.701215580944103E-002  9.00000000000013
```

6.651391514207509E-002 9.25000000000013
6.598008869178164E-002 9.50000000000014
6.541383273126178E-002 9.75000000000016
6.481849190041508E-002 10.0000000000002
6.419755130905430E-002 10.2500000000002
6.355458143321982E-002 10.5000000000002
6.289318480593495E-002 10.7500000000002
6.221693927827972E-002 11.0000000000002
6.152935010552888E-002 11.2500000000002
6.083379920102170E-002 11.5000000000002
6.013349379643222E-002 11.7500000000002
5.943141820596064E-002 12.0000000000002
5.873029156816448E-002 12.2500000000002
5.803253922500056E-002 12.5000000000003
5.734028538020131E-002 12.7500000000003
5.665535240235694E-002 13.0000000000003
5.597927593521582E-002 13.2500000000003
5.531332262585151E-002 13.5000000000003
5.465851218934085E-002 13.7500000000003
5.401564156385039E-002 14.0000000000004
5.338530897197524E-002 14.2500000000004
5.276793815847594E-002 14.5000000000004
5.216380227510645E-002 14.7500000000004
5.157304615586067E-002 15.0000000000004
0SPORTS TERMINATED NORMALLY

B.1.3 Calculations for Heat Exchanger K - Factor

The Exergy® shell-and-tube heat exchanger has 127 (3.2 mm OD, 0.32 mm thick) tubes, each 381 mm long. The K –factor for the heat exchanger was calculated as follows:

$$K = \frac{2\Delta P}{\rho U^2}$$

$$K = \frac{2\Delta P A^2}{(UA)^2 \rho}$$

Where ΔP is pressure drop in Pa.

A is area of cross section in m^2.

U is velocity in m^2/s.

ρ is density of fluid in kg/m^3.

K is coefficient depends on the nature of the local resistance to fluid flow.

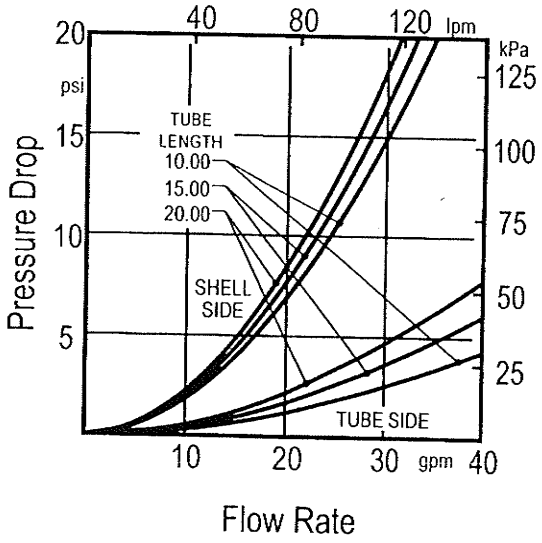

Figure B.1: Graph showing pressure Vs flow rate for shell and tube heat exchanger (EXERGY® miniature heat exchangers catalogue).

From the pressure loss graph of shell and tube heat exchanger (Figure B.1) for water we obtain the following parameters:

$UA = 0.001893 m^3/s \quad (30 gpm)$

$\Delta P = 25000 Pa$

$A = 6.5369 x 10^{-4} m^2$

$\rho = 998.21 Kg/m^3$ (For water at 101.33 KPa pressure and 20 °C)

Substituting these values in the equation $K = \frac{2\Delta P A^2}{(UA)^2 \rho}$ we obtain

$$K = \frac{2\Delta P A^2}{(UA)^2 \rho}$$

$$K = \frac{2x25000x(6.5369x10^{-4})^2}{(0.001893)^2 x998.21}$$

$$K = 5.97$$

B.1.4 Results of the Steady-State Simulations

	Case 1	Case 2	Case 3	Case 4
	Pressure: 7.5 MPa, Temperature: 25 °C, Inlet K: 0, Outlet K: 2	Pressure: 7.5 MPa, Temperature: 25 °C, Inlet K: 0, Outlet K: 5	Pressure: 7.5 MPa, Temperature: 25 °C, Inlet K: 0, Outlet K: 8	Pressure: 7.5 MPa, Temperature: 25 °C, Inlet K:0, Outlet K:10
Inlet Flow rate (kg/s)	Power (kW)	Power (kW)	Power (kW)	Power (kW)
0.2500000	0.0316997	0.0295735	0.0279453	0.0270495
0.5000000	0.0404661	0.0376346	0.0354730	0.0342814
0.7500000	0.0469933	0.0435878	0.0410080	0.0395919
1.0000000	0.0521028	0.0482364	0.0453217	0.0437262
1.2500000	0.0564166	0.0521485	0.0489421	0.0471902
1.5000000	0.0601921	0.0555595	0.0520882	0.0501942
1.7500000	0.0635682	0.0585968	0.0548791	0.0528526
2.0000000	0.0666312	0.0613397	0.0573888	0.0552364
2.2500000	0.0694395	0.0638416	0.0596665	0.0573927
2.5000000	0.0720340	0.0661398	0.0617469	0.0593546
2.7500000	0.0744452	0.0682618	0.0636550	0.0611456
3.0000000	0.0766958	0.0702280	0.0654092	0.0627826
3.2500000	0.0788035	0.0720539	0.0670229	0.0642780
3.5000000	0.0807821	0.0737513	0.0685062	0.0656409
3.7500000	0.0826424	0.0753292	0.0698665	0.0668780
4.0000000	0.0843932	0.0767945	0.0711097	0.0679954
4.2500000	0.0860411	0.0781525	0.0722410	0.0689992
4.5000000	0.0875915	0.0794076	0.0732658	0.0698958
4.7500000	0.0890487	0.0805639	0.0741897	0.0706918
5.0000000	0.0904162	0.0816257	0.0750185	0.0713941
5.2500000	0.0916971	0.0825974	0.0757583	0.0720088
5.5000000	0.0928944	0.0834837	0.0764146	0.0725414
5.7500000	0.0940113	0.0842892	0.0769925	0.0729970
6.0000000	0.0950510	0.0850187	0.0774965	0.0733804
6.2500000	0.0960170	0.0856764	0.0779309	0.0736958
6.5000000	0.0969127	0.0862659	0.0782997	0.0739468
6.7500000	0.0977416	0.0867909	0.0786064	0.0741364
7.0000000	0.0985071	0.0872547	0.0788541	0.0742669
7.2500000	0.0992120	0.0876605	0.0790451	0.0743403
7.5000000	0.0998591	0.0880111	0.0791815	0.0743403
7.7500000	0.1004511	0.0883090	0.0792648	0.0743403
8.0000000	0.1009904	0.0885563	0.0792648	0.0742291
8.2500000	0.1014794	0.0887547	0.0792648	0.0740852
8.5000000	0.1019204	0.0889057	0.0792069	0.0738893
8.7500000	0.1023153	0.0890105	0.0790875	0.0736425
9.0000000	0.1026661	0.0890700	0.0789199	0.0733459
9.2500000	0.1029741	0.0890700	0.0787046	0.0730006
9.5000000	0.1032409	0.0890700	0.0784426	0.0726079
9.7500000	0.1034674	0.0889831	0.0781348	0.0721694
10.0000000	0.1036547	0.0888679	0.0777821	0.0716866
10.2500000	0.1038037	0.0887105	0.0773858	0.0711618
10.5000000	0.1039149	0.0885116	0.0769471	0.0705973
10.7500000	0.1039891	0.0882720	0.0764676	0.0699957
11.0000000	0.1039891	0.0879922	0.0759490	0.0693601
11.2500000	0.1039891	0.0876729	0.0753934	0.0686939
11.5000000	0.1039891	0.0873151	0.0748032	0.0680005
11.7500000	0.1039891	0.0869196	0.0741807	0.0672839
12.0000000	0.1038170	0.0864874	0.0735289	0.0665477
12.2500000	0.1036780	0.0860196	0.0728507	0.0657961
12.5000000	0.1035039	0.0855178	0.0721492	0.0650328
12.7500000	0.1032960	0.0849832	0.0714279	0.0642616
13.0000000	0.1030548	0.0844176	0.0706900	0.0634862
13.2500000	0.1027806	0.0838228	0.0699388	0.0627099
13.5000000	0.1024740	0.0832009	0.0691776	0.0619359
13.7500000	0.1021356	0.0825539	0.0684097	0.0611669
14.0000000	0.1017658	0.0818842	0.0676381	0.0604054
14.2500000	0.1013654	0.0811940	0.0668657	0.0596533
14.5000000	0.1009351	0.0804858	0.0660951	0.0589124
14.7500000	0.1004758	0.0797622	0.0653288	0.0581842
15.0000000	0.0999883	0.0790256	0.0645688	0.0574696

	Case 5	Case 6	Case 7	Case 8
	Pressure: 7.5 MPa, Temperature: 25 °C, Inlet K: 0, Outlet K:13	Pressure: 7.5 MPa, Temperature: 25 °C, Inlet K: 2, Outlet K: 0	Pressure: 7.5 MPa, Temperature: 25 °C, Inlet K: 5, Outlet K: 0	Pressure: 7.5 MPa, Temperature: 25 °C, Inlet K: 8, Outlet K: 0
Inlet Flow rate (kg/s)	Power (kW)	Power (kW)	Power (kW)	Power (kW)
0.2500000	0.0259133	0.0317611	0.0296980	0.0281136
0.5000000	0.0327623	0.0405946	0.0378930	0.0358197
0.7500000	0.0377916	0.0471989	0.0439990	0.0415580
1.0000000	0.0417017	0.0523889	0.0488073	0.0460848
1.2500000	0.0449699	0.0567872	0.0528875	0.0499298
1.5000000	0.0477958	0.0606513	0.0564750	0.0533126
1.7500000	0.0502877	0.0641199	0.0596973	0.0563522
2.0000000	0.0525128	0.0672796	0.0626339	0.0591229
2.2500000	0.0545155	0.0701885	0.0653382	0.0616746
2.5000000	0.0563263	0.0728879	0.0678479	0.0640422
2.7500000	0.0579669	0.0754081	0.0701908	0.0662516
3.0000000	0.0594523	0.0777721	0.0723878	0.0683219
3.2500000	0.0607934	0.0799978	0.0744548	0.0702676
3.5000000	0.0619983	0.0820990	0.0764044	0.0720998
3.7500000	0.0630740	0.0840870	0.0782461	0.0738271
4.0000000	0.0640278	0.0859705	0.0799875	0.0754558
4.2500000	0.0648674	0.0877567	0.0816345	0.0769913
4.5000000	0.0656008	0.0894511	0.0831919	0.0784379
4.7500000	0.0662356	0.0910584	0.0846636	0.0797999
5.0000000	0.0667787	0.0925821	0.0860530	0.0810814
5.2500000	0.0672363	0.0940254	0.0873637	0.0822868
5.5000000	0.0676140	0.0953911	0.0885992	0.0834203
5.7500000	0.0679171	0.0966820	0.0897633	0.0844863
6.0000000	0.0681497	0.0979010	0.0908595	0.0854890
6.2500000	0.0683154	0.0990509	0.0918915	0.0864321
6.5000000	0.0684169	0.1001349	0.0928631	0.0873190
6.7500000	0.0684169	0.1011559	0.0937773	0.0881528
7.0000000	0.0684169	0.1021170	0.0946371	0.0889365
7.2500000	0.0683536	0.1030212	0.0954453	0.0896731
7.5000000	0.0682137	0.1038710	0.0962045	0.0903651
7.7500000	0.0680169	0.1046690	0.0969173	0.0910150
8.0000000	0.0677640	0.1054174	0.0975859	0.0916251
8.2500000	0.0674565	0.1061184	0.0982126	0.0921972
8.5000000	0.0670955	0.1067742	0.0987994	0.0927331
8.7500000	0.0666829	0.1073868	0.0993482	0.0932342
9.0000000	0.0662205	0.1079580	0.0998604	0.0937018
9.2500000	0.0657104	0.1084896	0.1003376	0.0941370
9.5000000	0.0651555	0.1089833	0.1007809	0.0945408
9.7500000	0.0645587	0.1094404	0.1011914	0.0949140
10.0000000	0.0639237	0.1098622	0.1015700	0.0952573
10.2500000	0.0632544	0.1102498	0.1019175	0.0955716
10.5000000	0.0625552	0.1106041	0.1022346	0.0958574
10.7500000	0.0618306	0.1109259	0.1025219	0.0961152
11.0000000	0.0610853	0.1112159	0.1027801	0.0963457
11.2500000	0.0603242	0.1114749	0.1030097	0.0965493
11.5000000	0.0595519	0.1117033	0.1032110	0.0967265
11.7500000	0.0587730	0.1119016	0.1033847	0.0968777
12.0000000	0.0579917	0.1120703	0.1035310	0.0970033
12.2500000	0.0572120	0.1122099	0.1036504	0.0971039
12.5000000	0.0564374	0.1123206	0.1037433	0.0971797
12.7500000	0.0556710	0.1124028	0.1038101	0.0972313
13.0000000	0.0549152	0.1124028	0.1038101	0.0972313
13.2500000	0.0541722	0.1124820	0.1038101	0.0972313
13.5000000	0.0534436	0.1124820	0.1038101	0.0972313
13.7500000	0.0527307	0.1124820	0.1038101	0.0972313
14.0000000	0.0520343	0.1123944	0.1038101	0.0971321
14.2500000	0.0513551	0.1123116	0.1036734	0.0970458
14.5000000	0.0506933	0.1122015	0.1035669	0.0969368
14.7500000	0.0500491	0.1120654	0.1034353	0.0968069
15.0000000	0.0494225	0.1119034	0.1032808	0.0966566

	Case 9	Case 10	Case 11	Case 12
	Pressure: 7.5 MPa, Temperature: 25 °C, Inlet K:10, Outlet K: 0	Pressure: 7.5 MPa, Temperature: 25 °C, Inlet K:13, Outlet K:0	Pressure: 7.5 MPa, Temperature: 28 °C, Inlet K: 0, Outlet K: 2	Pressure: 7.5 MPa, Temperature: 28 °C, Inlet K: 0, Outlet K: 5
Inlet Flow rate (kg/s)	Power (kW)	Power (kW)	Power (kW)	Power (kW)
0.2500000	0.0272407	0.0261323	0.0323295	0.0301056
0.5000000	0.0346731	0.0332078	0.0412317	0.0382687
0.7500000	0.0402124	0.0384965	0.0478254	0.0442558
1.0000000	0.0445871	0.0426798	0.0529568	0.0488964
1.2500000	0.0483049	0.0462373	0.0572611	0.0527697
1.5000000	0.0515767	0.0493691	0.0610010	0.0561153
1.7500000	0.0545171	0.0521841	0.0643186	0.0590634
2.0000000	0.0571975	0.0547502	0.0673022	0.0616945
2.2500000	0.0596657	0.0571126	0.0700109	0.0640618
2.5000000	0.0619555	0.0593031	0.0724861	0.0662024
2.7500000	0.0640914	0.0613447	0.0747577	0.0681428
3.0000000	0.0660915	0.0632541	0.0768479	0.0699028
3.2500000	0.0679694	0.0650440	0.0787738	0.0714987
3.5000000	0.0697355	0.0667234	0.0805490	0.0729443
3.7500000	0.0713976	0.0682995	0.0821849	0.0742525
4.0000000	0.0729618	0.0697781	0.0836918	0.0754349
4.2500000	0.0744330	0.0711645	0.0850793	0.0765024
4.5000000	0.0758160	0.0724643	0.0863563	0.0774647
4.7500000	0.0771155	0.0736826	0.0875309	0.0783302
5.0000000	0.0783362	0.0748249	0.0886110	0.0791062
5.2500000	0.0794827	0.0758966	0.0896032	0.0797993
5.5000000	0.0805599	0.0769024	0.0905136	0.0804157
5.7500000	0.0815723	0.0778468	0.0913475	0.0809605
6.0000000	0.0825239	0.0787336	0.0921098	0.0814386
6.2500000	0.0834183	0.0795666	0.0928052	0.0818537
6.5000000	0.0842590	0.0803494	0.0934377	0.0822093
6.7500000	0.0850492	0.0810852	0.0940110	0.0825082
7.0000000	0.0857919	0.0817769	0.0945285	0.0827526
7.2500000	0.0864900	0.0824272	0.0949930	0.0829445
7.5000000	0.0871460	0.0830385	0.0954069	0.0830856
7.7500000	0.0877624	0.0836126	0.0957724	0.0831775
8.0000000	0.0883409	0.0841514	0.0960912	0.0831775
8.2500000	0.0888835	0.0846562	0.0963649	0.0831775
8.5000000	0.0893914	0.0851283	0.0965949	0.0831775
8.7500000	0.0898661	0.0855688	0.0967824	0.0830746
9.0000000	0.0903087	0.0859789	0.0969284	0.0829369
9.2500000	0.0907202	0.0863592	0.0970338	0.0827565
9.5000000	0.0911014	0.0867106	0.0970997	0.0825347
9.7500000	0.0914531	0.0870339	0.0970997	0.0822726
10.0000000	0.0917761	0.0873298	0.0970997	0.0819713
10.2500000	0.0920710	0.0875988	0.0970997	0.0816322
10.5000000	0.0923383	0.0878416	0.0969798	0.0812567
10.7500000	0.0925788	0.0880586	0.0968583	0.0808462
11.0000000	0.0927928	0.0882506	0.0967010	0.0804024
11.2500000	0.0929809	0.0884179	0.0965092	0.0799270
11.5000000	0.0931435	0.0885611	0.0962837	0.0794217
11.7500000	0.0932813	0.0886807	0.0960250	0.0788887
12.0000000	0.0933945	0.0887771	0.0957342	0.0783300
12.2500000	0.0934836	0.0888509	0.0954120	0.0777477
12.5000000	0.0935490	0.0889024	0.0950594	0.0771441
12.7500000	0.0935490	0.0889024	0.0946773	0.0765215
13.0000000	0.0936090	0.0889024	0.0942668	0.0758821
13.2500000	0.0936090	0.0889024	0.0938289	0.0752283
13.5000000	0.0936090	0.0889024	0.0933649	0.0745625
13.7500000	0.0935316	0.0888380	0.0928760	0.0738867
14.0000000	0.0934637	0.0887650	0.0923636	0.0732033
14.2500000	0.0933740	0.0886728	0.0918288	0.0725143
14.5000000	0.0932643	0.0885624	0.0912733	0.0718218
14.7500000	0.0931352	0.0884345	0.0906984	0.0711276
15.0000000	0.0929871	0.0882896	0.0901056	0.0704335

	Case 13	Case 14	Case 15	Case 16
	Pressure: 7.5 MPa, Temperature: 28 °C, Inlet K: 0, Outlet K: 8	Pressure: 7.5 MPa, Temperature: 28 °C, Inlet K:0, Outlet K:10	Pressure: 7.5 MPa, Temperature: 28 °C, Inlet K:0, Outlet K:13	Pressure: 7.5 MPa, Temperature: 28 °C, Inlet K: 2, Outlet K: 0
Inlet Flow rate (kg/s)	Power (kW)	Power (kW)	Power (kW)	Power (kW)
0.2500000	0.0284098	0.0274789	0.0262995	0.0324044
0.5000000	0.0360189	0.0347825	0.0332098	0.0415405
0.7500000	0.0415660	0.0400941	0.0382266	0.0480808
1.0000000	0.0458512	0.0441890	0.0420838	0.0533090
1.2500000	0.0494120	0.0475822	0.0452672	0.0577184
1.5000000	0.0524713	0.0504876	0.0479791	0.0615688
1.7500000	0.0551501	0.0530210	0.0503288	0.0650023
2.0000000	0.0575227	0.0552532	0.0523825	0.0681072
2.2500000	0.0596379	0.0572305	0.0541836	0.0709427
2.5000000	0.0615293	0.0589849	0.0557626	0.0735504
2.7500000	0.0632215	0.0605406	0.0571441	0.0759603
3.0000000	0.0647339	0.0619174	0.0583493	0.0781949
3.2500000	0.0660836	0.0631334	0.0593973	0.0802713
3.5000000	0.0672859	0.0642048	0.0603054	0.0822031
3.7500000	0.0683548	0.0651461	0.0610878	0.0840015
4.0000000	0.0693031	0.0659699	0.0617566	0.0856764
4.2500000	0.0701416	0.0666866	0.0623226	0.0872368
4.5000000	0.0708795	0.0673057	0.0627947	0.0886910
4.7500000	0.0715251	0.0678354	0.0631807	0.0900467
5.0000000	0.0720860	0.0682828	0.0634867	0.0913112
5.2500000	0.0725684	0.0686537	0.0637175	0.0924912
5.5000000	0.0729777	0.0689528	0.0638769	0.0935925
5.7500000	0.0733186	0.0691840	0.0639681	0.0946203
6.0000000	0.0735946	0.0693504	0.0639681	0.0955792
6.2500000	0.0738087	0.0694545	0.0639681	0.0964737
6.5000000	0.0739635	0.0694545	0.0638547	0.0973077
6.7500000	0.0740609	0.0694545	0.0636949	0.0980850
7.0000000	0.0740609	0.0694545	0.0634775	0.0988088
7.2500000	0.0740609	0.0692859	0.0632049	0.0994822
7.5000000	0.0740609	0.0691066	0.0628791	0.1001079
7.7500000	0.0739091	0.0688753	0.0625026	0.1006882
8.0000000	0.0737436	0.0685942	0.0620780	0.1012251
8.2500000	0.0735295	0.0682652	0.0616084	0.1017206
8.5000000	0.0732687	0.0678904	0.0610970	0.1021760
8.7500000	0.0729628	0.0674719	0.0605475	0.1025928
9.0000000	0.0726135	0.0670122	0.0599637	0.1029721
9.2500000	0.0722226	0.0665139	0.0593497	0.1033152
9.5000000	0.0717920	0.0659801	0.0587100	0.1036228
9.7500000	0.0713241	0.0654138	0.0580488	0.1038959
10.0000000	0.0708211	0.0648185	0.0573704	0.1041352
10.2500000	0.0702857	0.0641976	0.0566793	0.1043415
10.5000000	0.0697205	0.0635546	0.0559795	0.1045155
10.7500000	0.0691285	0.0628932	0.0552749	0.1046578
11.0000000	0.0685126	0.0622169	0.0545691	0.1047690
11.2500000	0.0678759	0.0615294	0.0538654	0.1048497
11.5000000	0.0672215	0.0608338	0.0531665	0.1048497
11.7500000	0.0665525	0.0601335	0.0524749	0.1049205
12.0000000	0.0658719	0.0594314	0.0517926	0.1049205
12.2500000	0.0651825	0.0587303	0.0511214	0.1049205
12.5000000	0.0644873	0.0580325	0.0504624	0.1048096
12.7500000	0.0637889	0.0573403	0.0498168	0.1047176
13.0000000	0.0630897	0.0566554	0.0491851	0.1045976
13.2500000	0.0623920	0.0559793	0.0485681	0.1044511
13.5000000	0.0616978	0.0553133	0.0479658	0.1042788
13.7500000	0.0610089	0.0546585	0.0473785	0.1040810
14.0000000	0.0603266	0.0540156	0.0468061	0.1038585
14.2500000	0.0596525	0.0533853	0.0462485	0.1036118
14.5000000	0.0589875	0.0527679	0.0457056	0.1033415
14.7500000	0.0583325	0.0521638	0.0451770	0.1030484
15.0000000	0.0576884	0.0515730	0.0446624	0.1027330

	Case 17	Case 18	Case 19	Case 20
	Pressure: 7.5 MPa, Temperature: 28 °C, Inlet K: 5, Outlet K: 0	Pressure: 7.5 MPa, Temperature: 28 °C, Inlet K: 8, Outlet K: 0	Pressure: 7.5 MPa, Temperature: 28 °C, Inlet K:10, Outlet K: 0	Pressure: 7.5 MPa, Temperature: 28 °C, Inlet K:13, Outlet K: 0
Inlet Flow rate (kg/s)	Power (kW)	Power (kW)	Power (kW)	Power (kW)
0.2500000	0.0302568	0.0286136	0.0277099	0.0265637
0.5000000	0.0387117	0.0365528	0.0352587	0.0337508
0.7500000	0.0447611	0.0422394	0.0408513	0.0390861
1.0000000	0.0495971	0.0467861	0.0452430	0.0432807
1.2500000	0.0536790	0.0506257	0.0489512	0.0468231
1.5000000	0.0572446	0.0539799	0.0521903	0.0499165
1.7500000	0.0604241	0.0569698	0.0550767	0.0526712
2.0000000	0.0632982	0.0596705	0.0576821	0.0551547
2.2500000	0.0659206	0.0621315	0.0600537	0.0574112
2.5000000	0.0683289	0.0643871	0.0622242	0.0594714
2.7500000	0.0705499	0.0664621	0.0642172	0.0613581
3.0000000	0.0726038	0.0683751	0.0660512	0.0630899
3.2500000	0.0745062	0.0701418	0.0677419	0.0646829
3.5000000	0.0762702	0.0717755	0.0693031	0.0661514
3.7500000	0.0779074	0.0732882	0.0707472	0.0675083
4.0000000	0.0794281	0.0746911	0.0720855	0.0687648
4.2500000	0.0808420	0.0759941	0.0733279	0.0699304
4.5000000	0.0821580	0.0772060	0.0744830	0.0710134
4.7500000	0.0833840	0.0783344	0.0755580	0.0720211
5.0000000	0.0845271	0.0793860	0.0765597	0.0729602
5.2500000	0.0855934	0.0803668	0.0774941	0.0738364
5.5000000	0.0865885	0.0812822	0.0783665	0.0746549
5.7500000	0.0875173	0.0821372	0.0791817	0.0754201
6.0000000	0.0883846	0.0829363	0.0799438	0.0761355
6.2500000	0.0891944	0.0836831	0.0806563	0.0768044
6.5000000	0.0899506	0.0843811	0.0813223	0.0774293
6.7500000	0.0906566	0.0850331	0.0819443	0.0780127
7.0000000	0.0913150	0.0856414	0.0825246	0.0785564
7.2500000	0.0919286	0.0862083	0.0830651	0.0790623
7.5000000	0.0924994	0.0867355	0.0835674	0.0795318
7.7500000	0.0930292	0.0872246	0.0840330	0.0799664
8.0000000	0.0935199	0.0876771	0.0844634	0.0803672
8.2500000	0.0939727	0.0880942	0.0848595	0.0807354
8.5000000	0.0943889	0.0884771	0.0852227	0.0810721
8.7500000	0.0947697	0.0888267	0.0855537	0.0813782
9.0000000	0.0951161	0.0891440	0.0858537	0.0816547
9.2500000	0.0954291	0.0894300	0.0861234	0.0819024
9.5000000	0.0957094	0.0896854	0.0863637	0.0821221
9.7500000	0.0959579	0.0899109	0.0865753	0.0823147
10.0000000	0.0961753	0.0901075	0.0867589	0.0824808
10.2500000	0.0963624	0.0902756	0.0869154	0.0826212
10.5000000	0.0965197	0.0904161	0.0870453	0.0827366
10.7500000	0.0966479	0.0905295	0.0871493	0.0828276
11.0000000	0.0967476	0.0906165	0.0872281	0.0828950
11.2500000	0.0968195	0.0906777	0.0872823	0.0829394
11.5000000	0.0968195	0.0906777	0.0872823	0.0829394
11.7500000	0.0968803	0.0906777	0.0872823	0.0829394
12.0000000	0.0968803	0.0906777	0.0872823	0.0829394
12.2500000	0.0968803	0.0906777	0.0872823	0.0829394
12.5000000	0.0967744	0.0906126	0.0872003	0.0828325
12.7500000	0.0966902	0.0905299	0.0871191	0.0827532
13.0000000	0.0965805	0.0904256	0.0870170	0.0826537
13.2500000	0.0964476	0.0903003	0.0868955	0.0825367
13.5000000	0.0962918	0.0901549	0.0867552	0.0824029
13.7500000	0.0961139	0.0899899	0.0865969	0.0822530
14.0000000	0.0959145	0.0898060	0.0864213	0.0820877
14.2500000	0.0956943	0.0896040	0.0862290	0.0819076
14.5000000	0.0954539	0.0893846	0.0860207	0.0817135
14.7500000	0.0951941	0.0891484	0.0857972	0.0815059
15.0000000	0.0949155	0.0888962	0.0855591	0.0812857

	Case 21	Case 22	Case 23	Case 24
	Pressure: 7.5 MPa, Temperature: 31 °C, Inlet K: 0, Outlet K: 2	Pressure: 7.5 MPa, Temperature: 31 °C, Inlet K: 0, Outlet K: 5	Pressure: 7.5 MPa, Temperature: 31 °C, Inlet K: 0, Outlet K: 8	Pressure: 7.5 MPa, Temperature: 31 °C, Inlet K:0, Outlet K:10
Inlet Flow rate (kg/s)	Power (kW)	Power (kW)	Power (kW)	Power (kW)
0.2500000	0.0327915	0.0304164	0.0286229	0.0276439
0.5000000	0.0415821	0.0384061	0.0360180	0.0347128
0.7500000	0.0478688	0.0440290	0.0411622	0.0396013
1.0000000	0.0526378	0.0482527	0.0449928	0.0432219
1.2500000	0.0565218	0.0516526	0.0480447	0.0460885
1.5000000	0.0597894	0.0544773	0.0505531	0.0484293
1.7500000	0.0625930	0.0568706	0.0526554	0.0503779
2.0000000	0.0650322	0.0589265	0.0544405	0.0520202
2.2500000	0.0671765	0.0607097	0.0559694	0.0534154
2.5000000	0.0690764	0.0622670	0.0572864	0.0546064
2.7500000	0.0707694	0.0636335	0.0584249	0.0556254
3.0000000	0.0722847	0.0648365	0.0594104	0.0564969
3.2500000	0.0736455	0.0658978	0.0602628	0.0572392
3.5000000	0.0748708	0.0668344	0.0609973	0.0578667
3.7500000	0.0759759	0.0676599	0.0616258	0.0583904
4.0000000	0.0769735	0.0683851	0.0621578	0.0588190
4.2500000	0.0778739	0.0690186	0.0626009	0.0591599
4.5000000	0.0786856	0.0695677	0.0629616	0.0594192
4.7500000	0.0794155	0.0700383	0.0632453	0.0596021
5.0000000	0.0800696	0.0704354	0.0634566	0.0597133
5.2500000	0.0806528	0.0707635	0.0635998	0.0597133
5.5000000	0.0811693	0.0710262	0.0636786	0.0597133
5.7500000	0.0816229	0.0712270	0.0636786	0.0596550
6.0000000	0.0820168	0.0713690	0.0636786	0.0595163
6.2500000	0.0823539	0.0714549	0.0635590	0.0593244
6.5000000	0.0826368	0.0714549	0.0634111	0.0590827
6.7500000	0.0828677	0.0714549	0.0632140	0.0587945
7.0000000	0.0830490	0.0714549	0.0629710	0.0584634
7.2500000	0.0831825	0.0712844	0.0626849	0.0580929
7.5000000	0.0832701	0.0711258	0.0623589	0.0576867
7.7500000	0.0832701	0.0709246	0.0619959	0.0572484
8.0000000	0.0832701	0.0706835	0.0615992	0.0567817
8.2500000	0.0832701	0.0704049	0.0611718	0.0562901
8.5000000	0.0831931	0.0700910	0.0607169	0.0557773
8.7500000	0.0830746	0.0697442	0.0602376	0.0552467
9.0000000	0.0829198	0.0693667	0.0597370	0.0547016
9.2500000	0.0827300	0.0689611	0.0592181	0.0541452
9.5000000	0.0825068	0.0685296	0.0586838	0.0535804
9.7500000	0.0822517	0.0680745	0.0581369	0.0530100
10.0000000	0.0819663	0.0675984	0.0575802	0.0524366
10.2500000	0.0816521	0.0671034	0.0570161	0.0518623
10.5000000	0.0813106	0.0665918	0.0564469	0.0512891
10.7500000	0.0809435	0.0660660	0.0558748	0.0507189
11.0000000	0.0805524	0.0655280	0.0553017	0.0501531
11.2500000	0.0801387	0.0649798	0.0547294	0.0495929
11.5000000	0.0797043	0.0644236	0.0541594	0.0490396
11.7500000	0.0792505	0.0638612	0.0535930	0.0484938
12.0000000	0.0787791	0.0632942	0.0530314	0.0479564
12.2500000	0.0782916	0.0627243	0.0524756	0.0474279
12.5000000	0.0777896	0.0621530	0.0519263	0.0469088
12.7500000	0.0772745	0.0615817	0.0513844	0.0463992
13.0000000	0.0767479	0.0610115	0.0508503	0.0458996
13.2500000	0.0762112	0.0604436	0.0503245	0.0454098
13.5000000	0.0756658	0.0598789	0.0498074	0.0449301
13.7500000	0.0751132	0.0593183	0.0492991	0.0444604
14.0000000	0.0745544	0.0587625	0.0487999	0.0440006
14.2500000	0.0739909	0.0582122	0.0483099	0.0435506
14.5000000	0.0734237	0.0576679	0.0478291	0.0431103
14.7500000	0.0728539	0.0571301	0.0473575	0.0426795
15.0000000	0.0722825	0.0565992	0.0468951	0.0422580

	Case 25	Case 26	Case 27	Case 28
	Pressure: 7.5 MPa, Temperature: 31 °C, Inlet K:0, Outlet K:13	Pressure: 7.5 MPa, Temperature: 31 °C, Inlet K: 2, Outlet K: 0	Pressure: 7.5 MPa, Temperature: 31 °C, Inlet K: 5, Outlet K: 0	Pressure: 7.5 MPa, Temperature: 31 °C, Inlet K: 8, Outlet K: 0
Inlet Flow rate (kg/s)	Power (kW)	Power (kW)	Power (kW)	Power (kW)
0.2500000	0.0264088	0.0328995	0.0306324	0.0289124
0.5000000	0.0330587	0.0418098	0.0388587	0.0366209
0.7500000	0.0376278	0.0482329	0.0447487	0.0421182
1.0000000	0.0409865	0.0531445	0.0492523	0.0463193
1.2500000	0.0436225	0.0571780	0.0529455	0.0497591
1.5000000	0.0457556	0.0606011	0.0560747	0.0526695
1.7500000	0.0475141	0.0635654	0.0587814	0.0551849
2.0000000	0.0489801	0.0661692	0.0611581	0.0573926
2.2500000	0.0502106	0.0684816	0.0632687	0.0593527
2.5000000	0.0512466	0.0705527	0.0651591	0.0611082
2.7500000	0.0521185	0.0724197	0.0668640	0.0626918
3.0000000	0.0528489	0.0741115	0.0684101	0.0641289
3.2500000	0.0534546	0.0756511	0.0698188	0.0654395
3.5000000	0.0539484	0.0770572	0.0711073	0.0666395
3.7500000	0.0543406	0.0783452	0.0722896	0.0677414
4.0000000	0.0546393	0.0795276	0.0733769	0.0687555
4.2500000	0.0548513	0.0806152	0.0743783	0.0696899
4.5000000	0.0549827	0.0816164	0.0753015	0.0705515
4.7500000	0.0550387	0.0825385	0.0761527	0.0713460
5.0000000	0.0550387	0.0833875	0.0769371	0.0720780
5.2500000	0.0549406	0.0841685	0.0776593	0.0727518
5.5000000	0.0547956	0.0848860	0.0783231	0.0733708
5.7500000	0.0545922	0.0855436	0.0789319	0.0739384
6.0000000	0.0543349	0.0861447	0.0794888	0.0744572
6.2500000	0.0540278	0.0866922	0.0799962	0.0749297
6.5000000	0.0536751	0.0871887	0.0804567	0.0753582
6.7500000	0.0532813	0.0876364	0.0808723	0.0757448
7.0000000	0.0528507	0.0880374	0.0812451	0.0760913
7.2500000	0.0523877	0.0883938	0.0815768	0.0763995
7.5000000	0.0518968	0.0887071	0.0818690	0.0766709
7.7500000	0.0513822	0.0889791	0.0821233	0.0769071
8.0000000	0.0508482	0.0892112	0.0823412	0.0771094
8.2500000	0.0502987	0.0894048	0.0825239	0.0772792
8.5000000	0.0497376	0.0895613	0.0826727	0.0774177
8.7500000	0.0491685	0.0896818	0.0827889	0.0775261
9.0000000	0.0485944	0.0897675	0.0828737	0.0776056
9.2500000	0.0480184	0.0897675	0.0828737	0.0776574
9.5000000	0.0474430	0.0898381	0.0829515	0.0776574
9.7500000	0.0468704	0.0898381	0.0829515	0.0776574
10.0000000	0.0463026	0.0898381	0.0829515	0.0776574
10.2500000	0.0457410	0.0897089	0.0828591	0.0776574
10.5000000	0.0451870	0.0896086	0.0827770	0.0775305
10.7500000	0.0446417	0.0894797	0.0826700	0.0774384
11.0000000	0.0441058	0.0893244	0.0825399	0.0773240
11.2500000	0.0435800	0.0891439	0.0823878	0.0771902
11.5000000	0.0430648	0.0889390	0.0822148	0.0770379
11.7500000	0.0425604	0.0887108	0.0820217	0.0768682
12.0000000	0.0420670	0.0884604	0.0818096	0.0766819
12.2500000	0.0415847	0.0881887	0.0815794	0.0764799
12.5000000	0.0411136	0.0878968	0.0813321	0.0762631
12.7500000	0.0406534	0.0875857	0.0810687	0.0760325
13.0000000	0.0402041	0.0872564	0.0807900	0.0757887
13.2500000	0.0397654	0.0869100	0.0804969	0.0755328
13.5000000	0.0393373	0.0865473	0.0801904	0.0752654
13.7500000	0.0389194	0.0861695	0.0798714	0.0749874
14.0000000	0.0385115	0.0857775	0.0795406	0.0746995
14.2500000	0.0381133	0.0853723	0.0791990	0.0744024
14.5000000	0.0377245	0.0849549	0.0788474	0.0740970
14.7500000	0.0373449	0.0845261	0.0784865	0.0737837
15.0000000	0.0369742	0.0840870	0.0781172	0.0734633

	Case 29	Case 30
	Pressure: 7.5 MPa, Temperature: 31°C, Inlet K: 10,Outlet K: 0	Pressure: 7.5 MPa, Temperature: 31 °C, Inlet K:13, Outlet K:0
Inlet Flow rate (kg/s)	Power (kW)	Power (kW)
0.2500000	0.0279712	0.0267818
0.5000000	0.0353917	0.0338280
0.7500000	0.0406764	0.0388445
1.0000000	0.0447132	0.0426737
1.2500000	0.0480151	0.0458014
1.5000000	0.0508066	0.0484428
1.7500000	0.0532181	0.0507232
2.0000000	0.0553340	0.0527231
2.2500000	0.0572121	0.0544976
2.5000000	0.0588941	0.0560870
2.7500000	0.0604118	0.0575216
3.0000000	0.0617896	0.0588245
3.2500000	0.0630467	0.0600136
3.5000000	0.0641981	0.0611031
3.7500000	0.0652556	0.0621038
4.0000000	0.0662290	0.0630246
4.2500000	0.0671258	0.0638727
4.5000000	0.0679526	0.0646540
4.7500000	0.0687147	0.0653738
5.0000000	0.0694167	0.0660361
5.2500000	0.0700624	0.0666449
5.5000000	0.0706555	0.0672033
5.7500000	0.0711988	0.0677144
6.0000000	0.0716952	0.0681807
6.2500000	0.0721469	0.0686046
6.5000000	0.0725564	0.0689882
6.7500000	0.0729254	0.0693335
7.0000000	0.0732559	0.0696422
7.2500000	0.0735496	0.0699160
7.5000000	0.0738081	0.0701565
7.7500000	0.0740327	0.0703651
8.0000000	0.0742250	0.0705432
8.2500000	0.0743862	0.0706922
8.5000000	0.0745175	0.0708133
8.7500000	0.0746203	0.0709077
9.0000000	0.0746957	0.0709766
9.2500000	0.0747447	0.0710212
9.5000000	0.0747447	0.0710212
9.7500000	0.0747447	0.0710212
10.0000000	0.0747447	0.0710212
10.2500000	0.0747447	0.0710212
10.5000000	0.0746265	0.0709093
10.7500000	0.0745406	0.0708306
11.0000000	0.0744337	0.0707326
11.2500000	0.0743090	0.0706186
11.5000000	0.0741672	0.0704893
11.7500000	0.0740093	0.0703456
12.0000000	0.0738361	0.0701883
12.2500000	0.0736486	0.0700183
12.5000000	0.0734476	0.0698364
12.7500000	0.0732339	0.0696433
13.0000000	0.0730083	0.0694398
13.2500000	0.0727716	0.0692265
13.5000000	0.0725246	0.0690041
13.7500000	0.0722679	0.0687733
14.0000000	0.0720022	0.0685348
14.2500000	0.0717283	0.0682890
14.5000000	0.0714468	0.0680367
14.7500000	0.0711583	0.0677782
15.0000000	0.0708635	0.0675143

	Case 31	Case 32	Case 33	Case 34
	Pressure: 9.5 MPa, Temperature: 27 °C, Inlet K: 0, Outlet K: 2	Pressure: 9.5 MPa, Temperature: 27 °C, Inlet K: 0, Outlet K: 5	Pressure: 9.5 MPa, Temperature: 27 °C, Inlet K: 0, Outlet K: 8	Pressure: 9.5 MPa, Temperature: 27 °C, Inlet K: 0, Outlet K:10
Inlet Flow rate (kg/s)	Power (kW)	Power (kW)	Power (kW)	Power (kW)
0.2500000	0.0305579	0.0285472	0.0270054	0.0261574
0.5000000	0.0389812	0.0362985	0.0342417	0.0331050
0.7500000	0.0452111	0.0419868	0.0395331	0.0381827
1.0000000	0.0500818	0.0464248	0.0436554	0.0421356
1.2500000	0.0541887	0.0501566	0.0471139	0.0454475
1.5000000	0.0577792	0.0534089	0.0501204	0.0483221
1.7500000	0.0609880	0.0563061	0.0527912	0.0508714
2.0000000	0.0638995	0.0589258	0.0551989	0.0531653
2.2500000	0.0665706	0.0613205	0.0573925	0.0552509
2.5000000	0.0690418	0.0635273	0.0594068	0.0571615
2.7500000	0.0713430	0.0655736	0.0612673	0.0589216
3.0000000	0.0734969	0.0674804	0.0629933	0.0605497
3.2500000	0.0755214	0.0692637	0.0645997	0.0620602
3.5000000	0.0774305	0.0709366	0.0660987	0.0634644
3.7500000	0.0792357	0.0725093	0.0674996	0.0647716
4.0000000	0.0809464	0.0739903	0.0688106	0.0659894
4.2500000	0.0825705	0.0753869	0.0700380	0.0671240
4.5000000	0.0841145	0.0767050	0.0711875	0.0681806
4.7500000	0.0855840	0.0779496	0.0722637	0.0691638
5.0000000	0.0869838	0.0791252	0.0732707	0.0700772
5.2500000	0.0883182	0.0802354	0.0742117	0.0709241
5.5000000	0.0895907	0.0812836	0.0750898	0.0717074
5.7500000	0.0908046	0.0822725	0.0759076	0.0724296
6.0000000	0.0919626	0.0832047	0.0766674	0.0730930
6.2500000	0.0930673	0.0840824	0.0773714	0.0736996
6.5000000	0.0941208	0.0849075	0.0780214	0.0742515
6.7500000	0.0951251	0.0856819	0.0786193	0.0747503
7.0000000	0.0960819	0.0864073	0.0791666	0.0751978
7.2500000	0.0969929	0.0870850	0.0796649	0.0755954
7.5000000	0.0978596	0.0877167	0.0801156	0.0759442
7.7500000	0.0986832	0.0883035	0.0805200	0.0762456
8.0000000	0.0994650	0.0888467	0.0808791	0.0765004
8.2500000	0.1002062	0.0893476	0.0811939	0.0767099
8.5000000	0.1009079	0.0898071	0.0814654	0.0768748
8.7500000	0.1015710	0.0902262	0.0816945	0.0769961
9.0000000	0.1021966	0.0906057	0.0818819	0.0770748
9.2500000	0.1027856	0.0909464	0.0820286	0.0770748
9.5000000	0.1033389	0.0912490	0.0821352	0.0770748
9.7500000	0.1038572	0.0915143	0.0822026	0.0770748
10.0000000	0.1043413	0.0917429	0.0822026	0.0769775
10.2500000	0.1047918	0.0919354	0.0822026	0.0768544
10.5000000	0.1052093	0.0920925	0.0822026	0.0766934
10.7500000	0.1055944	0.0922147	0.0820919	0.0764957
11.0000000	0.1059476	0.0923026	0.0819731	0.0762621
11.2500000	0.1062695	0.0923026	0.0818189	0.0759938
11.5000000	0.1065604	0.0923774	0.0816306	0.0756919
11.7500000	0.1068209	0.0923774	0.0814089	0.0753577
12.0000000	0.1070515	0.0923774	0.0811547	0.0749924
12.2500000	0.1072525	0.0922450	0.0808690	0.0745976
12.5000000	0.1074243	0.0921384	0.0805528	0.0741748
12.7500000	0.1075675	0.0920006	0.0802073	0.0737257
13.0000000	0.1076824	0.0918329	0.0798336	0.0732519
13.2500000	0.1077693	0.0916359	0.0794330	0.0727556
13.5000000	0.1077693	0.0914102	0.0790069	0.0722385
13.7500000	0.1078601	0.0911565	0.0785567	0.0717027
14.0000000	0.1078601	0.0908756	0.0780840	0.0711504
14.2500000	0.1078601	0.0905682	0.0775904	0.0705836
14.5000000	0.1078601	0.0902351	0.0770776	0.0700045
14.7500000	0.1077214	0.0898773	0.0765473	0.0694153
15.0000000	0.1076229	0.0894956	0.0760013	0.0688178

	Case 35	Case 36	Case 37	Case 38
	Pressure: 9.5 MPa, Temperature: 27 °C, Inlet K: 0, Outlet K: 13	Pressure: 9.5 MPa, Temperature: 27 °C, Inlet K: 2, Outlet K: 0	Pressure: 9.5 MPa, Temperature: 27 °C, Inlet K: 5, Outlet K: 0	Pressure: 9.5 MPa, Temperature: 27 °C, Inlet K: 8, Outlet K: 0
Inlet Flow rate (kg/s)	Power (kW)	Power (kW)	Power (kW)	Power (kW)
0.2500000	0.0250827	0.0306089	0.0286511	0.0271463
0.5000000	0.0316531	0.0390875	0.0365130	0.0345299
0.7500000	0.0364626	0.0453802	0.0423257	0.0399868
1.0000000	0.0402035	0.0503159	0.0468926	0.0442809
1.2500000	0.0433321	0.0544905	0.0507588	0.0479187
1.5000000	0.0460418	0.0581513	0.0541509	0.0511118
1.7500000	0.0484389	0.0614330	0.0571931	0.0539765
2.0000000	0.0505901	0.0644199	0.0599630	0.0565854
2.2500000	0.0525400	0.0671689	0.0625130	0.0589876
2.5000000	0.0543201	0.0697204	0.0648803	0.0612178
2.7500000	0.0559535	0.0721043	0.0670924	0.0633017
3.0000000	0.0574578	0.0743434	0.0691702	0.0652588
3.2500000	0.0588464	0.0764556	0.0711301	0.0671043
3.5000000	0.0601302	0.0784549	0.0729850	0.0688504
3.7500000	0.0613179	0.0803529	0.0747454	0.0705068
4.0000000	0.0624164	0.0821590	0.0764199	0.0720817
4.2500000	0.0634318	0.0838811	0.0780159	0.0735817
4.5000000	0.0643689	0.0855259	0.0795393	0.0750126
4.7500000	0.0652319	0.0870989	0.0809954	0.0763793
5.0000000	0.0660242	0.0886050	0.0823887	0.0776859
5.2500000	0.0667491	0.0900485	0.0837230	0.0789362
5.5000000	0.0674092	0.0914330	0.0850018	0.0801332
5.7500000	0.0680071	0.0927618	0.0862280	0.0812799
6.0000000	0.0685450	0.0940378	0.0874043	0.0823785
6.2500000	0.0690251	0.0952634	0.0885330	0.0834314
6.5000000	0.0694492	0.0964410	0.0896161	0.0844405
6.7500000	0.0698191	0.0975726	0.0906555	0.0854077
7.0000000	0.0701361	0.0986599	0.0916530	0.0863346
7.2500000	0.0704015	0.0997046	0.0926101	0.0872228
7.5000000	0.0706167	0.1007083	0.0935283	0.0880737
7.7500000	0.0707827	0.1016722	0.0944089	0.0888886
8.0000000	0.0709008	0.1025977	0.0952531	0.0896689
8.2500000	0.0709718	0.1034858	0.0960621	0.0904158
8.5000000	0.0709718	0.1043378	0.0968371	0.0911304
8.7500000	0.0709718	0.1051547	0.0975790	0.0918137
9.0000000	0.0709125	0.1059374	0.0982890	0.0924665
9.2500000	0.0708048	0.1066868	0.0989679	0.0930897
9.5000000	0.0706552	0.1074038	0.0996166	0.0936841
9.7500000	0.0704647	0.1080893	0.1002358	0.0942503
10.0000000	0.0702345	0.1087441	0.1008261	0.0947892
10.2500000	0.0699658	0.1093689	0.1013884	0.0953013
10.5000000	0.0696601	0.1099643	0.1019230	0.0957874
10.7500000	0.0693189	0.1105310	0.1024308	0.0962479
11.0000000	0.0689437	0.1110695	0.1029121	0.0966834
11.2500000	0.0685364	0.1115803	0.1033676	0.0970946
11.5000000	0.0680988	0.1120639	0.1037978	0.0974818
11.7500000	0.0676332	0.1125208	0.1042031	0.0978457
12.0000000	0.0671416	0.1129514	0.1045840	0.0981866
12.2500000	0.0666264	0.1133563	0.1049410	0.0985051
12.5000000	0.0660900	0.1137357	0.1052744	0.0988015
12.7500000	0.0655351	0.1140902	0.1055848	0.0990764
13.0000000	0.0649643	0.1144200	0.1058724	0.0993300
13.2500000	0.0643800	0.1147256	0.1061378	0.0995628
13.5000000	0.0637848	0.1150073	0.1063812	0.0997751
13.7500000	0.0631814	0.1152655	0.1066029	0.0999674
14.0000000	0.0625719	0.1155004	0.1068035	0.1001399
14.2500000	0.0619587	0.1157124	0.1069830	0.1002930
14.5000000	0.0613439	0.1159019	0.1071420	0.1004270
14.7500000	0.0607294	0.1160690	0.1072806	0.1005423
15.0000000	0.0601169	0.1162141	0.1073992	0.1006392

	Case 39	Case 40	Case 41	Case 42
	Pressure: 9.5 MPa, Temperature: 27 °C, Inlet K: 10, Outlet K: 0	Pressure: 9.5 MPa, Temperature: 27 °C, Inlet K: 13, Outlet K: 0	Pressure: 9.5 MPa, Temperature: 30 °C, Inlet K: 0, Outlet K: 2	Pressure: 9.5 MPa, Temperature: 30 °C, Inlet K: 0, Outlet K: 5
Inlet Flow rate (kg/s)	Power (kW)	Power (kW)	Power (kW)	Power (kW)
0.2500000	0.0263176	0.0252666	0.0308035	0.0287450
0.5000000	0.0334308	0.0320239	0.0392720	0.0365260
0.7500000	0.0386947	0.0370442	0.0455203	0.0422190
1.0000000	0.0428411	0.0410047	0.0503949	0.0466488
1.2500000	0.0463552	0.0443630	0.0544955	0.0503627
1.5000000	0.0494405	0.0473124	0.0580712	0.0535889
1.7500000	0.0522089	0.0499593	0.0612578	0.0564522
2.0000000	0.0547304	0.0523704	0.0641402	0.0590310
2.2500000	0.0570521	0.0545905	0.0667758	0.0613781
2.5000000	0.0592076	0.0566514	0.0692055	0.0635309
2.7500000	0.0612216	0.0585766	0.0714595	0.0655172
3.0000000	0.0631127	0.0603837	0.0735607	0.0673581
3.2500000	0.0648955	0.0620867	0.0755271	0.0690701
3.5000000	0.0665818	0.0636967	0.0773732	0.0706664
3.7500000	0.0681810	0.0652225	0.0791106	0.0721577
4.0000000	0.0697008	0.0666718	0.0807490	0.0735530
4.2500000	0.0711477	0.0680506	0.0822965	0.0748595
4.5000000	0.0725273	0.0693643	0.0837599	0.0760835
4.7500000	0.0738443	0.0706172	0.0851451	0.0772302
5.0000000	0.0751027	0.0718133	0.0864571	0.0783043
5.2500000	0.0763061	0.0729559	0.0877001	0.0793098
5.5000000	0.0774574	0.0740479	0.0888780	0.0802500
5.7500000	0.0785593	0.0750919	0.0899941	0.0811282
6.0000000	0.0796143	0.0760903	0.0910515	0.0819471
6.2500000	0.0806246	0.0770452	0.0920526	0.0827094
6.5000000	0.0815921	0.0779585	0.0930001	0.0834173
6.7500000	0.0825185	0.0788322	0.0938959	0.0840730
7.0000000	0.0834057	0.0796678	0.0947423	0.0846786
7.2500000	0.0842551	0.0804669	0.0955409	0.0852358
7.5000000	0.0850681	0.0812312	0.0962936	0.0857461
7.7500000	0.0858463	0.0819617	0.0970018	0.0862108
8.0000000	0.0865908	0.0826598	0.0976673	0.0866315
8.2500000	0.0873029	0.0833265	0.0982913	0.0870091
8.5000000	0.0879834	0.0839628	0.0988750	0.0873450
8.7500000	0.0886335	0.0845696	0.0994194	0.0876401
9.0000000	0.0892539	0.0851477	0.0999257	0.0878954
9.2500000	0.0898455	0.0856982	0.1003947	0.0881120
9.5000000	0.0904091	0.0862216	0.1008274	0.0882906
9.7500000	0.0909454	0.0867188	0.1012246	0.0884323
10.0000000	0.0914550	0.0871904	0.1015871	0.0885378
10.2500000	0.0919388	0.0876372	0.1019156	0.0886079
10.5000000	0.0923972	0.0880598	0.1022108	0.0886079
10.7500000	0.0928309	0.0884587	0.1024735	0.0886079
11.0000000	0.0932405	0.0888345	0.1027042	0.0886079
11.2500000	0.0936265	0.0891879	0.1029037	0.0885485
11.5000000	0.0939895	0.0895192	0.1030724	0.0884521
11.7500000	0.0943298	0.0898291	0.1032110	0.0883248
12.0000000	0.0946481	0.0901180	0.1033201	0.0881674
12.2500000	0.0949448	0.0903863	0.1034001	0.0879806
12.5000000	0.0952202	0.0906345	0.1034001	0.0877653
12.7500000	0.0954749	0.0908630	0.1034745	0.0875223
13.0000000	0.0957092	0.0910722	0.1034745	0.0872526
13.2500000	0.0959235	0.0912626	0.1034745	0.0869569
13.5000000	0.0961182	0.0914345	0.1033804	0.0866364
13.7500000	0.0962937	0.0915883	0.1032964	0.0862920
14.0000000	0.0964503	0.0917244	0.1031863	0.0859249
14.2500000	0.0965884	0.0918431	0.1030512	0.0855360
14.5000000	0.0967083	0.0919449	0.1028916	0.0851266
14.7500000	0.0968104	0.0920300	0.1027079	0.0846978
15.0000000	0.0968950	0.0920989	0.1025007	0.0842509

	Case 43	Case 44	Case 45	Case 46
	Pressure: 9.5 MPa, Temperature: 30 °C, Inlet K: 0, Outlet K: 8	Pressure: 9.5 MPa, Temperature: 30 °C, Inlet K: 0, Outlet K: 10	Pressure: 9.5 MPa, Temperature: 30 °C, Inlet K: 0, Outlet K: 13	Pressure: 9.5 MPa, Temperature: 30 °C, Inlet K: 2, Outlet K: 0
Inlet Flow rate (kg/s)	Power (kW)	Power (kW)	Power (kW)	Power (kW)
0.2500000	0.0271708	0.0263064	0.0252120	0.0308604
0.5000000	0.0344277	0.0332703	0.0317941	0.0393907
0.7500000	0.0397151	0.0383397	0.0365903	0.0457092
1.0000000	0.0438213	0.0422725	0.0403063	0.0506566
1.2500000	0.0472542	0.0455548	0.0434002	0.0548332
1.5000000	0.0502266	0.0483912	0.0460663	0.0584879
1.7500000	0.0528554	0.0508941	0.0484116	0.0617564
2.0000000	0.0552137	0.0531340	0.0505029	0.0647237
2.2500000	0.0573510	0.0551584	0.0523854	0.0674472
2.5000000	0.0593022	0.0570009	0.0540910	0.0699675
2.7500000	0.0610932	0.0586864	0.0556434	0.0723150
3.0000000	0.0627437	0.0602339	0.0570605	0.0745125
3.2500000	0.0642692	0.0616582	0.0583564	0.0765782
3.5000000	0.0656819	0.0629710	0.0595423	0.0785264
3.7500000	0.0669919	0.0641821	0.0606273	0.0803688
4.0000000	0.0682073	0.0652992	0.0616187	0.0821152
4.2500000	0.0693350	0.0663288	0.0625228	0.0837737
4.5000000	0.0703808	0.0672767	0.0633451	0.0853510
4.7500000	0.0713496	0.0681475	0.0640903	0.0868532
5.0000000	0.0722457	0.0689455	0.0647623	0.0882853
5.2500000	0.0730729	0.0696745	0.0653651	0.0896515
5.5000000	0.0738347	0.0703378	0.0659018	0.0909558
5.7500000	0.0745340	0.0709384	0.0663755	0.0922015
6.0000000	0.0751736	0.0714791	0.0667884	0.0933915
6.2500000	0.0757562	0.0719622	0.0671429	0.0945287
6.5000000	0.0762839	0.0723899	0.0674411	0.0956153
6.7500000	0.0767587	0.0727639	0.0676847	0.0966537
7.0000000	0.0771823	0.0730861	0.0678756	0.0976457
7.2500000	0.0775563	0.0733581	0.0680154	0.0985932
7.5000000	0.0778822	0.0735813	0.0681056	0.0994980
7.7500000	0.0781615	0.0737572	0.0681056	0.1003616
8.0000000	0.0783954	0.0738870	0.0681056	0.1011855
8.2500000	0.0785852	0.0739722	0.0681056	0.1019712
8.5000000	0.0787320	0.0739722	0.0679985	0.1027199
8.7500000	0.0788369	0.0739722	0.0678616	0.1034328
9.0000000	0.0789011	0.0739722	0.0676835	0.1041108
9.2500000	0.0789011	0.0738880	0.0674658	0.1047551
9.5000000	0.0789011	0.0737664	0.0672102	0.1053664
9.7500000	0.0789011	0.0736069	0.0669182	0.1059456
10.0000000	0.0787678	0.0734109	0.0665917	0.1064934
10.2500000	0.0786425	0.0731796	0.0662326	0.1070108
10.5000000	0.0784819	0.0729144	0.0658428	0.1074983
10.7500000	0.0782875	0.0726167	0.0654244	0.1079566
11.0000000	0.0780605	0.0722880	0.0649798	0.1083863
11.2500000	0.0778019	0.0719298	0.0645111	0.1087881
11.5000000	0.0775129	0.0715439	0.0640209	0.1091626
11.7500000	0.0771949	0.0711319	0.0635115	0.1095102
12.0000000	0.0768492	0.0706957	0.0629855	0.1098315
12.2500000	0.0764771	0.0702371	0.0624453	0.1101270
12.5000000	0.0760802	0.0697582	0.0618934	0.1103972
12.7500000	0.0756599	0.0692610	0.0613322	0.1106425
13.0000000	0.0752179	0.0687475	0.0607639	0.1108634
13.2500000	0.0747558	0.0682197	0.0601907	0.1110604
13.5000000	0.0742753	0.0676797	0.0596146	0.1112337
13.7500000	0.0737782	0.0671295	0.0590374	0.1113838
14.0000000	0.0732661	0.0665710	0.0584608	0.1115112
14.2500000	0.0727410	0.0660061	0.0578863	0.1116160
14.5000000	0.0722044	0.0654364	0.0573152	0.1116988
14.7500000	0.0716581	0.0648638	0.0567488	0.1116988
15.0000000	0.0711038	0.0642897	0.0561881	0.1117982

	Case 47	Case 48	Case 49	Case 50
	Pressure: 9.5 MPa, Temperature: 30 °C, Inlet K: 5, Outlet K: 0	Pressure: 9.5 MPa, Temperature: 30 °C, Inlet K: 8, Outlet K: 0	Pressure: 9.5 MPa, Temperature: 30 °C, Inlet K: 10, Outlet K: 0	Pressure: 9.5 MPa, Temperature: 30 °C, Inlet K: 13, Outlet K: 0
Inlet Flow rate (kg/s)	Power (kW)	Power (kW)	Power (kW)	Power (kW)
0.2500000	0.0288604	0.0273272	0.0264840	0.0254155
0.5000000	0.0367647	0.0347479	0.0336321	0.0322055
0.7500000	0.0425965	0.0402198	0.0389089	0.0372364
1.0000000	0.0471705	0.0445179	0.0430578	0.0411975
1.2500000	0.0510350	0.0481514	0.0465662	0.0445484
1.5000000	0.0544179	0.0513331	0.0496387	0.0474832
1.7500000	0.0574442	0.0541797	0.0523877	0.0501090
2.0000000	0.0601920	0.0567643	0.0548837	0.0524927
2.2500000	0.0627141	0.0591364	0.0571741	0.0546796
2.5000000	0.0650479	0.0613311	0.0592927	0.0567017
2.7500000	0.0672214	0.0633742	0.0612646	0.0585829
3.0000000	0.0692555	0.0652857	0.0631088	0.0603415
3.2500000	0.0711670	0.0670810	0.0648403	0.0619916
3.5000000	0.0729690	0.0687726	0.0664711	0.0635448
3.7500000	0.0746724	0.0703706	0.0680111	0.0650103
4.0000000	0.0762861	0.0718835	0.0694681	0.0663958
4.2500000	0.0778176	0.0733182	0.0708491	0.0677077
4.5000000	0.0792732	0.0746805	0.0721597	0.0689515
4.7500000	0.0806583	0.0759757	0.0734047	0.0701320
5.0000000	0.0819775	0.0772080	0.0745885	0.0712532
5.2500000	0.0832349	0.0783812	0.0757148	0.0723188
5.5000000	0.0844341	0.0794989	0.0767869	0.0733322
5.7500000	0.0855781	0.0805640	0.0778079	0.0742962
6.0000000	0.0866698	0.0815792	0.0787804	0.0752136
6.2500000	0.0877118	0.0825471	0.0797069	0.0760868
6.5000000	0.0887063	0.0834700	0.0805897	0.0769181
6.7500000	0.0896555	0.0843498	0.0814310	0.0777093
7.0000000	0.0905614	0.0851888	0.0822324	0.0784622
7.2500000	0.0914258	0.0859884	0.0829958	0.0791783
7.5000000	0.0922503	0.0867504	0.0837224	0.0798592
7.7500000	0.0930366	0.0874760	0.0844138	0.0805061
8.0000000	0.0937860	0.0881666	0.0850712	0.0811203
8.2500000	0.0944997	0.0888234	0.0856958	0.0817030
8.5000000	0.0951789	0.0894474	0.0862886	0.0822553
8.7500000	0.0958246	0.0900397	0.0868507	0.0827782
9.0000000	0.0964379	0.0906014	0.0873832	0.0832726
9.2500000	0.0970196	0.0911332	0.0878868	0.0837395
9.5000000	0.0975707	0.0916362	0.0883624	0.0841797
9.7500000	0.0980919	0.0921110	0.0888110	0.0845940
10.0000000	0.0985841	0.0925585	0.0892331	0.0849832
10.2500000	0.0990479	0.0929793	0.0896296	0.0853480
10.5000000	0.0994841	0.0933743	0.0900011	0.0856890
10.7500000	0.0998933	0.0937439	0.0903483	0.0860069
11.0000000	0.1002762	0.0940890	0.0906718	0.0863023
11.2500000	0.1006334	0.0944099	0.0909722	0.0865758
11.5000000	0.1009653	0.0947074	0.0912500	0.0868280
11.7500000	0.1012727	0.0949819	0.0915057	0.0870593
12.0000000	0.1015559	0.0952340	0.0917400	0.0872703
12.2500000	0.1018155	0.0954641	0.0919532	0.0874615
12.5000000	0.1020520	0.0956727	0.0921459	0.0876334
12.7500000	0.1022657	0.0958604	0.0923185	0.0877865
13.0000000	0.1024573	0.0960274	0.0924715	0.0879212
13.2500000	0.1026269	0.0961743	0.0926053	0.0880381
13.5000000	0.1027752	0.0963015	0.0927204	0.0881374
13.7500000	0.1029025	0.0964094	0.0928172	0.0882197
14.0000000	0.1030091	0.0964984	0.0928961	0.0882855
14.2500000	0.1030956	0.0965690	0.0929575	0.0883351
14.5000000	0.1031621	0.0966214	0.0929575	0.0883351
14.7500000	0.1031621	0.0966214	0.0930276	0.0883860
15.0000000	0.1032358	0.0966724	0.0930276	0.0883860

	Case 51	Case 52	Case 53	Case 54
	Pressure: 9.5 MPa, Temperature: 32 °C, Inlet K: 0, Outlet K: 2	Pressure: 9.5 MPa, Temperature: 32 °C, Inlet K: 0, Outlet K: 5	Pressure: 9.5 MPa, Temperature: 32 °C, Inlet K: 0, Outlet K: 8	Pressure: 9.5 MPa, Temperature: 32 °C, Inlet K: 0, Outlet K: 10
Inlet Flow rate (kg/s)	Power (kW)	Power (kW)	Power (kW)	Power (kW)
0.2500000	0.0309521	0.0288595	0.0272628	0.0263870
0.5000000	0.0394391	0.0366476	0.0345196	0.0333476
0.7500000	0.0456838	0.0423264	0.0397863	0.0383931
1.0000000	0.0505444	0.0467330	0.0438633	0.0422934
1.2500000	0.0546232	0.0504162	0.0472594	0.0455358
1.5000000	0.0581703	0.0536049	0.0501883	0.0483255
1.7500000	0.0613222	0.0564248	0.0527674	0.0507754
2.0000000	0.0641646	0.0589547	0.0550705	0.0529568
2.2500000	0.0667553	0.0612478	0.0571475	0.0549176
2.5000000	0.0691355	0.0633420	0.0590339	0.0566920
2.7500000	0.0713357	0.0652656	0.0607560	0.0583054
3.0000000	0.0733793	0.0670401	0.0623340	0.0597772
3.2500000	0.0752846	0.0686822	0.0637836	0.0611224
3.5000000	0.0770664	0.0702056	0.0651174	0.0623532
3.7500000	0.0787365	0.0716211	0.0663456	0.0634794
4.0000000	0.0803049	0.0729378	0.0674767	0.0645094
4.2500000	0.0817798	0.0741632	0.0685178	0.0654499
4.5000000	0.0831682	0.0753038	0.0694751	0.0663072
4.7500000	0.0844760	0.0763652	0.0703540	0.0670863
5.0000000	0.0857084	0.0773523	0.0711592	0.0677921
5.2500000	0.0868699	0.0782692	0.0718948	0.0684286
5.5000000	0.0879646	0.0791199	0.0725645	0.0689992
5.7500000	0.0889960	0.0799078	0.0731717	0.0695071
6.0000000	0.0899673	0.0806360	0.0737192	0.0699549
6.2500000	0.0908814	0.0813073	0.0742093	0.0703453
6.5000000	0.0917409	0.0819240	0.0746445	0.0706803
6.7500000	0.0925482	0.0824884	0.0750268	0.0709622
7.0000000	0.0933056	0.0830025	0.0753581	0.0711927
7.2500000	0.0940151	0.0834679	0.0756403	0.0713739
7.5000000	0.0946785	0.0838863	0.0758749	0.0715073
7.7500000	0.0952972	0.0842594	0.0760635	0.0715945
8.0000000	0.0958727	0.0845885	0.0762077	0.0715945
8.2500000	0.0964065	0.0848750	0.0763088	0.0715945
8.5000000	0.0968998	0.0851201	0.0763680	0.0715945
8.7500000	0.0973538	0.0853250	0.0763680	0.0715094
9.0000000	0.0977695	0.0854908	0.0763680	0.0713866
9.2500000	0.0981480	0.0856186	0.0763062	0.0712261
9.5000000	0.0984903	0.0857095	0.0762098	0.0710294
9.7500000	0.0987973	0.0857095	0.0760775	0.0707981
10.0000000	0.0990698	0.0857837	0.0759106	0.0705336
10.2500000	0.0993088	0.0857837	0.0757106	0.0702376
10.5000000	0.0995149	0.0857212	0.0754785	0.0699118
10.7500000	0.0996890	0.0856407	0.0752158	0.0695578
11.0000000	0.0998318	0.0855285	0.0749238	0.0691775
11.2500000	0.0999439	0.0853858	0.0746041	0.0687729
11.5000000	0.1000261	0.0852134	0.0742580	0.0683457
11.7500000	0.1000261	0.0850124	0.0738871	0.0678979
12.0000000	0.1001023	0.0847837	0.0734930	0.0674317
12.2500000	0.1001023	0.0845284	0.0730774	0.0669489
12.5000000	0.1001023	0.0842474	0.0726419	0.0664516
12.7500000	0.1000072	0.0839418	0.0721882	0.0659418
13.0000000	0.0999221	0.0836128	0.0717180	0.0654214
13.2500000	0.0998110	0.0832615	0.0712332	0.0648923
13.5000000	0.0996747	0.0828891	0.0707353	0.0643564
13.7500000	0.0995140	0.0824967	0.0702262	0.0638152
14.0000000	0.0993294	0.0820857	0.0697074	0.0632705
14.2500000	0.0991216	0.0816572	0.0691805	0.0627236
14.5000000	0.0988913	0.0812126	0.0686472	0.0621761
14.7500000	0.0986392	0.0807531	0.0681087	0.0616290
15.0000000	0.0983659	0.0802801	0.0675667	0.0610837

	Case 55	Case 56	Case 57	Case 58
	Pressure: 9.5 MPa, Temperature: 32 °C, Inlet K: 0, Outlet K: 13	Pressure: 9.5 MPa, Temperature: 32 °C, Inlet K: 2, Outlet K: 0	Pressure: 9.5 MPa, Temperature: 32 °C, Inlet K: 5, Outlet K: 0	Pressure: 9.5 MPa, Temperature: 32 °C, Inlet K: 8, Outlet K: 0
Inlet Flow rate (kg/s)	Power (kW)	Power (kW)	Power (kW)	Power (kW)
0.2500000	0.0252792	0.0310138	0.0289846	0.0274319
0.5000000	0.0318543	0.0395681	0.0369064	0.0348665
0.7500000	0.0366227	0.0458891	0.0427360	0.0403333
1.0000000	0.0403024	0.0508290	0.0472994	0.0446187
1.2500000	0.0433526	0.0549905	0.0511464	0.0482329
1.5000000	0.0459680	0.0586237	0.0545058	0.0513895
1.7500000	0.0482561	0.0618652	0.0575032	0.0542058
2.0000000	0.0502848	0.0648002	0.0602172	0.0567553
2.2500000	0.0520995	0.0674868	0.0627011	0.0590880
2.5000000	0.0537330	0.0699659	0.0649927	0.0612394
2.7500000	0.0552092	0.0722681	0.0671202	0.0632359
3.0000000	0.0565467	0.0744168	0.0691050	0.0650976
3.2500000	0.0577597	0.0764304	0.0709643	0.0668404
3.5000000	0.0588597	0.0783235	0.0727113	0.0684769
3.7500000	0.0598564	0.0801080	0.0743572	0.0700175
4.0000000	0.0607576	0.0817940	0.0759111	0.0714707
4.2500000	0.0615701	0.0833895	0.0773806	0.0728437
4.5000000	0.0622998	0.0849018	0.0787721	0.0741426
4.7500000	0.0629519	0.0863366	0.0800912	0.0753727
5.0000000	0.0635309	0.0876993	0.0813427	0.0765387
5.2500000	0.0640405	0.0889943	0.0825310	0.0776447
5.5000000	0.0644841	0.0902256	0.0836598	0.0786942
5.7500000	0.0648645	0.0913968	0.0847324	0.0796907
6.0000000	0.0651845	0.0925111	0.0857519	0.0806371
6.2500000	0.0654467	0.0935713	0.0867212	0.0815361
6.5000000	0.0656532	0.0945800	0.0876427	0.0823899
6.7500000	0.0658062	0.0955397	0.0885188	0.0832008
7.0000000	0.0659077	0.0964524	0.0893514	0.0839704
7.2500000	0.0659595	0.0973205	0.0901423	0.0847007
7.5000000	0.0659595	0.0981455	0.0908933	0.0853931
7.7500000	0.0659595	0.0989291	0.0916057	0.0860492
8.0000000	0.0658323	0.0996729	0.0922810	0.0866702
8.2500000	0.0657020	0.1003781	0.0929205	0.0872575
8.5000000	0.0655303	0.1010461	0.0935255	0.0878122
8.7500000	0.0653191	0.1016779	0.0940969	0.0883355
9.0000000	0.0650705	0.1022747	0.0946359	0.0888283
9.2500000	0.0647862	0.1028375	0.0951435	0.0892916
9.5000000	0.0644683	0.1033673	0.0956206	0.0897263
9.7500000	0.0641188	0.1038649	0.0960681	0.0901333
10.0000000	0.0637400	0.1043312	0.0964867	0.0905133
10.2500000	0.0633340	0.1047670	0.0968773	0.0908672
10.5000000	0.0629032	0.1051731	0.0972406	0.0911956
10.7500000	0.0624499	0.1055502	0.0975774	0.0914993
11.0000000	0.0619767	0.1058989	0.0978881	0.0917788
11.2500000	0.0614860	0.1062200	0.0981736	0.0920348
11.5000000	0.0609801	0.1065140	0.0984344	0.0922679
11.7500000	0.0604615	0.1067815	0.0986710	0.0924786
12.0000000	0.0599326	0.1070231	0.0988840	0.0926675
12.2500000	0.0593955	0.1072392	0.0990739	0.0928351
12.5000000	0.0588524	0.1074306	0.0992413	0.0929820
12.7500000	0.0583052	0.1075975	0.0993866	0.0931086
13.0000000	0.0577558	0.1077405	0.0995103	0.0932154
13.2500000	0.0572058	0.1078601	0.0996129	0.0933029
13.5000000	0.0566567	0.1079566	0.0996948	0.0933716
13.7500000	0.0561100	0.1080307	0.0997566	0.0934219
14.0000000	0.0555667	0.1080307	0.0997566	0.0934219
14.2500000	0.0550280	0.1081116	0.0998199	0.0934219
14.5000000	0.0544947	0.1081116	0.0998199	0.0934219
14.7500000	0.0539675	0.1081116	0.0998199	0.0934219
15.0000000	0.0534472	0.1081116	0.0998199	0.0934219

	Case 59	Case 60
	Pressure: 9.5 MPa, Temperature: 32 °C, Inlet K: 10, Outlet K: 0	Pressure: 9.5 MPa, Temperature: 32 °C, Inlet K: 13, Outlet K: 0
Inlet Flow rate (kg/s)	Power (kW)	Power (kW)
0.2500000	0.0265790	0.0254991
0.5000000	0.0337392	0.0322993
0.7500000	0.0390096	0.0373221
1.0000000	0.0431446	0.0412679
1.2500000	0.0466328	0.0445972
1.5000000	0.0496793	0.0475048
1.7500000	0.0523971	0.0500982
2.0000000	0.0548572	0.0524449
2.2500000	0.0571075	0.0545907
2.5000000	0.0591822	0.0565682
2.7500000	0.0611070	0.0584017
3.0000000	0.0629011	0.0601096
3.2500000	0.0645798	0.0617066
3.5000000	0.0661554	0.0632042
3.7500000	0.0676378	0.0646120
4.0000000	0.0690353	0.0659379
4.2500000	0.0703548	0.0671886
4.5000000	0.0716022	0.0683700
4.7500000	0.0727829	0.0694871
5.0000000	0.0739013	0.0705443
5.2500000	0.0749614	0.0715456
5.5000000	0.0759669	0.0724946
5.7500000	0.0769211	0.0733943
6.0000000	0.0778268	0.0742473
6.2500000	0.0786865	0.0750561
6.5000000	0.0795024	0.0758229
6.7500000	0.0802765	0.0765495
7.0000000	0.0810108	0.0772379
7.2500000	0.0817069	0.0778896
7.5000000	0.0823663	0.0785062
7.7500000	0.0829906	0.0790891
8.0000000	0.0835810	0.0796397
8.2500000	0.0841387	0.0801591
8.5000000	0.0846650	0.0806485
8.7500000	0.0851610	0.0811089
9.0000000	0.0856275	0.0815413
9.2500000	0.0860657	0.0819468
9.5000000	0.0864763	0.0823260
9.7500000	0.0868603	0.0826799
10.0000000	0.0872184	0.0830093
10.2500000	0.0875513	0.0833148
10.5000000	0.0878597	0.0835971
10.7500000	0.0881444	0.0838570
11.0000000	0.0884060	0.0840951
11.2500000	0.0886450	0.0843119
11.5000000	0.0888622	0.0845081
11.7500000	0.0890579	0.0846843
12.0000000	0.0892329	0.0848409
12.2500000	0.0893875	0.0849787
12.5000000	0.0895225	0.0850979
12.7500000	0.0896381	0.0851993
13.0000000	0.0897351	0.0852833
13.2500000	0.0898137	0.0853504
13.5000000	0.0898746	0.0854010
13.7500000	0.0898746	0.0854010
14.0000000	0.0899432	0.0854535
14.2500000	0.0899432	0.0854535
14.5000000	0.0899432	0.0854535
14.7500000	0.0899432	0.0854535
15.0000000	0.0898891	0.0853822

APPENDIX - C

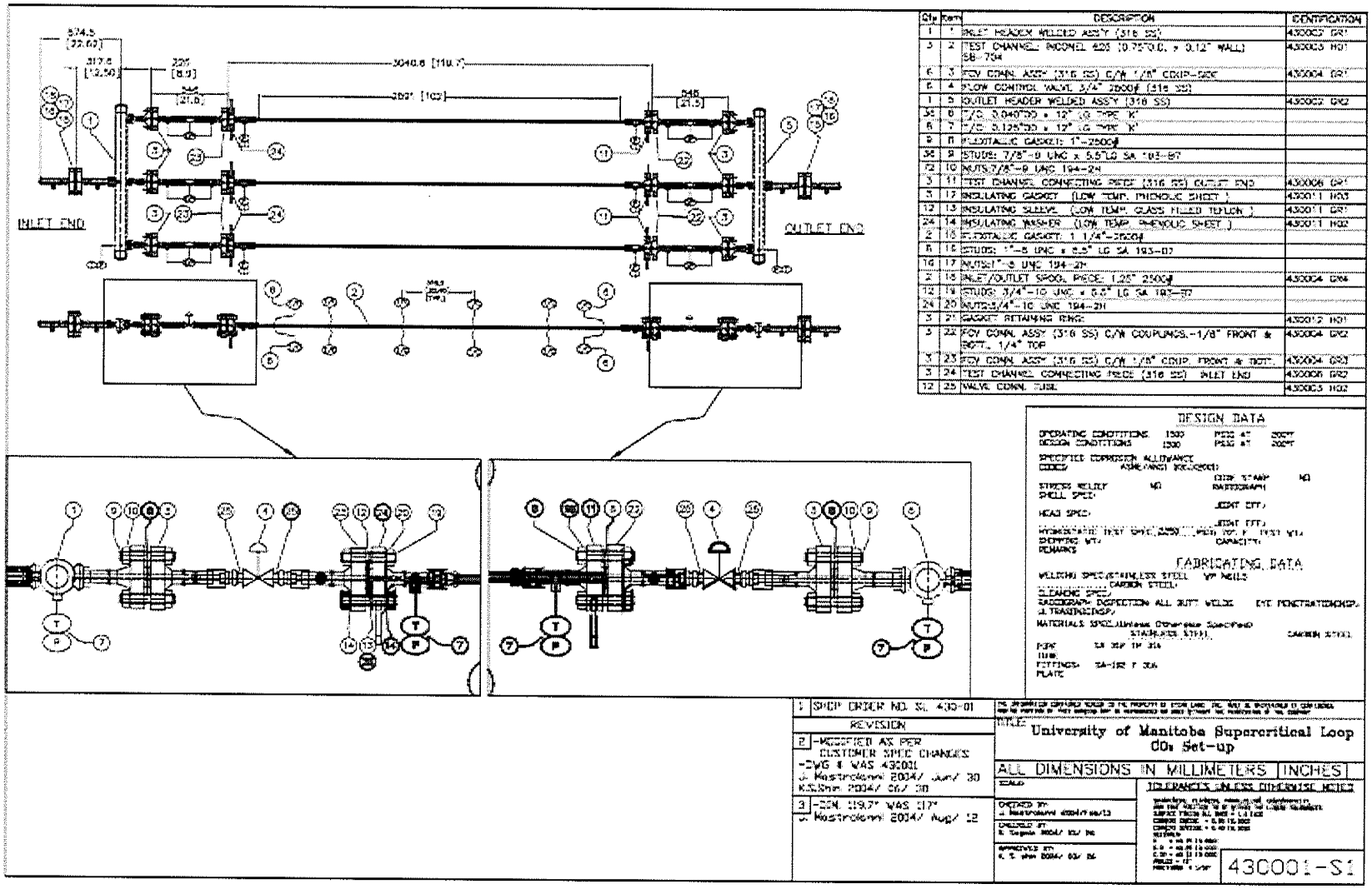

Figure C.1: Schematic drawing of test section for carbon dioxide experiments.

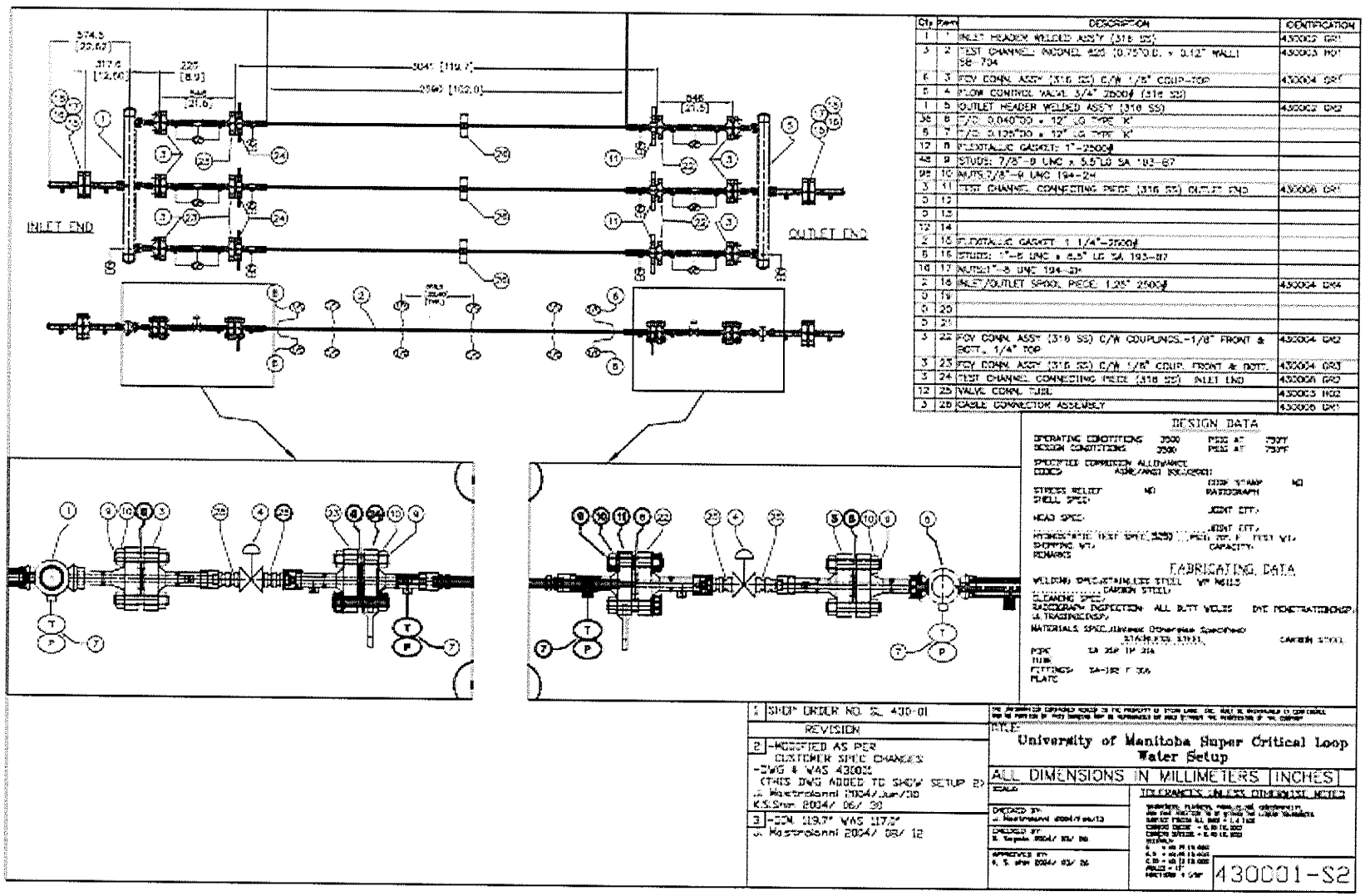

Figure C.2: Schematic drawing of the test section for water experiments.

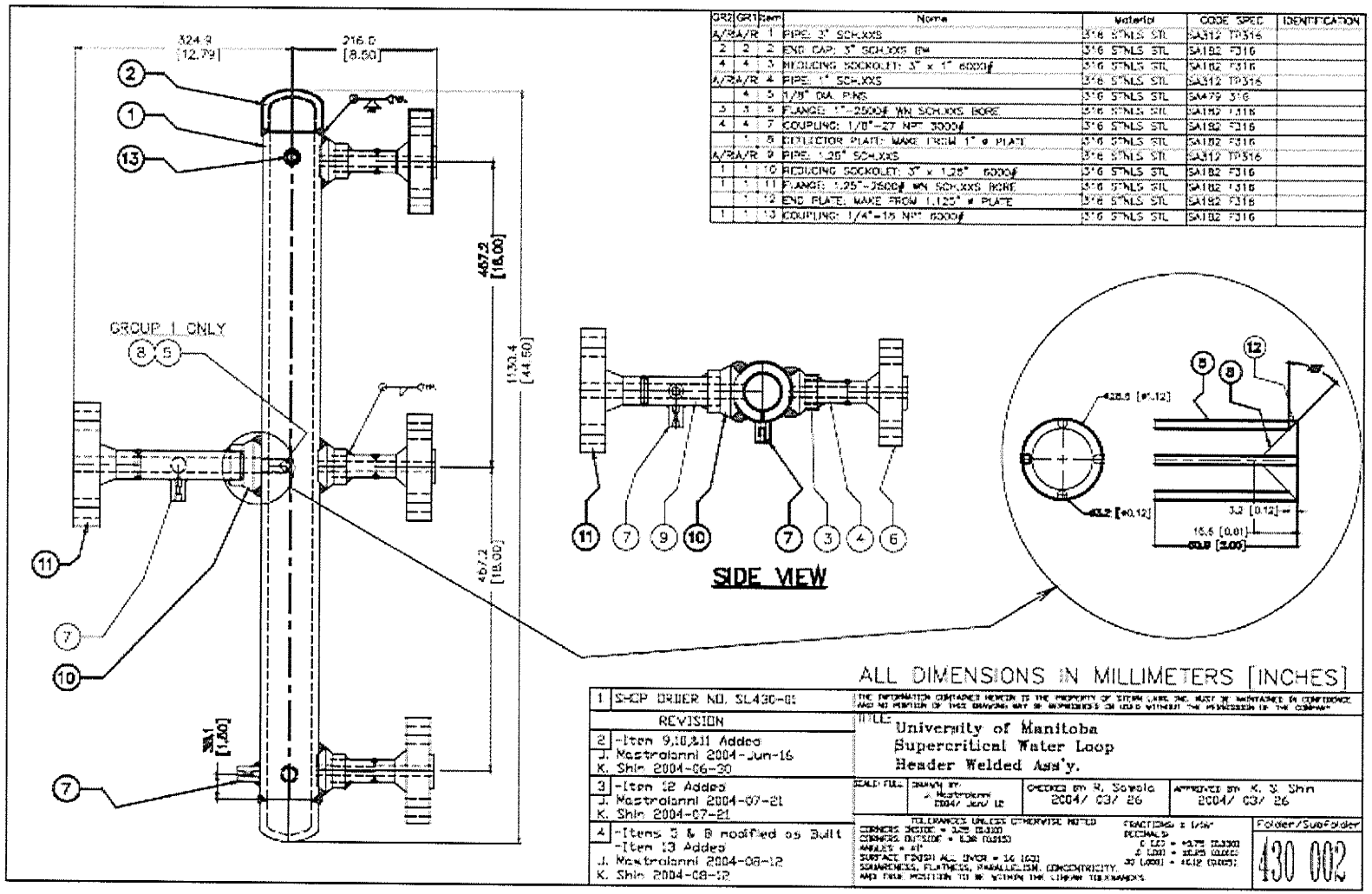

Figure C.3: Schematic drawing of test section header assembly.

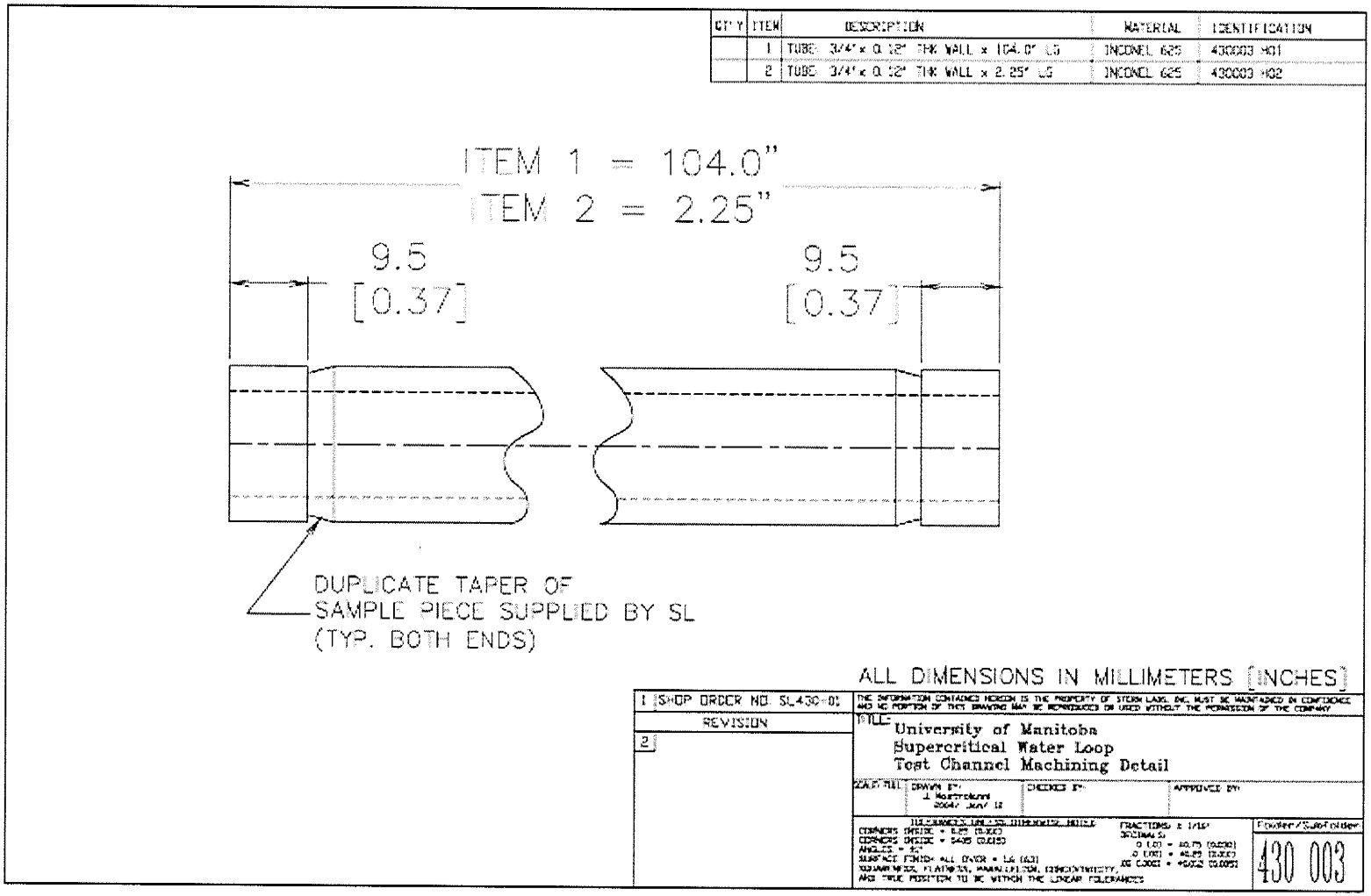

Figure C.4: Schematic drawing of test section channel machining details.

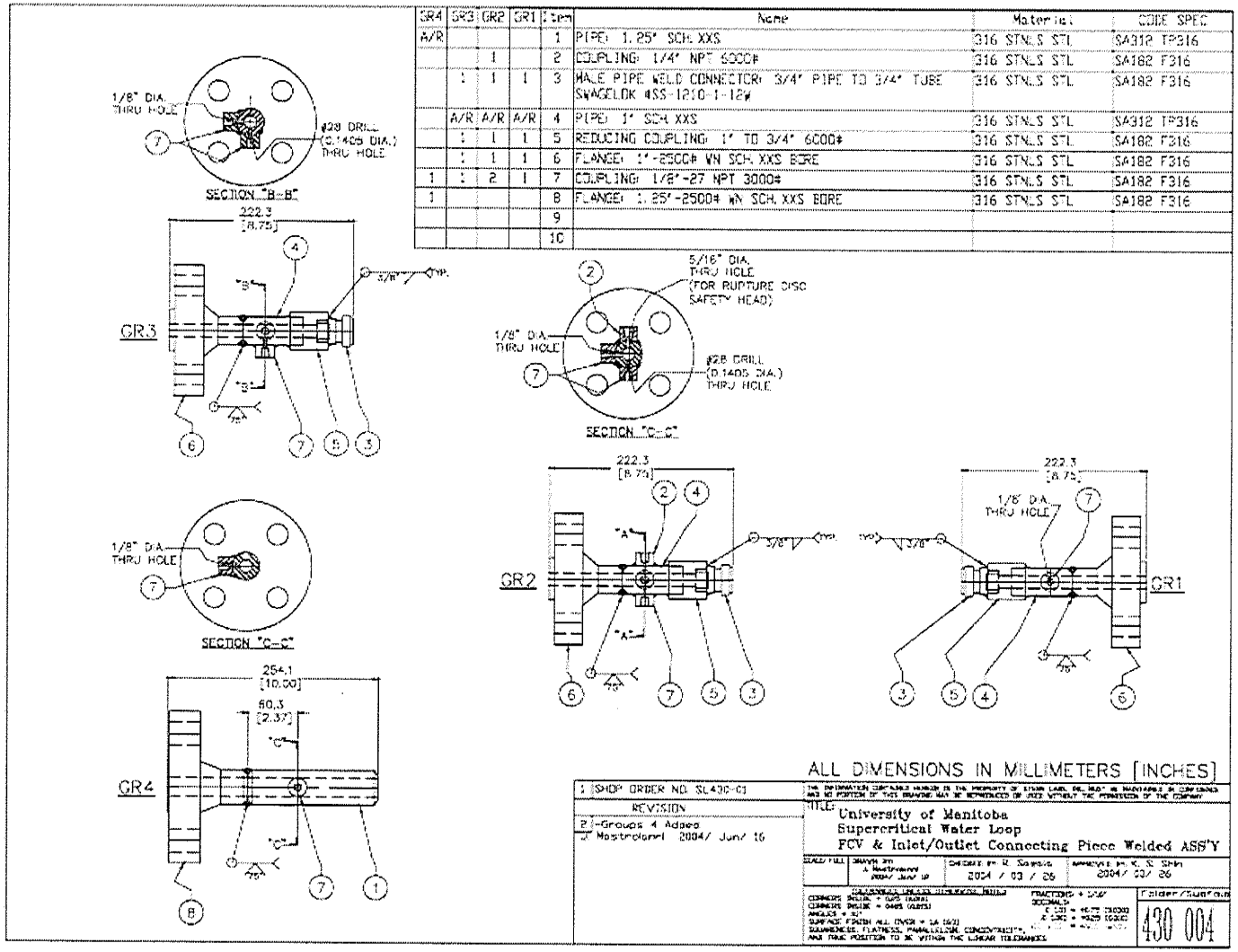

Figure C.5: Schematic drawing of flange couplings.

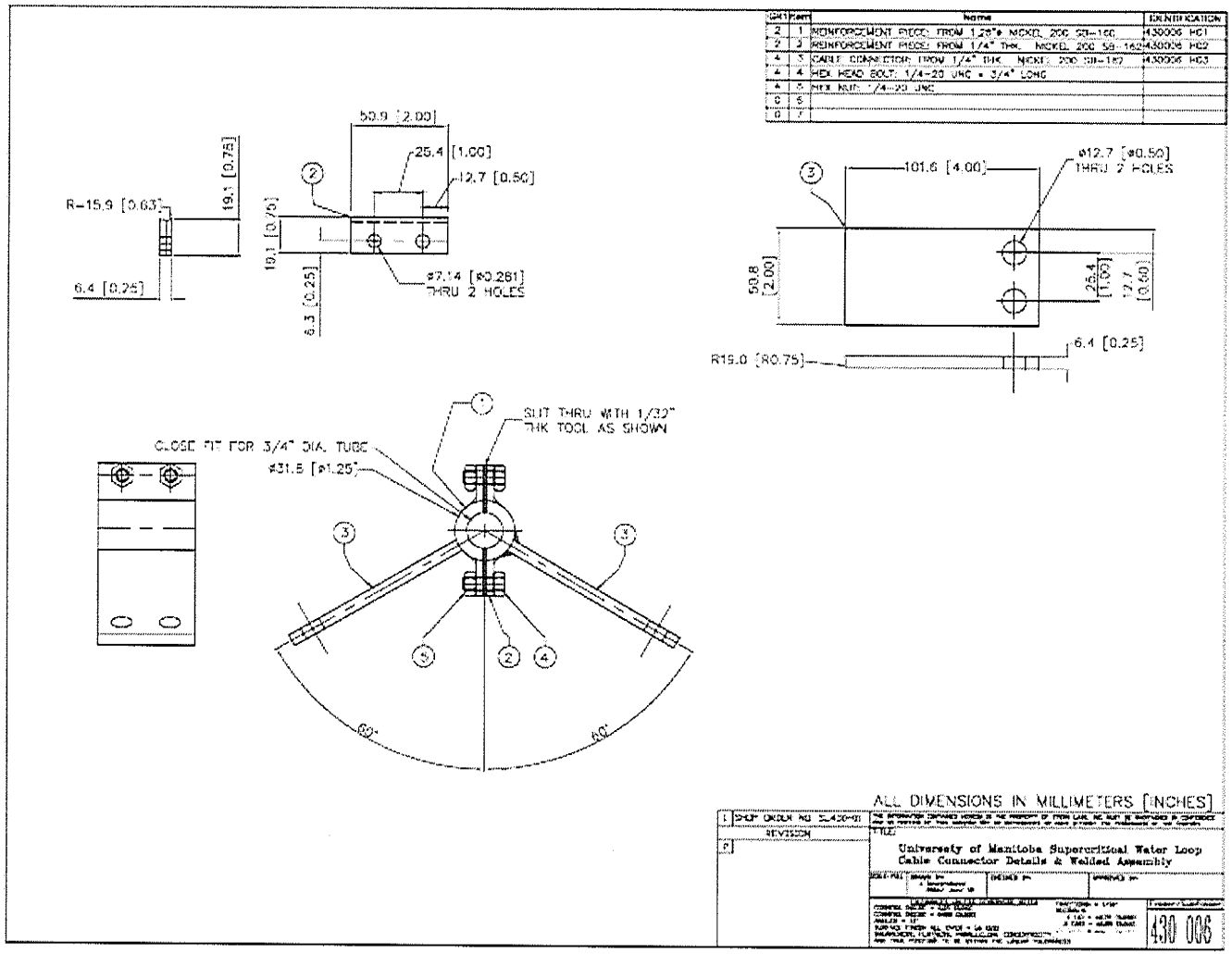

Figure C.6: Schematic drawing of electrical cable connector details (I).

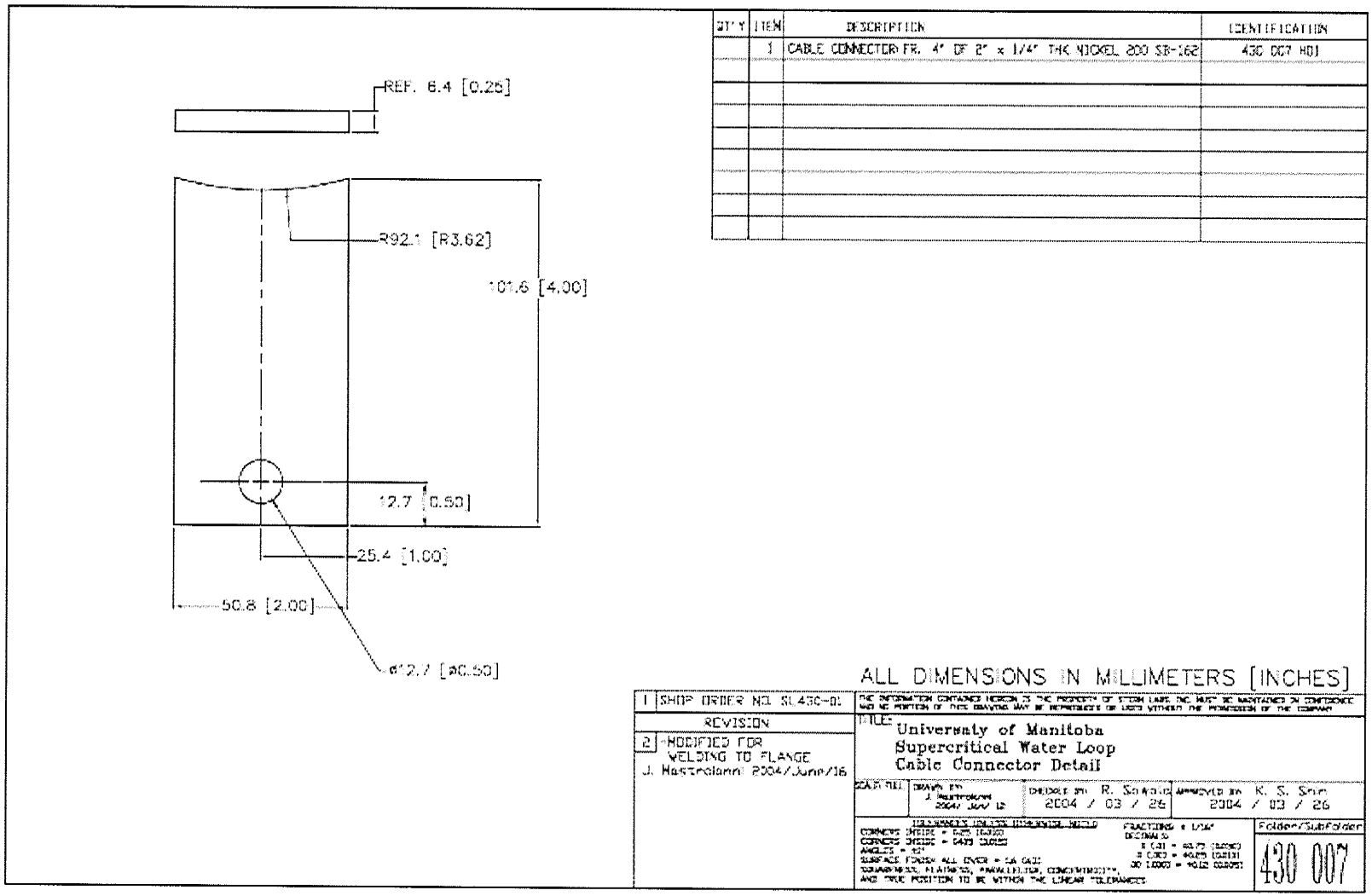

Figure C.7: Schematic drawing of electrical cable connector details (II).

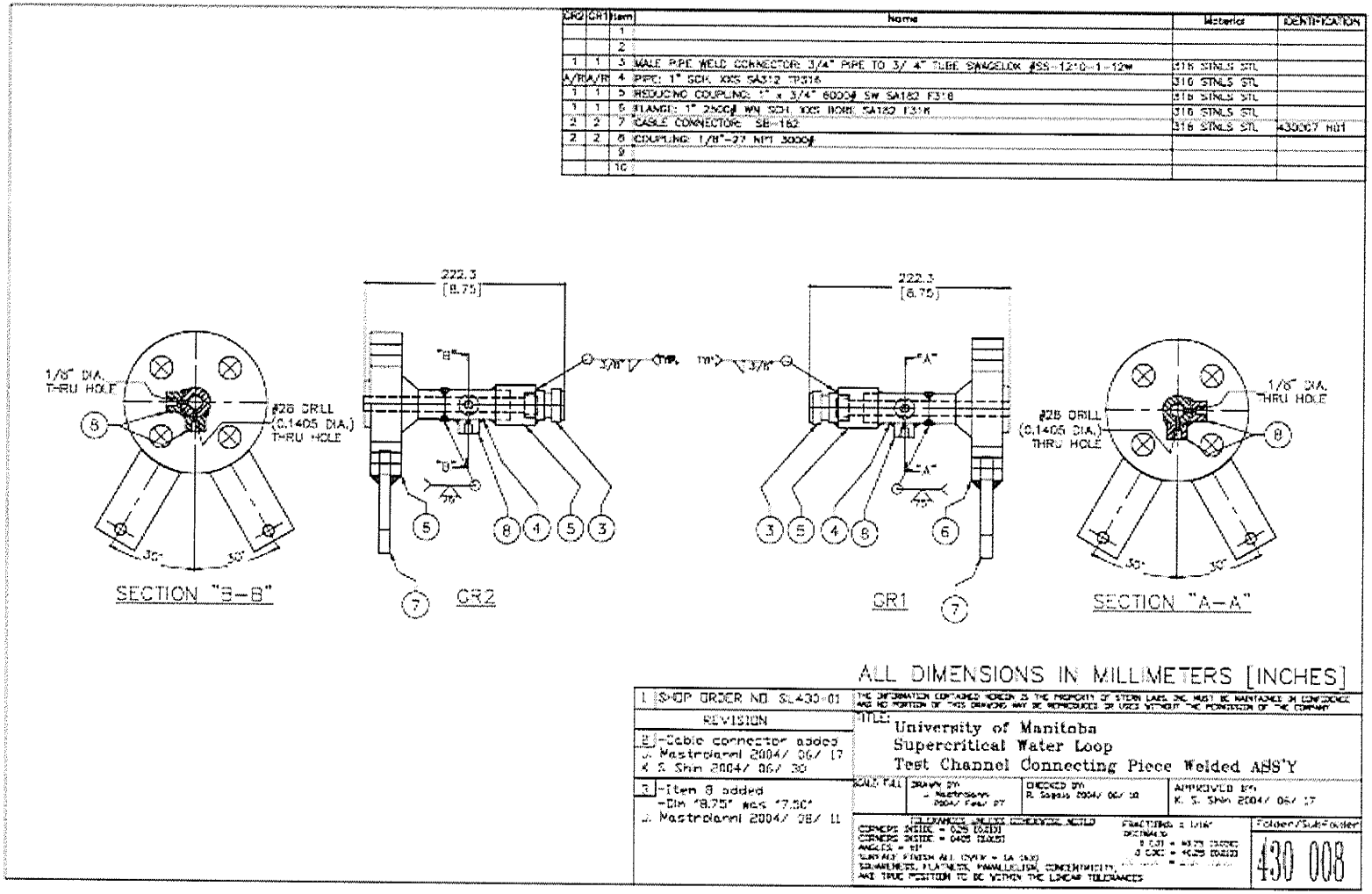

Figure C.8: Schematic drawing of test section flange couplings.

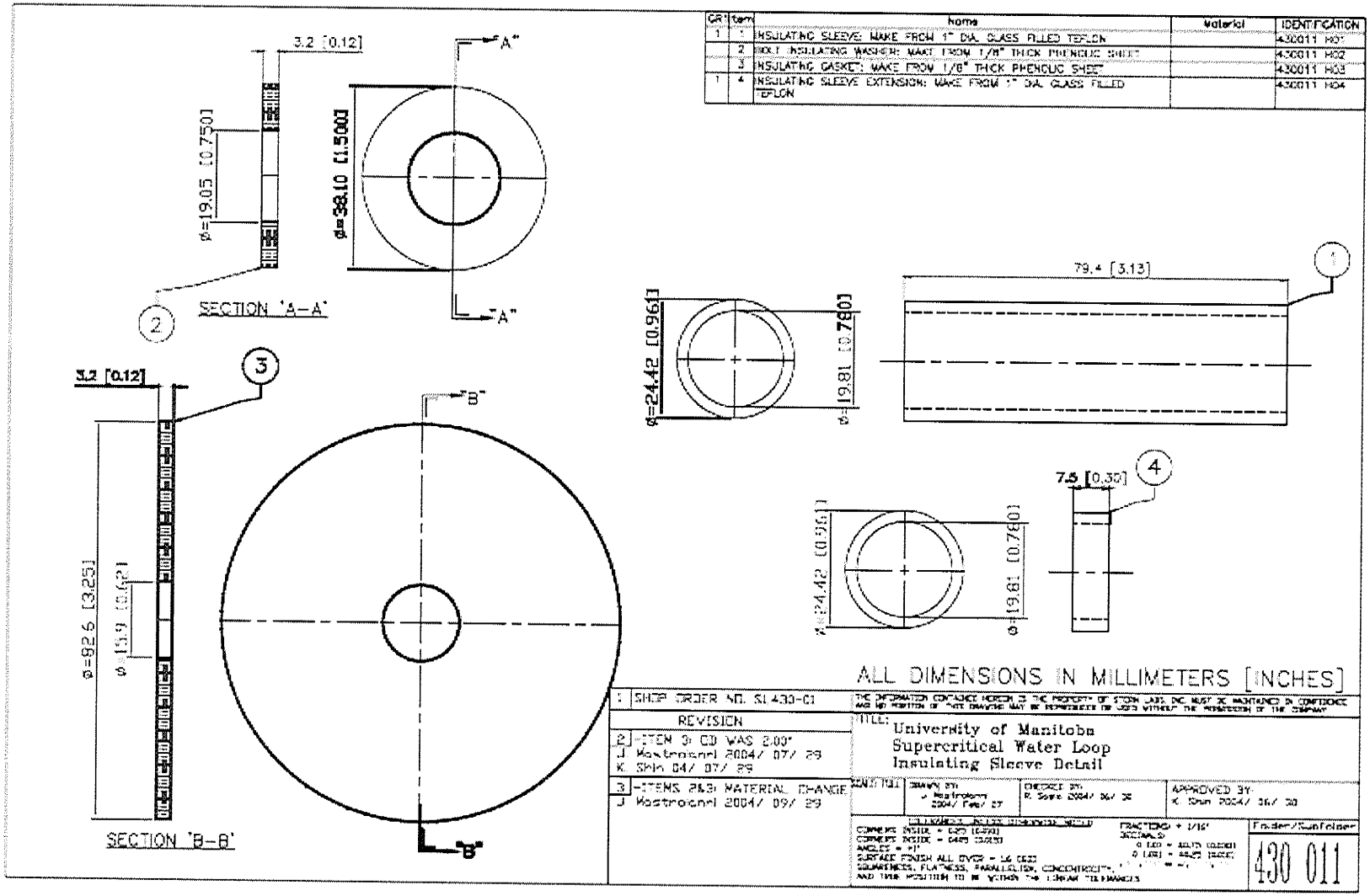

Figure C.9: Schematic drawing of test section electrical insulation sleeve details.

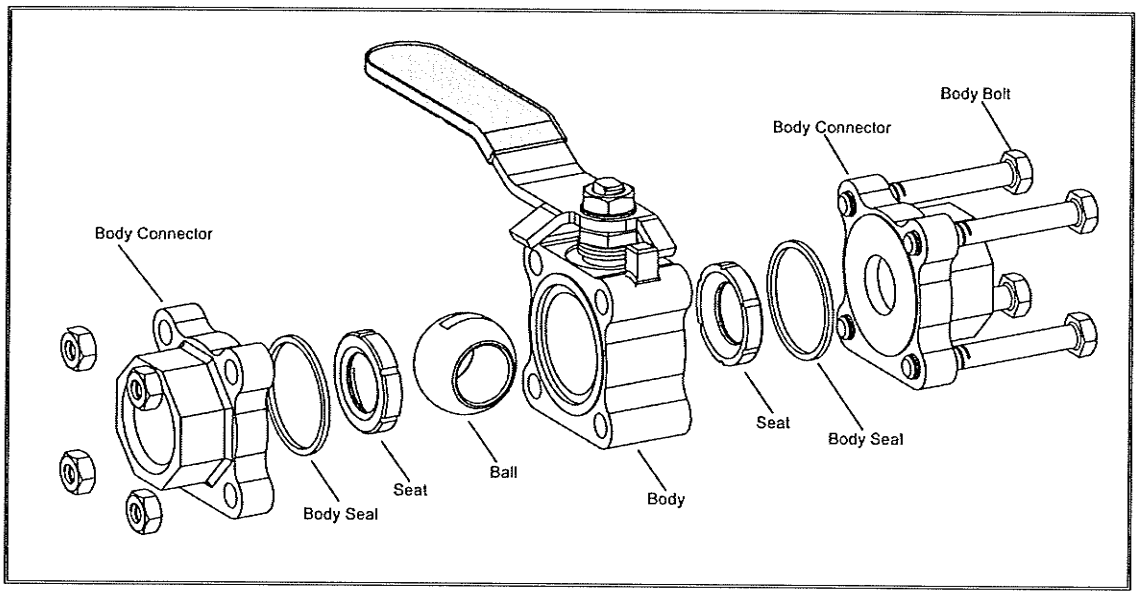

Figure C.10: Schematic drawing of the flow control ball valve assembly (Habonim®).